ÇUKUROVA UNIVERSITY
INSTITUTE OF NATURAL AND APPLIED SCIENCES

PhD THESIS

Suat ÖNAL

INVESTIGATION OF FLOW CHARACTERISTICS AROUND A SINGLE AND STAGGERED SLOTTED-CYLINDERS

DEPARTMENT OF MECHANICAL ENGINEERING

ADANA, 2010

ÇUKUROVA UNIVERSITY
INSTITUTE OF NATURAL AND APPLIED SCIENCES

INVESTIGATION OF FLOW CHARACTERISTICS AROUND A SINGLE AND STAGGERED SLOTTED-CYLINDERS

Suat ÖNAL

PhD THESIS

DEPARTMENT OF MECHANICAL ENGINEERING

We certify that the thesis titled above was reviewed and approved for the award of degree of the Doctor of Philosophy by the board of jury on 06/08/2010.

…….....	……..	…….....
Prof. Dr. Beşir ŞAHİN	Prof. Dr. Recep YURTAL	Assoc. Prof. Dr. Hüseyin AKILLI
SUPERVISOR	MEMBER	MEMBER

…….	……
Assoc. Prof. Dr. Ahmet PINARBAŞI	Assoc. Prof. Dr. Muammer ÖZGÖREN
MEMBER	MEMBER

This PhD Thesis is written at the Department of Institute of Natural And Applied Sciences of Çukurova University.
Registration Number:

Prof. Dr. İlhami YEĞİNGİL
Director
Institute of Natural and Applied Sciences

ABSTRACT

PhD THESIS

INVESTIGATION OF FLOW CHARACTERISTICS AROUND A SINGLE AND STAGGERED SLOTTED-CYLINDERS

Suat ÖNAL

ÇUKUROVA UNIVERSITY
INSTITUTE OF NATURAL AND APPLIED SCIENCES
DEPARTMENT OF MECHANICAL ENGINEERING

Supervisor : Prof. Dr. Beşir ŞAHİN
Year: 2010, Pages: 118
Jury : Prof. Dr. Beşir ŞAHİN
: Prof. Dr. Recep YURTAL
: Assoc. Prof. Dr. Hüseyin AKILLI
: Assoc. Prof. Dr. Ahmet PINARBAŞI
: Assoc. Prof. Dr .Muammer ÖZGÖREN

The aim of this experimental study is to determine the flow characteristics of a single and multiple slotted-staggered cylinders placed in a rectangular water channel with a narrow gap using the Particle Image Velocimetry technique. Qualitative flow visualization was initially employed in order to observe the overall nature of the vortical flow patterns for different configurations of cylinders. Quantitative flow visualization was secondly employed for whole configurations of cylinders in order to understand the physics of complex flow behaviour that gives rise to unsteady loading with the eventual intent of implementing control schemes to enchance the rate of heat transfer hydrodynamically.

Key words: Confined flow, vorticity, staggered cylinders, slotted-cylinders

ÖZ

DOKTORA TEZİ

TEK VE ÇOK SLOTLU ŞAŞIRTILMIŞ SİLİNDİRLER ETRAFINDAKİ AKIŞ YAPISININ İNCELENMESİ

Suat ÖNAL

ÇUKUROVA ÜNİVERSİTESİ
FEN BİLİMLERİ ENSTİTÜSÜ
MAKİNA MÜHENDİSLİĞİ ANABİLİM DALI

Danışman : Prof. Dr. Beşir ŞAHİN
Yıl: 2010, Pages: 118
Jüri : Prof. Dr. Beşir ŞAHİN
: Prof. Dr. Recep YURTAL
: Doç. Dr. Hüseyin AKILLI
: Doç. Dr. Ahmet PINARBAŞI
: Doç. Dr. Muammer ÖZGÖREN

Bu tezin amacı, dikdörtgen kesitli sığ kanal içerisine yerleştirilmiş tek ve çoklu silindirler etrafındaki akış karakteristiklerini Parçacık Görüntülemeli Hız Tekniği ile deneysel olarak hesaplamaktır. Başlangıçta, değişik sıralanmış silindirler etrafındaki doğal akış girdap parametrelerini baştanbaşa nitel olarak gözlemlemek amacıyla boya deneyi yapılmıştır. İkinci olarakta hidrodinamik açıdan ısı transferi miktarını artırma amaçlı daimi olmayan akış kontrol uygulamalarındaki kompleks akış davranışının fiziğini anlamak için PIV ile akış yapısı nicel olarak incelenmiştir.

Anahtar Kelimeler: Sınırlandırılmış akış, girdap, şaşırtmalı dizilmiş silindir, oyuklu silindir

TEŞEKKÜR

Yapılan çalışmaların her aşamasında, desteğini ve yakın ilgisini esirgemeyen ve her aşamada beni motive eden değerli hocam Prof. Dr. Beşir ŞAHİN'e en içten saygı ve şükranlarımı sunmak isterim.

Tez konusu deney çalışmalarında yardımlardan ve katkılarından dolayı Doç. Dr. Hüseyin AKILLI ve Dr. Sedat Yayla'ya ve Proje Asist. Engin Pınar'a teşekkür ederim.

Bir hayli uzun süren bu çalışma süresi boyunca her zaman manevi desteğini yanımda hissettiğim sevgili eşim Münire ÖNAL' a, oğlum Taha Ökkeş ve kızım T.Sena ÖNAL'a sonsuz teşekkür ederim.

Ayrıca yaşam felsefesinde her zaman topluma faydalı bir fert olma duygusuyla beni yetiştiren merhum babam Kemal ÖNAL'a, annem Türkan ÖNAL'a, başta Yrd.Doç.Dr. Servet ÖNAL olmak üzere tüm ağabeylerime, Atelye sorumlusu Ali AYUR ve Boğaç ERSOY'a sonsuz şükranlarımı sunarım.

Çukurova Üniversitesi Mühendislik Mimarlık Fakültesi Makine Mühendisliği Bölümünde Doktora çalışması yaptığım süre içerisinde beraber çalıştığım tüm akademik ve idari görevlilere ayrıca teşekkür ediyorum.

Bu çalışmanın ülkemize faydalı olmasını temenni ediyorum.

CONTENTS **PAGE**

LIST OF FIGURES **PAGE**

NOMENCLATURE

D	: Cylinder diameter, m
A	: Cross-sectional area of the pipe, m^2
h_l	: Distance between the plate surface and the laser sheet in plan view planes (m)
h_w	: water level (m)
H	: Depth of the water in the channel (m)
Δt	: Time interval (s)
S_x	: Saddle point
Ls	: Seperation line
B	: Slot width of cylinder (m)
S_t	: Strouhal number
Re_d	: Reynolds number based on cylinder diameter
Re_h	: Reynolds number based on hydraulic diameter of the open channel
$<V>$	: Time averaged velocity (m/sn)
V	: Instantaneous velocity (m/sn)
$<\psi>$	: Time averaged streamline
ψ	: Instantaneous streamline
$<\omega>$	: Time averaged vorticity (1/sn)
ω	: Instantaneous vorticity (1/sn)
U	: Free stream velocity (m/sn)
u	: Instantaneous velocity (m/sn)
u_{rms}	: Fluctuations of u (m/sn)
v_{rms}	: Fluctuations of v (m/sn)
$u'v'$	: Reynolds stress correlation
F_x	: Focus
N_a	: Nodal point of attachment
N_s	: Nodal point of separation
μ	: Dynamic viscosity (kg/ms)
ρ	: Density (kg/m^3)

1. INTRODUCTION

1.1. Overview of the Present Work

A large amount of work has been devoted to the study of the flow around bluff bodies which have different geometries but especially circular cylinders. Flow around circular cylinders has practical significance in many branches of engineering such as design and analysis of flows past tall towers, chimneys, heat exchangers and offshore structures. Therefore, investigation of flow characteristic is so important. Nowadays, flow configuration still presents one of the challenging subject to study in fluid mechanics, such aspects as aerodynamic forces, vortex shedding phenomena, instantaneous pressure field, governing the wake formation and its downstream evolution etc. In addition to that all these interconnected phenomena are influenced by a large number of factors, including Reynolds and Strouhal numbers, flow conditions (laminar, turbulence, steady, unsteady, compressible, incompressible), geometry (interaction between several cylinders, length to diameter ratio etc). Flow past bluff bodies has received a great deal of attention. Particularly the flow around a circular cylinder has been well studied up to now but flow around multiple bluff bodies is less well studied and understood. Therefore, in this study, flow around single-slot cylinder and multiple slot-cylinders have been investigated.

Energy is presently the most common issue in the world, because it is known that energy shortage will rise in all areas in the common decade. That is reason all countries around the world try to investigate alternative energy sources and also work on the energy saving technologies. As it is known heat exchanger is one of the devices that can be developed further in the energy saving aspects. Heat exchangers technology is used in a wide variety of industrial, thermal, commercial and household applications. Thermal power plants based on fossil fuels also degrade the quality of environment in large scale. A rapid increase of energy demands in the world is due to the rate of population growth, the high rate of industrialization, social and economical development of countries. With this in mind, progress in

technological development of heat exchanger systems must continue. Heat transfer problem and the efficiency in the heat exchanger are strongly depended on the flow structure. Plate fin and tube heat exchangers are most commonly used in space heating and cooling devices and in heat recovery systems. Due to the complex flow geometry, in recent years, most of the research work performed on the fin-tube heat exchanger is numerical. In the present work, flow structure in the flow passage of the fin-tube type heat exchanger has been studied experimentally both by dye visualization and using particle image velocimetry technique in order to examine the influence of flow structure on the performance of the heat exchangers.

1.2. Description of Heat Exchangers

A heat exchanger can be defined as a heat transfer device that is used to transfer of internal thermal energy between two or more fluids available at different temperatures. In most heat exchangers the fluids are separated by a heat transfer surface, and ideally they do not mix (Kuppan, 2000).

In other term, a heat exchanger is a device which transfers heat energy from one fluid (or gas) to another fluid (or gas), and without mixing the two different fluids or gases.

A common example of heat exchanger is automotive radiators. Heat from the hot engine water is pumped through the radiator, while air is blown through the radiator fins. The hot engine water's heat energy is transferred to the air, thus keeping the water at the desired temperature, and thus the engine is kept at the right temperature. Generally, heat exchangers are widely used in cooling, heating, ventilating, air conditioning and refrigeration systems.

There are a number of specially configured fin patterns and tube shapes used in the plate fin and tube heat exchangers to effectively improve the thermal performance and to significantly reduce the size and weight of the heat exchangers. These types of heat exchangers consist of round, elliptical, flat, oval and rectangular tubes with various fin configurations such as plain, wavy, louvered, multi louvered, corrugated, etc. In the plate fin and tube type heat exchangers, fins are attached to the

tubes and are primarily used to increase the surface area and consequently to increase the total rate of heat transfer. Plain or specially configured fins are used on the outside of the array of tubes of staggered or in-lined arrangement passing perpendicularly through the plates to improve the heat transfer coefficient on that side. Generally, liquid flows inside of the tubes and gas is forced to flow through the fins. In these types of heat exchangers, generally plain fins are used because of their long term operation and lower friction characteristics. Similarly, generally round tubes are preferred because of their easy construction as seen Figure 1.1.

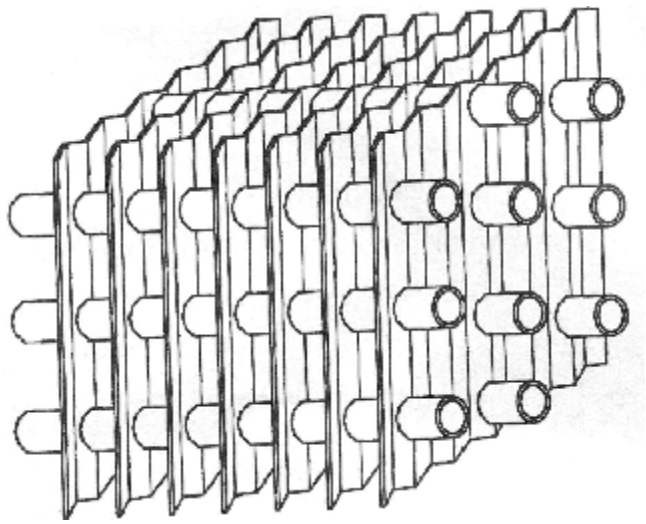

Figure 1.1. Fin configuration with round tubes (Wang et al., 1999)

Therefore some investigators such as Mon and Gross (2004), Kim and Song (2002), Tiwari et al., (2003), Bouris et al., (2001), Méndez et al. (2000), Jang et al., (1997), Tsai and Sheu, (1998), used elliptical and round tubes in their investigations.

Typical geometrical parameters of a plate fin and tube heat exchanger are illustrated in Figure 1.2. The flow is in the x-direction. The meanings of these parameters are as follows;

d tube diameter

s distance between lower and upper fin plates

l_c distance measured from the leading edge of the fin plate to the center of the tube

l_f fin length

w fin width

l_{x1} distance between the leading edge of the plate and the inlet of the heat exchanger flow passage

l_{x2} distance between the trailing edge of the plate and the outlet of the heat exchanger flow passage

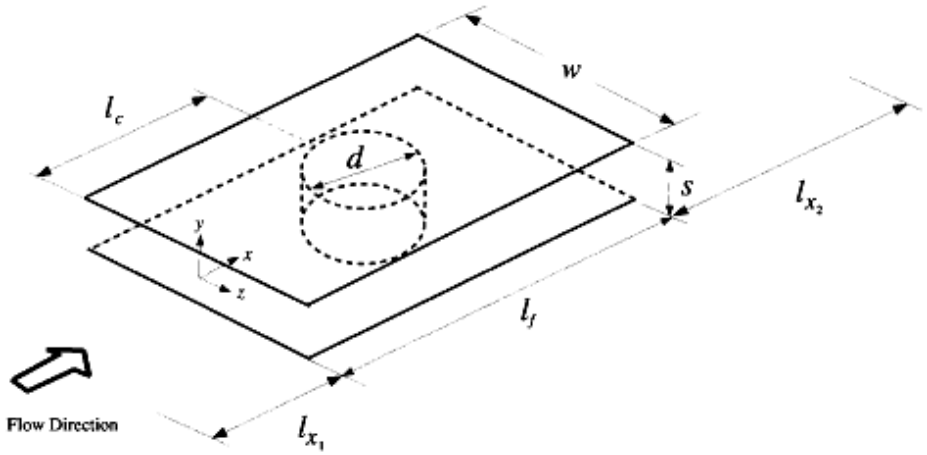

Figure 1.2. Geometrical parameters of a typical plate fin and tube heat exchanger (Mendez et al., 2000)

Various fin geometries are preferred because of better mixing of cold and hot fluids. Similarly, staggered tube layout is more efficient in terms of heat transfer characteristics compared with the in-lined tube layout. In order to get flow control and increase heat transfer, staggered slotted cylinder arrangements have been used in the present work. Various fin geometries and tube layout are shown in Figure 1.3.

Figure 1.3. Flat or continuous fins on an array of tubes; (a) Wavy fin, (b) Multilouver fin, (c) Fin with structured surface roughness (Rohsenow et al, 1998).

Flat plate heat exchangers are used to heat or cool various fluids or gases. Specifically, they are used for refrigerant to fluid applications, fluid to fluid, and sometimes gas applications. This type of heat exchanger is widely used in residential, commercial and industrial applications as shown Figure 1.4.

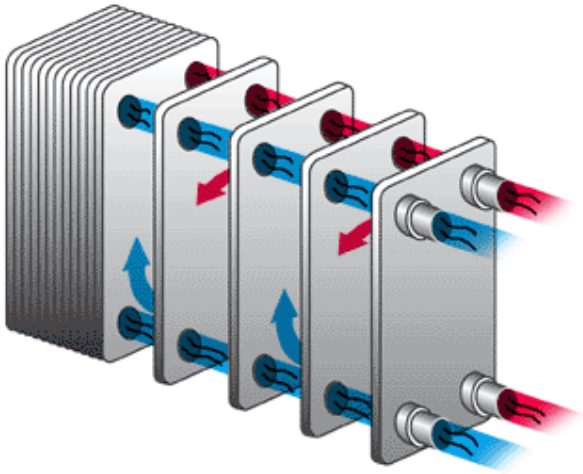

Figure 1.4. A flat plate heat exchanger (Ozturk, 2006)

1.3. Vortex Formation around a Circular Cylinder

When a flow goes across a circular cylinder, in the vicinity of the cylinder surface and the wake region, flow separation, vortex shedding and shear-layer instability etc., are usually occured in different regimes of Reynolds numbers.

Two types of stream wise vortices have been mentioned in the laminar and transitional wakes of cylinders. At a sufficiently high value of Reynolds number, so-called “transition waves” appears in the shear layer separating from the surface of the cylinder. These waves are detectable in the region of the wake extending from the separation point on the body to the first appearance of the large-scale Karman vortex. As a result, a vortex is shed from the cylinder when the local pressure changes each time. When the value of Reynolds number is sufficiently high, then these transition waves take the form of train of Kelvin-Helmholtz vortices shown in Figure 1.5.

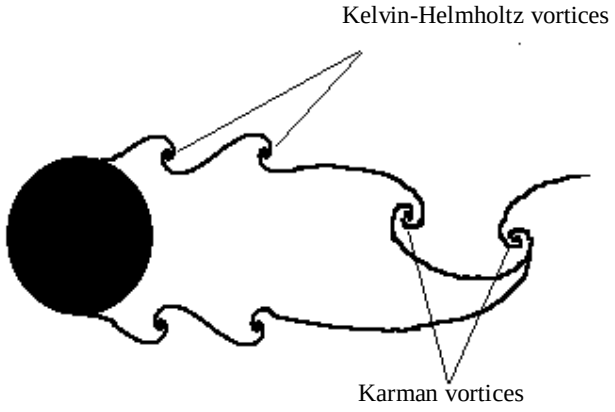

Figure 1.5. The Kelvin-Helmholtz (secondary) vortices and the Karman vortices from circular cylinder. (Akar, 2008)

Kelvin-Helmholtz vortices in the shear layer are an essential feature of the transition from a laminar to turbulent state. As a consequence of this transition process, the first Karman vortex formed from the cylinder at higher value of

Reynolds number is essentially turbulent. A Karman vortex from circular cylinder is also shown in Figure 1.5.

When more than one cylinder is placed in a uniform flow, the aerodynamic parameters and vortex-shedding patterns are completely different from the case of a single body. Because their wakes or vortex streets interference each other in a complex manner depending on the arrangement or spacing of the cylinders. Thus the flow characteristics around variable arrangement of inline and staggered circular cylinders have been recently investigated by Hassan and Barsamian (2004) in order to enhancement heat transfer in heat exchangers. Three dimensional vorticity magnitudes plot at contour level of 85 Hz for tube bundle is shown in Figure 1.6.

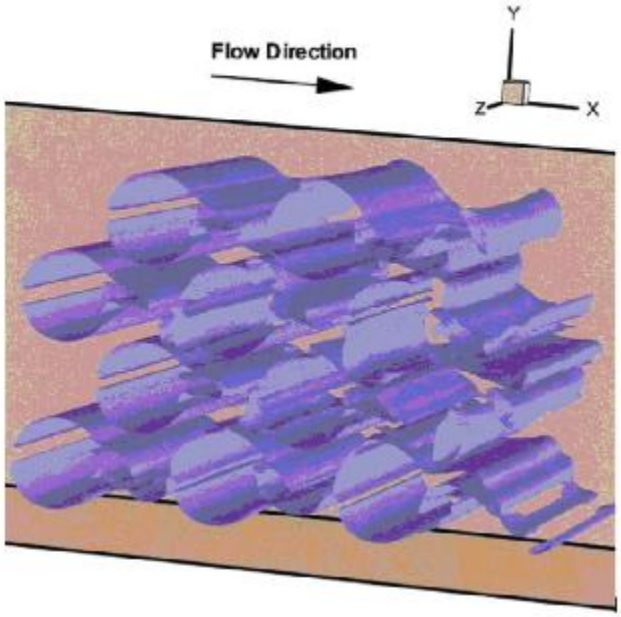

Figure 1.6. Three dimensional vorticity magnitudes plot for tube bundle (Hassan and Barsamian, 2004)

2. LITERATURE SURVEY AND OUTLINE OF THE PRESENT STUDY

2.1. Literature Survey

2.1.1. Vortex Formation and Flows Around Cylinders

One of the main problems in the fluid mechanics is to determine the flow characteristics around bluff bodies and especially cylinders. Of course, formation and shedding of vortices from a cylinder have fundamental research values in the areas of vortex dynamics and bluff body flows. In recently years, lots of researches have been carried out on vortex dynamics of a cylinder. Therefore, vortex shedding from a bluff body at different Reynolds numbers has been a topic of interest for many fluid dynamics researchers for a long time.

Nakamura (1996) has investigated vortex shedding and vortex shedding frequency experimentally for different type of bluff bodies which are rectangular, semi-circular and circular with splitter plates in a wind tunnel. He reported that when increasing the length and diameter of pipe ratio, L/D, the strouhal number of a bluff body decreases, the reduction not being dependent on the details of the cross-sectional geometry but only the value of L/D=1.0

Zdravkovich (1988) reported overall idea about different modes of vortex shedding. He categorized the observed modes of vortex shedding into 3 groups. The first one is the low-speed mode caused by the mechanics of vortex formation and shedding. Second is the synchronized vortex shedding. Third one is another synchronized vortex shedding is described that is caused by the streamwise oscillation of a cylinder or when a stationary cylinder is submerged in oscillatory flows.

Ozono (1999) Performed an experimental studying using a low-speed wind tunnel and investigated flow control of vortex shedding by a short splitter plate asymmetrically arranged downstream of a cylinder. The diameter of circular cylinder used were d=50 mm to 110 mm and splitter plate thickness was 2 mm and the cord lenght used were 50 mm to 110 mm corresponding to the cylinder

diameters. Experimental data was taken between Z/d=0 and Z/d=0,5 and also between G/d=0 and G/d=6. As a result of experimental result, he obtained that when the splitter plate is well-removed from the cylinder, strouhal number is kept around 0,2.When the splitter plate reaches a gap of G/d=2, strouhal number jumped down to 0,13 and that result showed good agreement with those of Roshko who had done same study for G/d=2,7. He reported that in the circular cylinder case with Z/d = 0.5-1.3, the variation of both base suction coefficient and Strouhal number with G/d depends on Z/d significantly.

Kang, Choi and Lee (1999) studied numerically about laminar flow past a rotating circular cylinder for the purpose of controlling vortex shedding and understanding the underlying flow mechanism. They made numerical simulations for Re=40, 60, 100 and 160 in the range of circumferential speed at the cylinder surface between 0-2,5.They reported that the rotation of a cylinder can suppress vortex shedding effectively, vortex shedding exist at low rotational speed and completely disappears over critical rotational speeds which shows logarithmic dependence on Reynolds number. The strouhal number remains nearly constant regardless of circumferential speed while vortex shedding exist.

Sumner et al. (1999) measured the flow patterns downstream of two and three side-by-side circular cylinders in the range of G/D=1~6 and Re_D =500-3000 using flow visualization and the particle image velocimetry techniques. They noted considerable variation in the flow patterns at a given G/D ratio.

Zhou et al. (2002) measured the velocity, temperature and their fluctuations at Re=1800 in the cases of two-and-three-cylinders. They observed that the cross-stream distributions of the Reynolds stresses and heat flux varied significantly, which were ascribed to different flow patterns, as G/D ratio was reduced from 3.0 to 1.5.

Sumner et al (2000) investigated flow characteristics for two staggered circular cylinders of equal diameter in cross-flow, using flow visualization and PIV. They did experiments within the low subcritical Re number regime from 850 to 1900 for centre to centre pitch ratio P/D=1 to 5 and angle of incidence α = 0 to 90 degree. After all, they reported that some different flow patterns were identifed in the low

subcritical regimes which are the pitch ratio, incidence angle boundaries, shear layer reattachment, induced separation, vortex pairing, synchronization and vortex impingement. They also explained that existing of vortex shedding from the upstream cylinder is intrinsically linked the flow through the gap between cylinders.

Mittal and Raghuvanshi (2001) have studied numerically control of vortex shedding behind circular cylinder and they investigated the effect of the placement of a control cylinder in the near wake of the main cylinder for flows at low Reynolds numbers. They took parameters as following that P/D=2, T/D=0,8 ; P/D=5, T/D=5 and P/D=2, T/D=1 for Re number of 60, 70, 80 and 100.They reported that their numerical studies and experimental findings of other researchers are good agreement as pressure, stream function, vorticity fields and also it is obvious that proper placement of the control cylinder leads to suppression of the vortex shedding behind the main cylinder.

Zovato and Pedrizzetti (2001) made a numerical studying flow past a circular cylinder between paralel walls, at various distances from the walls, for values of Reynolds number from those corresponding to steady flows and the initiation of vortex shedding regime. They reported that two-dimensional transition form steady to unsteady flow significantly delayed by the presence of a close wall and then, in the steady regime, the presence of a wall inhibits the creation of a vortex pair and the wakes which become a single row of vortex filaments whereas the transition from two-dimensional to three-dimensional flow in the wake of an unbounded cylinder is caused by the self-induced stretching of vortex pairs. They also reported that the transition form steady flow to a periodic vortex shedding regime occurs at larger Reynolds numbers as the cylinder approaches one wall, because the wake interacts with the wall boundary layer. The periodic shedding is delayed because the vorticity shed from the cylinder's wall side couples with the wall vorticity which arrests its evolution.

Keles (2002) performed experimental work on active control of vortex shedding in the far wake of a cylinder using wind tunnel. He reported that active control shedding of vortices achieved locally in the beginning of distance x/d=7 of far wake which extends to x/d=20 further downstream behind the cylinder and

reductions in the amplitude of flactuation's behind the cylinder were suppressed in the beginning of far wake distance x/d=7. In the further downstream of the far wake distance x/d=20 no active control shedding of vortices was achieved. Significant reductions of the amplitude of the velocity fluctuations in the Karman vortex street were observed when the active control was turned on in the beginning of far wake distance x/d=7.

Lim and Lee (2002) investigated flow around cylinders with different grooved surfaces experimentally. They measured the drag force, wake velocity and surface pressure distribution for Reynolds number based on the cylinder diameter in the range $8x10^3 \leq Re_d \leq 1.4x10^5$. Their main findings were; i) the u-grooved cylinder reduces the drag coefficients as much as 18.6% comparing to the smooth cylinder at $Re_d=1.4x10^5$ on the other hand, the drag reduction for the v-grooved cylinder is only 2.5% , ii) the length of the vortex formation region and the level of Strouhal number increase with an increase of Reynolds number in the case of the u-grooved cylinder comparing to the smooth and v-grooved cylinders, iii) in the case of u-grooved cylinder the vortex formation behind the u-grooved cylinder elongates more than 50% comparing to the case of smooth cylinder.

Akilli and Rockwell (2002) investigated the vortex formation in the base of a vertical cylinder in shallow water flow using a combination of flow visualization and PIV techniques. Their dye visualization demonstrated the formation of counter-clock-wise spanwise rotating vortices near the cylinder-plate juncture in the wake region. While moving from the bed surface to the free surface, the characteristics of the wake flow region changes for a certain extent indicating that flow is three-dimensional.

Kahraman et al. (2002) tried to control vortex formation for a vertical cylinder in shallow water flow by placing a narrow transverse strip of roughness element with small size on the flat plate surface in downstream base of the cylinder. They concluded that the existence and the height of the roughness element change the wake flow parameters. Reynolds stress, both at the bed and mid plane showed decreasing peak values with increasing height of the roughness elements.

Wang and Zhou (2005) studied experimentally in a water tunnel for investigation of vortex interactions in a two side-by-side cylinder near wake. They classified the flow as three regimes which are single street, the cylinder center-to-center spacing T/d<1.2., asymmetrical flow, 1.2<T/d<2.0, and two coupled street, T/d>2.0. They gave special attention to the asymmetrical flow regime which is characterized by one narrow and one wide wake.. They reported that the flow structure and its downstream evolution are closely linked to the phase relationship between the gap vortex in the wide wake and that in the narrow wake. When the gap vortex in the wide wake leads in phase, the two opposite-signed vortices in the narrow wake are typically engaged in pairing, which yields a relatively low pressure region between them, thus drawing in the gap vortex along with fluid in the wide wake. When lagging behind in fase, the gap vortex in the wide wake fails to merge with the vorticies in the narrow wake.. Interactions between vortices in the two wakes lead to changeover of the gap flow deflection from one side to another.

Konstantinidis et al. (2004) investigated the effects of imposed pulsations on the cross-flow over tube arrays in the subcritical regime both experimentally and numerically. They reported that the arrangement of the tubes exerts a strong influence on the vortex shedding characteristics in steady flow. Pulsing the flow resulted in lock-on in all arrays when the pulsation frequency was close to the frequency of unforced vortex shedding or its first harmonic but resonance was more pronounced in the latter case. The amplitude of the velocity fluctuations increased with lock-on due to an increase of organised periodic motion of the flow associated with vortex shedding, whereas the level of random fluctuations remained approximately the same as in steady flow.

Iwaki, Cheong, Monji and Matsui (2004) investigated shell-side cross-flow in tube bundles experimentally using PIV method. They conducted experiments using two types of model; inlined and staggered bundles with a pitch-to-diameter ratio of 1.5, containing 20 rows of five tubes of 15 mm diameter in each column. They reported that, in the in-line array, the flow was characterized by two flow regions, i.e., a vortex region behind the tubes and a straight flow region of high velocity in the horizontal spaces between the adjacent tubes. On the other hand, in the staggered

array, the flow was characterized by three kinds of flow regions; a vortex region, a branching region, and a meeting region. In the in-line array, three typical patterns of vortex were observed in the mean velocity field; a symmetric pair of vortices, an asymmetric pair of vortices and a single large vortex. In the staggered array, only a symmetric pair of vortices formed behind all of the tubes.

Sarpkaya (2004) reported a comprehensive review of the progress made during the past two decades on vortex induced vibration His extensive review covers the fundamental aspect of bluff body flows, mostly vortex induced vibration of circular cylindrical structure subjected to steady uniform flow, with a powerful theoretical discussion, experimental methods and numerical models regarding the strengths and weaknesses of the current state of the understanding of the complex fluid/structure interaction. Unsteady flow structure can cause a severe problem depending on the location of the cylinder.

Akilli et al (2004) performed the PIV technique and flow visualizations so as to find out flow characteristics of circular cylinders arranged side-by-side in shallow water arranged different transverse gap ratio in the range of G/D =1.0-3.0 with an increment of 0.25 for the Reynolds number of 5000. They reported that the effect of jet-like flow on the flow characteristics behind cylinders was negligible for larger gap ratios ($G/D \geq 2.5$), jet-like flow between cylinders was remarkably effective for small gap ratios ($G/D \leq 1.5$), bistable nature of the flow observed especially for the gap ratio of G/D = 1.25 both for two and three side-by-side cylinders arrangements.

Dong and Karniadakis (2005) presented results of direct numerical simulations for turbulent flow past a stationary and a rigid circular cylinder for Re=10.000 and compared their results with available experimental data.

Naudascher and Rockwell (1994) reported that a cylinder with high aspect ratio produces a regular vortex shedding leading to create resonances which may fail whole structures. In some cases, a massive flow separation can cause high drag forces on the bluff body.

Itoh and Himeno (2001) studied on numerical simulation of three-dimensional flow around two circular cylinders in tandem arrangement. They ranged the distance between the centers of the two circular cylinders from 2.0 D to 5.0 D and L/D ratio

from 2.0 to 5.0. They reported that their computation results of strouhal number and time-averaged drag coefficient are in good agreement with the previous experimental results.

Igarashi and Terachi (2002) made an experimental study on drag reduction of flat plate normal to airstream by flow control using a rod. They chosen chord lenght of the plate, D, was 50 mm and the diameter of the rod, d, ranged from 2 to 20 mm. and the distance between the axes of the rod and plate, L/D, was varied from 1.0 to 2.6. The Reynolds number ranged from 19.000 to 77.000. According to the result of experiments they reported that the larger the rod diameter, the more efficient is the drag reduction. The maximum reduction of total drag coefficient that includes the additional force from the rod is about 20-30 % for d/D = 0.4 and L/ D = 2.0 in comparision to the value obtained without the rod.

Mittal and Kummar (2003) studied numerically on vortex induced vibrations of two equal-sized cylinders in tandem and staggered arrangement placed in uniform incompressible flow of Reynolds number 1000. In this arrangement, the cylinders are seperated by 5.5 times the cylinder diameter in the stream wise direction. For the staggered arrangement, the spacing between two cylinders is 0.7 times the cylinder diameter. They reported that the downstream cylinder lies in the wake of upstream cylinder. In almost all the cases the upstream cylinder responds like an isolated single cylinder. in certain cases, the oscillations of the cylinders result in an alternate mode of vortex shedding. Vibration of cylinders is usually accompanied by an increase in drag.

Liao, Dong and Lu (2004) studied on a numerical simulation in order to investigate the vortex structure and force characteristics of a foil placed in the wake of a circular cylinder. According to position of the foil and the cylinder, they classified into three groups which are as the foil placed inside the cylinder wake (ICW), on the edge of the cylinder wake (ECW) and outside the cylinder wake (OCW). Some basic vortex structures, corresponding to these classifications, are identifed in the near region of the foil. They reported that a preferred vortex shedding frequency of the foil is synchronized with that of the circular cylinder. As the foil under the interaction of an incident vortex street shed from the cylinder, it is

interesting to find that the mean lift and drag coefficients acting on the foil for the classification of ICW are smaller than those for the classification of OCW.

Lee and Park (2004) investigated drag characteristics and wake structure behind a circular cylinder by upstream installation of a small control rod. The Reynolds number based on the main cylinder (D=30 mm) is about Re= 20.000 and the diameters of control rods ranged from d/D=0.133 to 0.267. They reported that the drag coefficient of main circular cylinder decreases about 29% when a control rode of diameter d=7 mm and the maximum reduction of the total system drag including that of the control rod (about 25%) was observed at a pitch ratio of L/D=1.833 with a control rod diameter of d/D=0.233.

2.1.2. Wakes Control Around Bluff Bodies

Bluff body is a widely studied subject since Strouhal (1878) observed vortex shedding from a circular cylinder. So far most of works were carried out on the cylinders having circular, square and rectangular cross-section, but the flow around circular cylinders remains the principal subject of researchers because, despite the geometric simplicity, the mechanisms involved are complex and the flow patterns are not easy to understand, especially for large Reynolds numbers and when control processes are implemented.

There are many important reviews and studies in the literature regarding structure of wake region downstream of the circular cylinder. Chen and Aubry (2005) stated that the appearance of vortex shedding is accompanied by a large fluctuation of drag and lift forces, which may cause structural vibrations and acoustic noises, and shorten the life of the solid structure. Therefore, control of wakes of bluff bodies is very important in many engineering applications, such as in aircraft and automobile industry. Zdravkovich (1981) reviewed techniques of controlling vortex structure. Anagnostopoulos (1997) studied the laminar vortex shedding behind a circular cylinder using the finite element method. Mavridis et al. (1998) performed detailed measurements of temperatures and turbulent statistics in the wake region of square cylinders operated with and without jet injection into the

vortex formation region using laser velocimetry technique. Persillion and Braza (1998) studied physical analysis of the transition to turbulent flow in the wake region of a circular cylinder using three-dimensional numerical simulation of the Navier-Stokes equations.

Souza et al. (1999) investigated turbulent boundary layer interacting with the wake of a circular cylinder. They indicated that this flow configuration was of interest in terms of both heat transfer and surface friction control.

Grosche and Meier (2001) pointed out that unsteady vortex shedding into the wake flow can lead to severe buffeting of the body, especially if the resonance effects occur. This unsteady flow separation is the main source of wind noise.

Gossler and Marshall (2001) examined the secondary vorticity field generated by a cylinder during interaction with a normal vortex filament under several flow conditions. They performed a computational study to give limiting streamlines, surface pressure contours, and vortex lines on the cylinder surface at various time frames.

Akıllı et al. (2004) investigated experimentally the flow around two and three side-by-side circular cylinders of equal diameter (Re_D=5000) in shallow water using the particle image Velocimetry (PIV) technique, over a transverse gap ratio in the range of G/D= 1.0-3.0 with an increment of 0.25 For the two side-by-side cylinder case, They found that the flow structure behind the cylinders is asymmetrical at small gap ratios as a result of jet-like flow between the cylinders. The jet-like flow tends to deflect toward the narrow wake region that has a higher vortex shedding frequency. In the case of three cylinders, they observed both an asymmetrical flow structure at small gap ratio (G/D= 1.25) and a symmetrical flow structure at intermediate gap ratios (1.5<G/D<2.0). He also observed bistable wake regions for the asymmetrical cases.

Akıllı et al. (2005) investigated the effect of splitter plate on the suppression of vortex shedding in shallow water using the Particle Image Velocimetry (PIV) technique. Splitter plates with a length of 50 mm, which is equal to the diameter of the cylinder (D), were used during the experiments. Gap distance between the base of the cylinder and the leading edge of the splitter plate ranged from 0 to 2D.

Velocity vector field and corresponding vorticity contours and streamline topology and Reynolds stress concentrations were used to explain the characteristics of the flow. The splitter plates having different thicknesses presented the same influence on the flow characteristics. The splitter plate has a substantial effect on suppression of the vortex shedding for the gap ratio between 0 and 1.75D. In this gap ratios, shear layers extend up to the trailing edge of the splitter plate preventing the entrainment of the free- stream flow into the base region. For G/D=1.75, the normalized Reynolds stress has a peak value of 0.0158 which is approximately 8.5 times smaller than the concentrations occurring for a bare cylinder. After passing the splitter plate, the flow starts to oscillate with smaller frequency compared to the natural frequency of the bare cylinder. When the splitter plate was located at 2D location, no effect of the splitter plate was observed.

Akıllı et al. (2008) investigated experimentally passive control of vortex shedding behind a circular cylinder by splitter plates of various lengths attached on the cylinder base in shallow water flow (Re=6300). At this study the length of the splitter plate was varied from L/D=0.2 to L/D=2.4 in order to see the effect of the splitter plate length on the flow characteristics. Instantaneous and time-averaged flow data clearly indicate that the length of the splitter plate has a substantial effect on the flow characteristics. They found the flow characteristics in the wake region of the circular cylinder sharply change up to the splitter plate length of L/D=1.0. and above this plate length, small changes occur in the flow characteristics.

2.1.3. Flow Past a Surface Mounted Object (Junction Flows)

Not only the flows around and in the wake of bluff bodies but also flows around and downstream of the intersection of a bluff body with a flat surface are also an interesting topic to be investigated. Because such flows have a complicated three-dimensional flow structure. Practical examples of these types of flows can be seen applications in nuclear, coastal, wind, and heat transfer engineering, for example, flow past aircraft wing-body junctions, turbine blade-hub junctions, building-ground junctions, pipelines, bridge piers, heat exchangers, etc.

Due to importance of these types of flows, some researchers performed either numerical and/or experimental studies to determine flow characteristics of junction flows. Sumer et al. (1997) conducted experiments to determine the flow around the base of a vertical wall-mounted cylinder exposed to waves. Simson (2001) discussed the physical features of some practical junction flows around bluff bodies for both laminar and turbulent approaching boundary layers. Becker et al. (2002) studied the flow around three-dimensional rectangular obstacles of different aspect ratios and provided the distribution of turbulent energy downstream of the obstacle at various sections experimentally. Martinuzzi and Havel (2004) investigated periodic vortex shedding from two surface mounted cubes in tandem arrangement using laser doppler velocimetry. Kairouz and Rahai (2005) presented the results of the experimental study for turbulent junction flows. Chang et al. (2005) and Roulund et al. (2005) performed both numerical and experimental studies of flow around obstacles.

Sahin and Ozturk (2009) investigated the flow behaviour at the junction of cylinder and base plate in deep water by using the PIV method experimentally for Reynolds numbers between 1500 and 9600. By analysis of instantaneous flow data, the time-averaged velocity vectors map, streamlines, vorticity patterns, Reynolds stress correlations and fluctuations of the velocity component, they showed that the flow structure occurred in the base of cylinder is three dimensional and the area of flow field affected by the horseshoe vortex system around the cylinder varies as a function of the Reynolds number.

Ozturk et al (2009) performed PIV measurements in order to find out the flow characteristics downstream of a circular cylinder mounted on a flat surface for Reynolds numbers of 4000 and 7000. They reported that the horseshoe vortex system emerging from the upstream of the cylinder conveys fresh fluid into the wake flow region aiding interaction of the horseshoe vortices with the shear layer vortices caused by shedding vortices. They also reported that the strength of the normalized Reynolds stress increases while the value of X_L/d increases, the peak value of the normalized Reynolds stress obtained at the saddle point where

shedding shear layers merge and from the saddle point, further downstream, the strength of the normalized Reynolds stress decreases gradually.

2.1.4. Definition and Properties of Horseshoe Vortex System

When a flow passes through a wall-mounted object of sufficient size, this flow accelerates around the object and vertical velocity gradient of the flow is transformed into a pressure gradient on the leading edge of the structure. This pressure gradient results in a downward flow that impacts the object's base as seen in Fig. 2.1. This downflow forms a vortex sweps around and downstream of the object and is called as "horseshoe vortex" or "necklace vortex" due to its horseshoe shape.

The horseshoe vortex can be seen in every day life at any time a boundary layer encounters a wall mounted bluff body obstruction and is very important in various engineering applications.

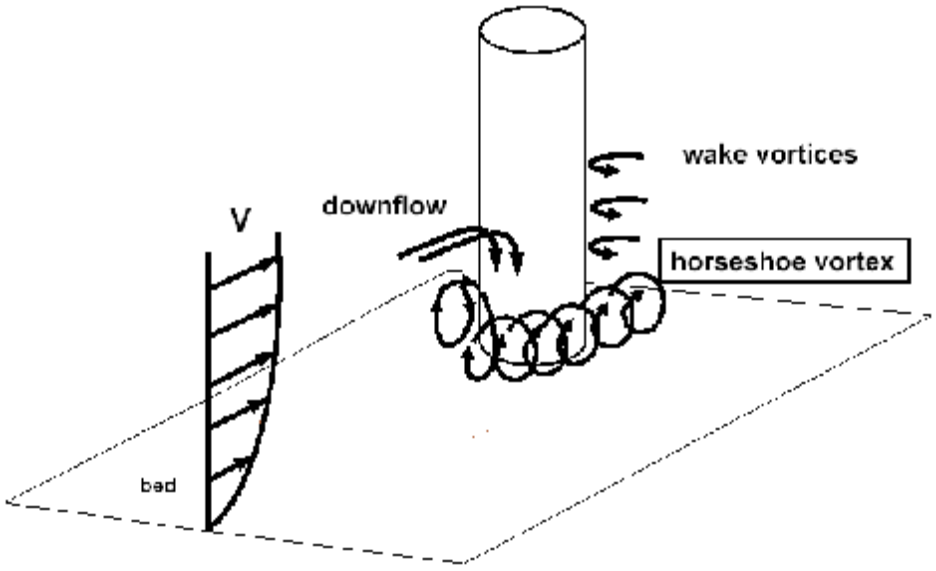

Figure 2.1. Local scour mechanism at the base of the bridge pier (Sheppard, 2004).

The horseshoe vortices are generated in the junction of a bluff body and a relatively flat surface and are important for many fluid mechanics applications. The main cause of the horseshoe vortex system is the rotation in the incoming flow at the junction of a flat surface and a vertically placed bluff body. Figure 2.2 illustrates a horseshoe vortex mechanism formed in front of a circular cylinder.

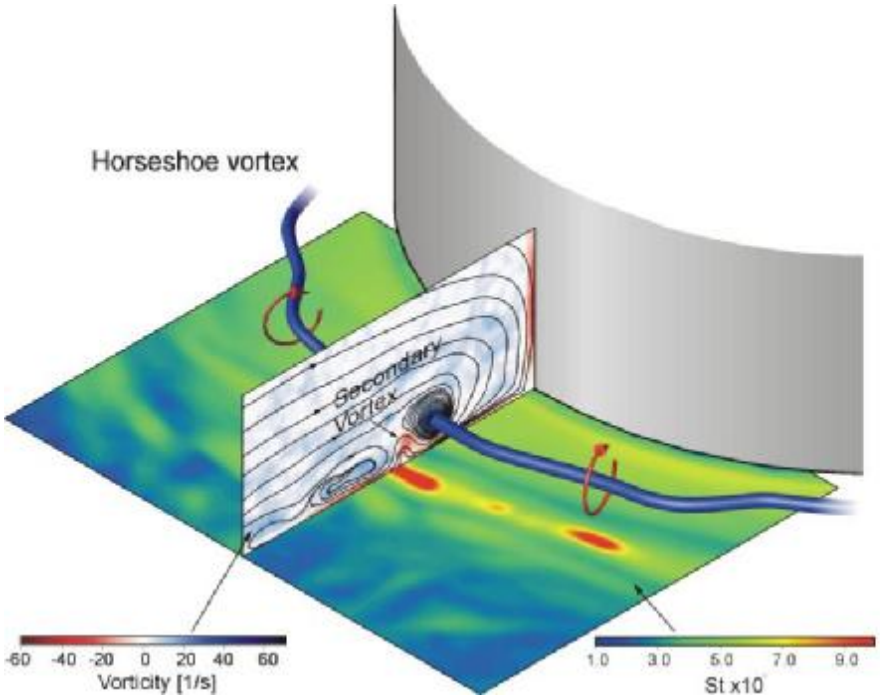

Figure 2.2. Horseshoe vortex mechanism in front of a circular cylinder (Praisner, 2001)

Figure 2.3. illustrates time-averaged streamline patterns <ψ> upstream of the cylinder. Two symmetrical horseshoe vortex is formed upstream of the cylinder in the vicinity of the tube and the fin junction area.

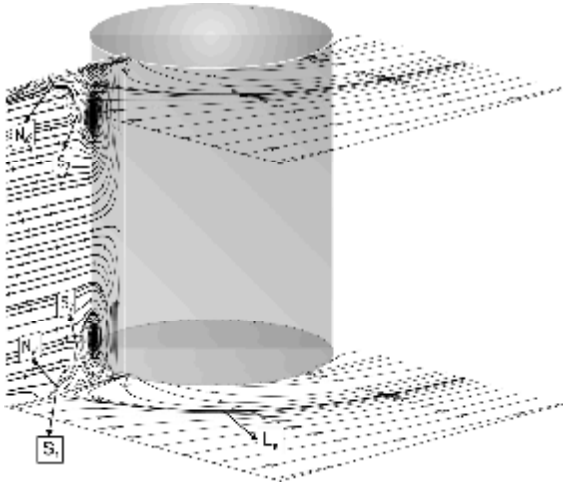

Figure 2.3. Time-averaged streamline patterns upstream of the cylinder (Ozturk, 2006)

Kelso and Smith (1995) studied the horseshoe vortex system resulting from the interaction between a laminar boundary layer and a round transverse jet for the Reynolds number range of $1200<Re_d<4600$ based on the pipe diameter using a hydrogen bubble wire visualization in a water channel. They concluded that the interaction of round transverse jet and laminar boundary layer can cause steady, oscillating or coalescing horseshoe vortex system depending on the flow condition. Their results suggest that there is a strong connection between the unsteadiness in the wake and the unsteadiness in the horseshoe vortex system.

Seal and Smith (1997) reported that the existence of the horseshoe vortex cause a significant impact on the flow characteristics in junction regions of a cylinder and a flat plate relating to the hydrodynamic and thermal effects. So, it is useful to control these vortex systems. They also performed an experimental work to control the turbulent end-wall boundary layers using surface suction. Their results indicate that the surface suction in front of the cylinder weakens both the instantaneous turbulent vortex and its associated surface interactions.

Faracci et al. (2000) investigated flow structures at the base of a vertical cylinder in the presence of an oscillating flow. They reported that Keulegan-Carpenter KC, in the case of fixed bed, along with the Reynolds number Re_d is the

key parameters to control the horseshoe vortex formation and development. The horseshoe vortex does not exist for KC<6 and Reynolds number, Re_δ<50 based on boundary layer thickness.

Simpson (2001) reported some physical features of junction flows around bluff bodies such that, horseshoe vortices form in all types of bluff bodies' junction causing high rate of turbulent intensities, pressure fluctuations, circulatory motions and heat transfer rate around the bluff bodies base.

Lin et al. (2003) studied simultaneous measurements using PIV and LDV techniques in the periodical oscillatory horseshoe vortex system near the base of square cylinder–plate juncture. They stated that the combination of PIV and LDV provide a better understanding of horseshoe vortex system using the spatial distribution and time history of velocity near the juncture and phase averaging of the PIV data. They classified the horseshoe vortex system as three types which are the steady vortex system, the periodical oscillatory vortex system and turbulence-like chaotic vortex system.

Sau et al. (2003) studied interaction of trailing vortices in the wake of a wall-mounted rectangular cylinder and they conducted numerical simulations to investigate three-dimensional unsteady vortex-vortex and vortex-surface interactions in the junction of a wall-mounted rectangular cylinder.

Muzzammil and Gangadariah (2003) investigated the characteristics of the primary horseshoe vortex on the plane of the symmetry in front of a circular cylinder.

Contantinescu and Koken (2005) used a kind of simulation to reveal the physical behavior of the horseshoe vortex system at the base of the surface mounted cylinder. They concluded that the structure of the horseshoe vortex system is very organized and periodic when approaching boundary layer is laminar. In the case of turbulent flow horseshoe vortex system has wide range of a coherent structure with a wide range of energetic frequencies in velocity and pressure spectra. The highest value of the bed shear stress occurs beneath the horseshoe vortex system.

Pattenden et al. (2005) performed PIV experiments to visualize flow details on different planes and examined the location and motion of the horseshoe vortex system in front of the cylinder mounted on a ground plane.

Fu and Rockwell (2005) studied horseshoe vortex system in shallow water flow with a shallow water layer height of h_w=6.3mm. The approaching flow was laminar. Their main findings are; i) An instability of the horseshoe vortex system emerging from the forward face region of the cylinder stimulates instability of flow in the near wake, ii) Increasing amplitude level of the fluctuation in the horseshoe vortex system causes a formation of coherent vortical structures earlier in the separating shear layer, iii) Rotational perturbation of the cylinder can destabilize the wake flow region.

Roulund et al. (2005) performed numerical and experimental studies and revealed that the boundary-layer thickness, Reynolds number and bed roughness influence the horseshoe vortex system. The size of horseshoe vortex system and bed shear stress in laminar flow rise up as a function of Reynolds number, but in the case of turbulent flow regime a reduction takes place.

2.1.5. Flows in the Heat Exchanger Flow Passages

As it is known, heat and momentum transfer characteristics around the tubes are strongly affected by the flow structure and have a great importance in design and optimization of heat exchangers. In the literature there are a number of studies regarding flow and heat transfer characteristics and horseshoe vortex system formed in the heat exchangers composed of parallel plates passing through cylinders.

Wung and Chen (1989) studied numerically studies on the flow and heat transfer characteristics of heat exchanger configurations. They predicted heat transfer and flow data and found that heat transfer tended to peak in the upstream surface of the cylinder, and became minimum at the separation point and in the recirculation zone.

Kundu et al. (1992) measured heat transfer and pressure drop data for laminar and turbulent flow over an inline cylinder array for eight cylinders with three different aspect ratios (ratio of fin spacing to cylinder diameter) in the $220<Re<2800$ range concerning flow transition from laminar to turbulent flow regime.

Jang et al. (1996) have performed experimental studies over a 3-D multi-row (1-6 cylinders) plate fin and tube heat exchanger to investigate effects of tube arrangement, tube row number and fin pitch (8-12 fins per inch) for fin spacing-based Reynolds number in the range of $60<Re<900$. The experiments were conducted using the wind tunnel. The average heat transfer coefficient of the staggered arrangement was 15-27% higher than that of the in-lined arrangement, while the pressure drop of the staggered arrangement was 20-25 % higher than that of the in-lined arrangement.

Kim et al. (1997) used a multiple regression technique to correlate wavy fin geometries for both staggered and in-line arrays of circular tubes with varying number of tube rows, tube diameter, fin spacing and distance between tubes in the direction either normal to the flow or parallel to the flow.

Wang et al. (1997) conducted several tests on wavy fin and tube heat exchangers with different geometrical parameters including the number of tube rows, fin pitch, and also tube arrangement for $400<Re<8000$ range in the wind tunnel. They observed that for the staggered layout at higher Reynolds numbers, downstream turbulence causes a higher heat transfer coefficient with an increase in the number of tube rows. Also the heat transfer coefficients for wavy fin geometry show a 55% to 70% increase compared to the plain fin geometry while the corresponding values for the friction factor was 66% to 140%.

Ballio et al. (1998), stated that the presence of horseshoe vortex system increases the local shear stresses, heat transfer, drag in the plate fin and tube heat exchanger flow passages, as the flow approaches to the tubes, the horseshoe vortex system forms in front of each tube near the tube and the fin junction region and reveals the mixing of hot and cold fluids, thus, creates a natural heat transfer augmentation in that area.

Tsai and Sheu (1998) conducted a three-dimensional numerical study in order to examine flow structure and performance of a conjugate heat transfer in a finned-tube heat exchanger element. They reported that the rate of heat transfer increases due to the presence of helical horseshoe vortices which form in forward base of the tube both in close region of lower and upper fin plates and wrap around tube.

Spiraling motions of horseshoe vortices adjacent to their central lines enables exchange of fluids between main and wake flow regions.

Sheu et al. (1999) numerically studied the heat transfer in two-row tubes heat exchanger having slotted fins and laminar flow. Because this type of fin can be divided into louvered, forgo, radial-strip, parallel-strip and wavy-strip types. In this type of geometry, the physical complexity comes from the three-dimensional boundary layer development and the subsequent flow separation. Their study revealed that three-dimensional vortical flow structure becomes more energetic because of the perforated fin surface leading to an increase in the heat transfer rate but causing further pressure losses.

Mendez et al. (2000) examined effect of fin spacing on a single cylinder heat exchanger with plain fin configuration in the $260<Re<1460$ range through dye visualization technique. They showed that the horseshoe vortex development depends on the fin spacing and corresponds to the peak in the Nusselt number.

Kim and Song (2002) studied the effects of distance between plates and tube placement for a single tube row in the $114<Re<2660$ range using naphthalene sublimation technique. They observed a subsidiary horseshoe vortex when the Reynolds number is as large as 2660. They found that total mass transfer rate is increased up to 25% by proper positioning of the tube.

Kim and Song (2002) used naphthalene sublimation technique in order to measure local heat and mass transfer coefficients on the fin surface and examined a main and a subsidiary horseshoe vortex causing a substantial increase in total heat and mass transfer rates in front of the cylinders, whereas low heat and mass transfer coefficients in the wake region downstream of the cylinders. Authors suggested an optimal non-dimensional length between two-cylinder centers as 0.5, considering high heat transfer rates and minimum pressure drops.

Leu et al. (2004) performed numerical and experimental analysis so as to investigate the heat transfer rate and the flow structure in the plate-fin and tube heat exchangers with vortex generator mounted downstream the tubes. Using vortex generator can significantly improve the heat transfer performance but causes an

increase in pressure. They visualized the horseshoe vortex system using dye injection.

Akkoca (2004) presented detailed instantaneous and time-averaged flow and heat transfer data as well as structure of the horseshoe vortex system in the heat exchanger flow passage having different geometrical and operating parameters for Reynolds numbers in the range $500 \leq Re \leq 7500$ by using PIV technique and FLUENT finite volume code. The influence of the Reynolds number Re, on the size of horseshoe vortex is significant. In the laminar flow, the size of the horseshoe vortex and bed shear stress increase with increasing Reynolds number, on the other hand, in turbulent regime, opposite case happens.

Tutar and Akkoca (2004) studied numerically time evolution of horseshoe vortices in the circumference of the first and the second cylinders and local heat transfer coefficients on the plate surface in the heat exchanger flow passage. They reported that, in front of the tubes, the horseshoe vortex contributes to the heat transfer rate and in the wake of the tubes, a dead flow zone indicating poor heat transfer rate forms.

Hassan and Barsamian (2004) studied numerically on Large Eddy simulation (LES) of a three-dimensional tube bundle at Reynolds number of 21,700, based on the inlet velocity and the tube diameter. They compared their numerical predictions with available data. Their calculations were consistent with the experimental data and the flapping effect in the tube wake was captured. They concluded that the large Eddy simulation technique can be utilized as a tool in predicting the unsteady behavior of flow in some industrial applications. They explained Three definitive characteristics. First, the largest rotational structures in the flow occur in the tube wakes and are generated due to viscous forces. Second,there is a clear shedding of the vortices behind the tubes. Third, the rotating structures that separate because of the shedding are carried from the low velocity region into the high velocity region in a manner comparable to the shedding frequency from either side of a given tube. Their enhanced visualization of the shedding process through the vorticity magnitude for the same temporal profile is shown in Fig.2.4.

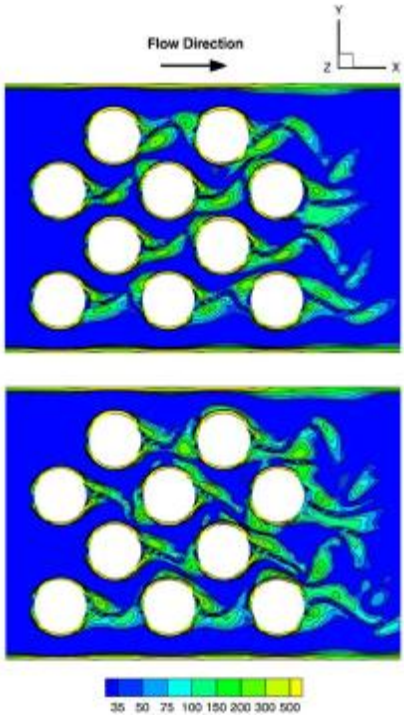

Figure 2.4. Vorticity magnitude at midplane for tube bundle (Hassan and Barsamian, 2004)

Xu and Zhou (2005) reported Heat and momentum transfer characteristics downstream of heated cylinders are also strongly affected by the interaction of wake flow structures

Sahin et al (2006) investigated the flow structure in a plate fin and tube heat exchanger model composed of single cylinder located between two parallel plates for duct height to the cylinder diameter ratio of 0.365 for Reynolds numbers of 4000 and 7500 experimentally by using PIV method. They showed that the structure of turbulent flow, size of wake flow region, position of the peak values of turbulence quantities such as concentration of vorticity, Reynolds stress are strongly effected by the variation of the Reynolds number. The presence of horseshoe vortex system in close region of the plate fin-circular cylinder junction magnifies the level of these flow characteristics. They also reported that the increase of heat, mass and momentum transfer are seen the presence of horseshoe vortex for Z=Fs/9 which is near to surface plate.

Sahin et al (2008) investigated the horseshoe vortex in a rectangular duct with a narrow gap which is designed to simulate a fin-tube heat exchanger containing a single circular cylinder for Reynolds numbers range of 1500 and 6150 experimentally by using the PIV method. They reported that although the plates are closely spaced, a horseshoe vortex system appears along both sides of the plate surfaces and these vortices magnify the entrainment process which occurs between the main flow and wake-flow regions that causes enhancing the heat transfer rate in fin-tube heat exchangers.

Ziada (2006) studied on the vorticity shedding excitation in tube bundles and its relation to the acoustic resonance mechanism experimentally. He explained that the natural vorticity shedding, which prevails before the onset of resonance, is not always the source exciting acoustic resonance, especially, in the case for in-line tube bundles. Therefore, separate "acoustic" Strouhal number charts must be used when appropriate to design against acoustic resonances. The resonant structure shown in Fig.5 can couple with a fluid resonance, which induces a particle velocity in the transverse direction. On the other hand, the vorticity-shedding excitation, As shown in this figure, the vortex pattern confined to a tube column is 180° out of phase with those confined to the neighboring columns. The resultant-flow excitation produced by this vortex pattern in the transverse direction is, therefore, practically zero. Since the flow instabilities causing the resonance and the vorticity-shedding excitation are basically different, it is logical to expect them to occur at different Strouhal numbers. This is compatible with the experimental observation that the acoustic resonance Strouhal numbers are different from the Strouhal number of vorticity shedding. These findings give support to the supposition that Strouhal numbers of vorticity shedding should not be determined from resonance cases.

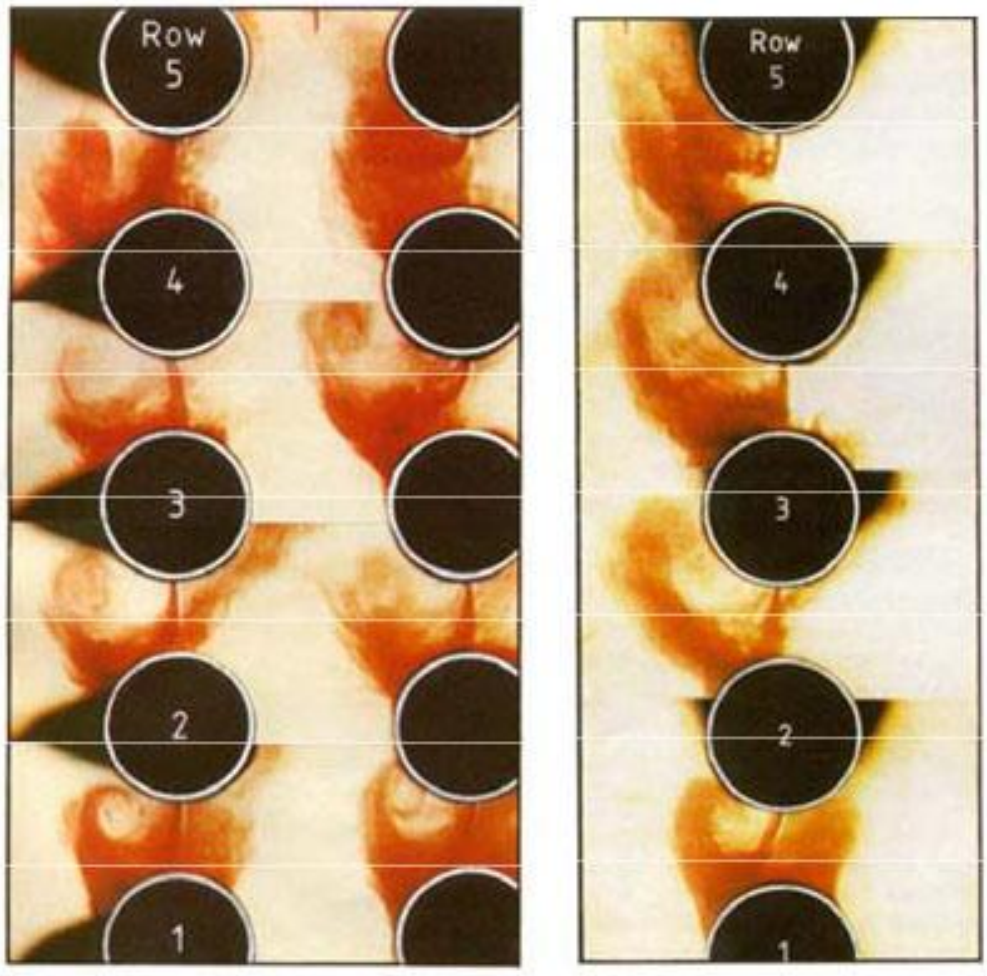

Figure 2.5. Overview of the resonant flow structure in the array at the same instant of time in a period of surface wave resonance. (Ziada, 2006)

2.2. Outline of Dissertation

It is concluded after examining the literature survey that, heat transfer efficiency around the cylinders in the heat exchanger flow passages is strongly related to the flow structure and hydrodynamics. It is well known that the most famous bluff body is the circular cylinder because of its industrial relevance. Studies of flow around circular cylinder provide most fundamental basics of fluid dynamics. Due to this reason, circular cylinder has attracted the attention of researcher most among the other bluff-bodies.

Therefore in the present study, firstly, qualitative flow visualization was employed during the initial scope of experiments in order to determine the overall flow patterns for a circular cylinder of 50 mm diameter, a circular slotted-cylinder of 50 mm diameter and 5 mm slot's width, multiple circular cylinders of 50 mm diameter and multiple circular slotted-cylinders of 50 mm diameter and 5 mm slot's width mounted over a flat plate and also located between two parallel plates.

Secondly in order to determine the instantaneous velocity fields around the surface mounted cylinders in the heat exchanger flow passages, high-image-density Particle Image Velocimetry (PIV) technique was employed. The use of PIV technique is very famous in modern fluid mechanics, because it helps to understand unsteady flow phenomena by scanning technique over a certain area of flow field. The Laser Doppler Velocity and hot wire velocity measuring devices can only measure once at a point. It is not possible to perform measurements at multiple points.

Both dye visualization and the PIV experiments were employed at Mechanical Engineering Department of Cukurova University, in the Fluid Dynamics Research Laboratory.

The interaction between primary, incoming, and counter-clock-wise rotating vortices and the trail of the horseshoe vortex formed in the upstream base of the cylinder are clearly identified with the time-averaged and the instantaneous flow data. It is shown that the position and the strength of the horseshoe vortex and the location of the saddle point formed upstream of it vary rapidly with an increase in

the Reynolds number. The secondary and the primary flow interactions in the upstream and downstream bases of the cylinder with the flat plate surface results in a three-dimensional and a complex flow behavior.

Introduction part introduces briefly the practical application and importance of the present work.

Literature survey part summarizes the modern research on vortex-bluff body interactions, physical aspects of vortical flow, and control of vortices.

Material and method part describes the details of the experimental system and measurement techniques. Specifically, the details of technological developments in Particle Image Velocimetry (PIV) and image processing used in the present study are given.

2.3. Objective and Scope of the Present Work

In this dissertation plain fin and circular slotted-cylinder configurations are investigated in terms of heat transfer and fluid flow characteristics

As it is outlined in the previous sections, the heat exchanger flow passage that consists of plain or specially configured parallel channels located on the outside of the tube bundle results in a very complex geometry. This complex geometry causes formation of a highly complex and three dimensional flow and heat transfer characteristics. Formation of horseshoe vortices in front of and at the rear the cylinders, interaction of secondary flows of opposite vorticity at the front and sides of the tubes, vortices in the wake of the fins; improved air mixing and thinning of boundary layers along with lateral swirl mixing due to the corrugated geometry formed by the wavy fins.

Due to the rate of population growth, the high rate of industrialization and development of countries, a quick increase of energy demands in the world is reality. Therefore, progress of technological development in heat exchanger systems must carry on. Because heat transfer rate in the heat exchangers is strongly related to the flow structure. Heat exchangers are one of the devices that can be developed further in the energy saving aspects. Thus in recent years, there have been significant

improvements in heat exchanger technology in order to rationalize the use of available energy and reduction of lost energy. The investigation of the flow through fin-tube heat exchanger has been and will continue to be a challenge to the sciences of thermal fluid mechanics in the future. Understanding of complex three-dimensional flow mechanisms around surface mounted cylinders is a subject of considerable interest in that the flow field is affected both from the presence of the cylinder and the flat plate. As far as we know, there is little study published in the literature demonstrating details of flow interactions around slotted-cylinders. So the details of the flow captured experimentally by the PIV technique and dye visualization around the single slotted-cylinder and multiple slotted-cylinders at different Reynolds numbers are carried out.

A deeper physical understanding of local flow structure in the heat exchanger flow passage is very important for design and optimization purposes. Therefore in the present study the physics of the flow and the horseshoe vortex mechanism are investigated in detail using time-averaged, instantaneous, and phase averaged flow statistics obtained by the Particle Image Velocimetry (PIV) technique.

The main purpose of this study is to gain insight into the mechanisms which are responsible for the performance of the heat exchangers. The dynamics of horizontal large-scale turbulent flow structure dominate the transverse exchange of momentum and heat. So, it can be stated that the present study also has the following main objectives;

I) Analyzing the structure of turbulent flow using data which consist of time series of two dimensional velocity components measured in some selected cross-sections at various elevations and in vertical planes. The turbulence intensities and transports are going to be investigated with the help or transverse and vertical profiles of Reynolds stresses.

II) Observation are focused in close region of cylinders-plate junctions in order to see the generation and behavior of the horseshoe vortex system and their effect on turbulence structure

III) Finally it is aimed to observe vortices how they stimulate the heat transfer rate through flow passages.

Qualitative flow visualization was employed during the initial scope of experiments in order to determine the overall nature of the complex flow patterns for different configurations of the heat exchanger.

The present study is extended to investigate the flow characteristics around of single and multiple slotted-cylinders located between two parallel plates. Numbers of circular tube were designed seven rows and seven column both in-line and staggered case. It is known that staggered tube arrangements are more efficient than in-lined tube arrangements. So, it is planned to examine the effect of various tube combination on the flow characteristics. The result of the present investigation is compared with the results available in the literature. Consequently, a final comment is made on the performances of the defined heat exchanger geometries in terms of flow characteristics.

3. MATERIAL AND METHOD

3.1. Particle Image Velocimetry (PIV)

Particle Image Velocimetry (PIV) is a non-intrusive measurement technique used to simultaneously determine the velocities at many points in a fluid flow. The technique involves seeding the flow field, illuminating the region under investigation and capturing two images of that region in rapid succession. From the displacement of the tracer particles, provided that the time interval between image captures is known, a velocity vector map can be calculated in the flow field.

3.2 Principles of PIV

The general principle of PIV is to illuminate tracer particles in the flow field of interest with a plane sheet of light, and acquire two images of the flow field with a known time separation. When a digital CCD camera is used for image acquisition, one uses the acronym DPIV. The displacement field is determined from the motion of the tracer particles between the two images, and by dividing this with the known time separation one obtains the velocity field. The problem in PIV is to determine the displacement field. The time separation is assumed to be known with sufficient accuracy. The technique of PIV can be considered as consisting of two stages; image acquisition and image evaluation.

3.3 Image Acquisition

Figure 3.1 shows a typical experimental arrangement for carrying out PIV measurements. Tracer particles added to flow under investigation are illuminated by laser sheet and images of the illuminated flow field are captured and stored for later analysis.

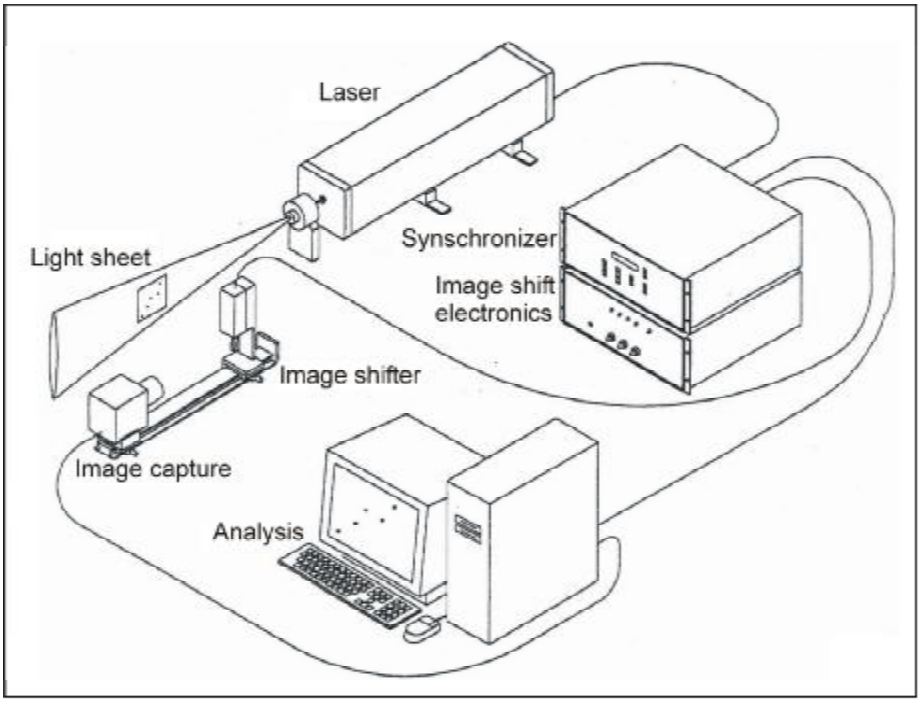

Figure 3.1. Schematic of experimental apparatus and digital PIV instrumentation

3.3.1 Seeding

Particle size and density, and fluid density and viscosity, determine the effects of buoyancy and inertia. Exact neutral buoyancy is difficult to achieve, but particles must remain suspended throughout an experiment. In general, seeding is easier in fluids. Lower velocities and accelerations combined with the higher density and viscosity of liquid means larger, more easily detectable images. In fluids, they may be up to tens of microns in diameter; in air diameters range from 5 microns to sub micron. For very large accelerations, such as in aero shock waves, particle lag cab can introduce gross errors and requires careful optimization with other requirements. The light scattered from the particles is only a fractions of the light introduced into the flow. Of this scattered light, only that within the solid angle defined by the lens aperture of the imaging system will be collected to form an image. Conventional PIV set-ups record side-scattered light, which can be orders of magnitude weaker than

forward-scattered light. The size and material of the seed particles can affect scattering efficiency and small particles also affect particle image intensity. The average particle image should exceed the fog level of photographic emulsions or the noise level of solid-state detectors. Seeding is, in general, easier in water than in air. Lower velocity and accelerations combined with the higher density and viscosity of liquid mean larger, more easily detectable particles can be used.

3.3.2 Ilumination

In PIV, the displacement field is determined as average displacements within so-called interrogation areas of the image plane. A typical size of these interrogation areas is 32x32 pixels, which means that one gets about 1000 vectors from an image with a resolution of 1008x1016 pixels. For single exposed images, the displacement is determined by forming the cross-correlation of corresponding interrogation areas in the first and second images. The location of the highest correlation peak in the correlation plane corresponds to the most likely average particle displacement in the interrogation area. Sub-pixel accuracy of the displacement is obtained by fitting a Gaussian distribution to the correlation peak, and finding the exact peak location. Since the cross-correlation method uses all information within the interrogation area for finding the displacement, the method is robust and often provides reasonable results even for non-ideal conditions. Another advantage is that the displacement field is obtained on a regular grid.

For the illumination, it is preferable to use a laser, since the laser beam is easy to form into a sheet by a cylindrical lens. A pulsed laser is preferred, since one obtains a high light energy during a very short time interval (typically 5 ns for a YAG-laser), which means that the particle images will be practically frozen even for high velocities (> 100 m/s). The repetition rate of a YAG-laser is typically 10-30 Hz, which is too low except for very low velocities (< 1 cm/s). One therefore needs two lasers to get full freedom in terms of time separation between the pulses. Special PIV YAG-lasers are available that combine two laser cavities with a common beam outlet.

3.3.3 Image Capturing

To be able to acquire two single exposed images with a time separation of the order of microseconds, one uses a so-called full-frame interline transfer progressive scan CCD camera, also called a cross-correlation CCD-camera. The basic idea is that the image exposed by the first laser pulse is transferred very rapidly to light-hidden areas on the CCD-chip. This is done on a pixel-by-pixel basis, i.e. each pixel has its own storage site in immediate vicinity of the light sensitive pixel area. After the second exposure, both images are transferred to the computer. Since a lot of data has to be transferred, it is only possible to take a few double-images per second. The temporal resolution of the flow is thus in general very poor with this technique.

A very important issue for obtaining accurate PIV measurements is appropriate seeding of the flow with tracer particles. To closely follow the flow the particles should be as small as possible, but on the other hand they may not be too small, because then very small particles will not scatter enough light, and hence produce too weak images.

3.4 Image Evaluation

Since the introduction of the first PIV image evaluation methods, alternative analysis algorithms have been developed as well as error correction and post-processing procedures designed to improve speed and accuracy of the PIV method. However, the classical PIV analysis method is still the most frequently used and forms the basis of many other algorithms. (Figure 3.2). The heart of the PIV analysis is the correlation of regions of the input images (known as interrogation areas) with each other to determine the displacement vector of the flow in that part. Knowing the time interval between the images captures enables a velocity vector to be calculated from the displacement vector. The correlation technique can be used for a single frame multiply exposed (auto-correlation) or multiple frames singly exposed (cross-correlation). To speed up the convolution process, correlation of each pair of interrogation areas is carried out in Fourier space. After interrogating the images in this way and generating the vector map, post-processing is carried out to validate the

data and to improve the vector map resolution and accuracy. Using this vector map, vorticity and Reynolds stress contours and streamline topology can be obtained.

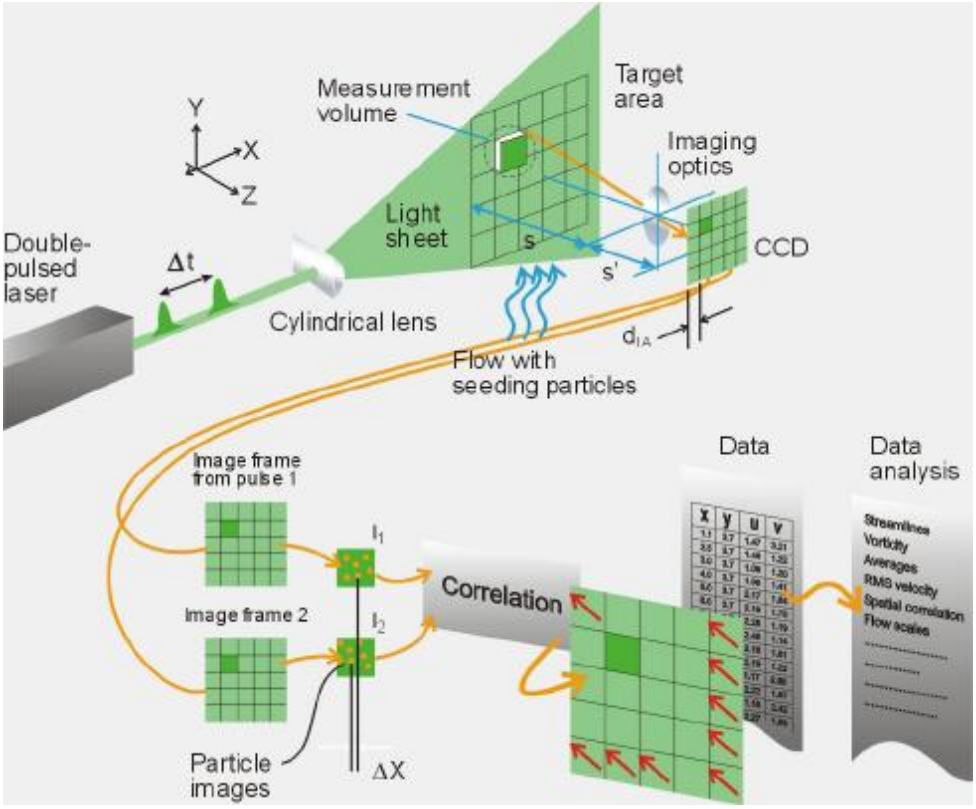

Figure 3.2. Basic PIV analysis process (Schiwietz, T., Westermann, R., 2004)

3.5. Time-Averaging of PIV Images

Time-averaging of PIV images were performed using following formulation. Time-averaged horizontal component of velocity:

$$\langle u \rangle = \frac{1}{N} \sum_{n=1}^{N} u_n(x, y) \tag{3.1}$$

Time-averaged transverse component of velocity:

$$\langle v \rangle = \frac{1}{N} \sum_{n=1}^{N} v_n(x, y) \tag{3.2}$$

Time-averaged vorticity:

$$\langle \omega \rangle = \frac{1}{N} \sum_{n=1}^{N} \omega_n(x, y) \tag{3.3}$$

Root-mean-square of u component fluctuation:

$$u_{rms} = \left\{ \frac{1}{N} \sum_{n=1}^{N} \left[u_n(x, y) - \langle u(x, y) \rangle \right]^2 \right\}^{1/2} \tag{3.4}$$

Root-mean-square of v component fluctuation:

$$v_{rms} = \left\{ \frac{1}{N} \sum_{n=1}^{N} \left[v_n(x, y) - \langle v(x, y) \rangle \right]^2 \right\}^{1/2} \tag{3.5}$$

Averaged value of Reynolds stress correlation:

$$\langle u'v' \rangle = \frac{1}{N} \sum_{n=1}^{N} \left[u_n(x, y) - \langle u(x, y) \rangle \right] \left[v_n(x, y) - \langle v(x, y) \rangle \right] \tag{3.6}$$

Where N is the total number of instantaneous images used for the time-averaged values and n refers to the instantaneous images.

3.6. Phase-Averaging of PIV Images

In addition to time-averaging, phase-averaging of images were pursued. The phase-reference to be employed depends on the type of experiment. In cases, where a periodic signal is recorded along with the PIV images, it is possible to employ this signal as phase-reference, provided that the timing of PIV images is known. In this study where such a signal is not available, it is necessary to make use of the PIV images themselves and search for characteristic motion representing the phase-oscillations.

The equations employed for phase-averaging are directly analogous to those employed for time-averaging, except the average was performed for the total number of M images at a given phase ϕ, as described in the foregoing.

Phase-averaged horizontal component of velocity:

$$\langle u \rangle_p = \frac{1}{M} \sum_{m=1}^{M} u_m(x, y) \tag{3.7}$$

Phase-averaged transverse component of velocity:

$$\langle v \rangle_p = \frac{1}{M} \sum_{m=1}^{M} v_m(x, y) \tag{3.8}$$

Phase-averaged transverse component of vorticity:

$$\langle \omega \rangle_p = \frac{1}{M} \sum_{m=1}^{M} \omega_m(x, y) \tag{3.9}$$

Where M is total number of instantaneous images used for the phase-averaged values and m refers to the instantaneous images.

3.7 Dye Visualization Experiments

A fluorescent dye which shines under laser sheet was used to create color change in water to visualize flow characteristics around the cylinders during the dye experiments. Dye was located in a small container which is located 500 mm above the free surface of the water channel. Dye was injected at the entrance of confined plate by plastic pipe and dye was passed through the confined plates. The video camera which was SONY HD-SR1 was used to capture the instantaneous video images of the vortex flow structures. The images were captured by frame grabber software of camera. The dye visualization technique gives no numerical information about flow structure of vortical flow, but demonstrates a brief and rough idea about flow structure around the cylinders

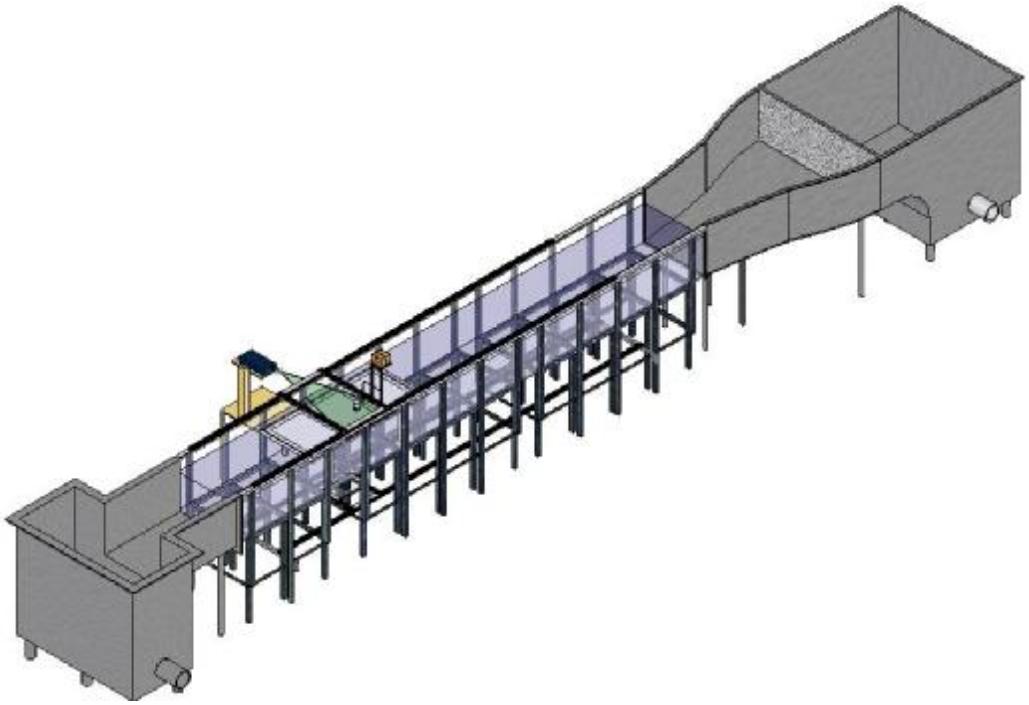

Figure 3.3. General view of Water Channel for dye visualization and the PIV Experiments (Akar, 2008)

3.8 PIV Experimental Setup

Experiments were performed in a large-scale water channel, having a test section length of 650 mm and width 750 mm. In order to study the case of a confined flow, the test section, which has a total height of 610 mm was filled with water. In order to characterize the flow structure downstream of single and multiple staggered slotted-cylinders, a technique of high-image-density particle image velocimetry was employed.

During the period of the experiment, images taken were indicated in the schematic of Figure 3.4.

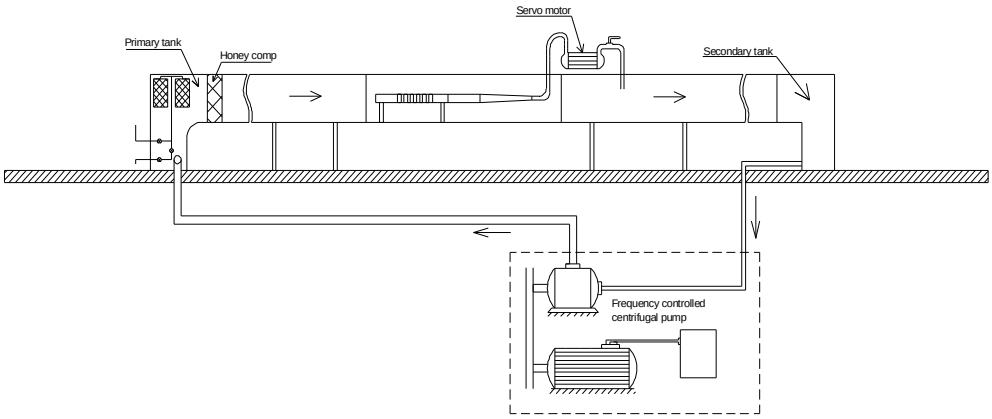

Figure 3.4. Schematics of channel and its mechanism

This approach is necessary in order to attain sufficient spatial resolution. Images acquired in each of these fields of view are averaged, and by splicing them together, it is possible to define this flow structure over a relatively long streamwise distance of the water flow. The experimental set-up of PIV system typically consists of several subsystems. In most applications tracer particles have to be added to the flow. These particles have to be illuminated in a plane of the flow at least twice within a short time interval. The light scattered by the particles has to be recorded

either on single or on a sequence of frames. The displacement of the particle images between the light pulses has to be determined through evaluation of the PIV recordings. In order to be able to handle the great amount of data which can be collected employing the PIV technique, sophisticated post-processing is required. Figure 1 briefly explains a typical set up for PIV recording. Small tracer particles are added to the flow. A plane (light sheet) within the flow is illuminated twice by means of a laser (the time delay between pulses depending on the mean flow velocity and the magnification at imaging). It is assumed that the tracer particles move with local velocity between the two illuminations. After development the photographical PIV recording is digitized by means of a scanner. The output of the CDD camera is stored in real time in the memory of a computer directly. As the resolution and image format of CDD camera is several orders of magnitude lower than that of a photographic medium, digitization cannot be ignored.

For evaluation, the digital PIV recording is divided in small sub-areas called interrogation areas (windows). The local displacement vector for the images of the tracers particle of the first and second illumination is determined for each interrogation area by means of methods. It is assumed that all particles within one interrogation area have moved homogenously between the two illuminations. The projection of the vector of the local velocity into the plane of the light sheet is calculated by taking into account the time delay between the two illuminations and the magnification at imaging.

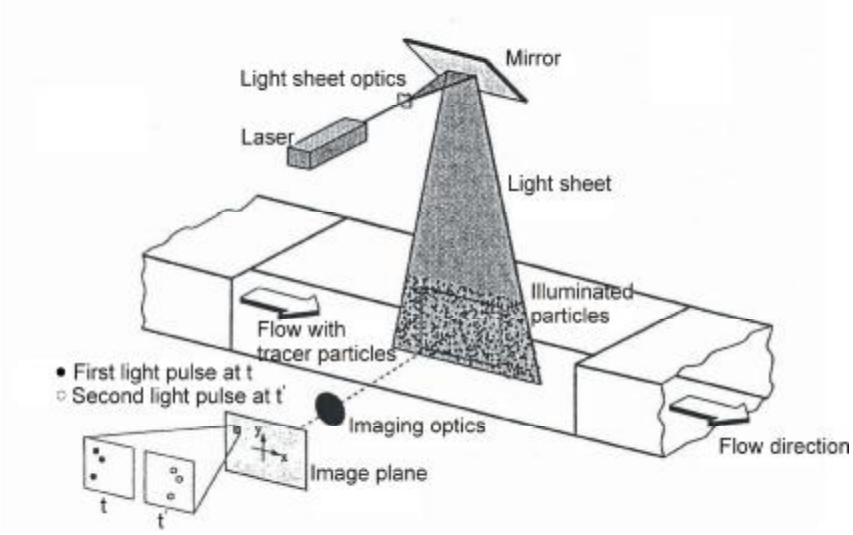

Figure 3.5. A typical experimental set-up for PIV technique is shown.

The process of interrogation is repeated for all interrogation areas of the PIV recording. With CDD cameras it is possible to capture more than 100 PIV recordings per minute. The evaluation of one camera PIV recording with 3600 instantaneous velocity vectors (depending on the size of the recording and of the interrogation area) is of order of a few seconds with standard computers. If even faster availability of the data is required for on line monitoring of the flow, dedicated hardware processors are commercially available which perform evaluations of similar quality within fractions of a second.

3.9. Examination of PIV on the Shear and Wake of Surface Mounted Cylinder

One of the most challenging problems in fluid mechanics is the measurement of the overall flow field properties, such as the velocity, vorticity and pressure. Hot-Wire and Laser Doppler velocimetry can only measure velocity at a single point. However as it is known, many flow fields such as coherent structures in shear flows or wake flows are highly unsteady. For these types of flow, it is required measuring whole flow field instantly in order to interpret these types of flow in detail.

In all test geometries the cylinders and the plates are made from Plexiglas material so that the laser light propagates easily. Before the image processing, all the spurious vectors are detected and removed using Cleanvec software and then the digital images were improved and smoothed by neighborhood averaging technique.

In this study three different geometries were taken and experiments have been carried out. These arrangements are single completed cylinder, single slotted-cylinder and multiple staggered slotted-cylinders in a narrow gaped rectangular duct respectively as seen figure 3.6, figure 3.7 and figure 3.8.

In the part of study, dye visualization and the PIV Technique have been used to determine the velocity field around the surface mounted cylinder in the passage having laser sheet height to water height ratio of 0.1. The cylinder is cutted in to 2 pieces with a 5 mm of whole cross-section slot and allows flow between semi-cylinders. Cylinder height is 20 mm and the diameter is 50 mm. The flow Reynolds numbers are Re_d=1500 and Re_d=4000 based on the cylinder diameter.

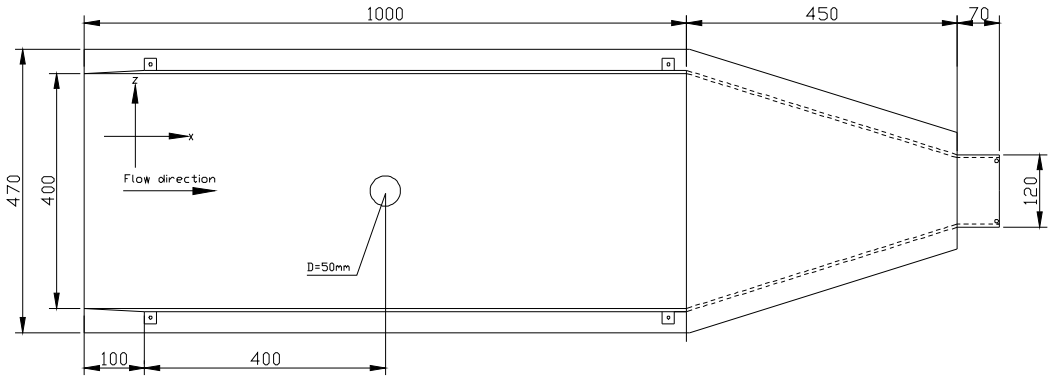

Figure 3.6. Test geometry of single cylinder in plan view plane (Dimensions in mm).

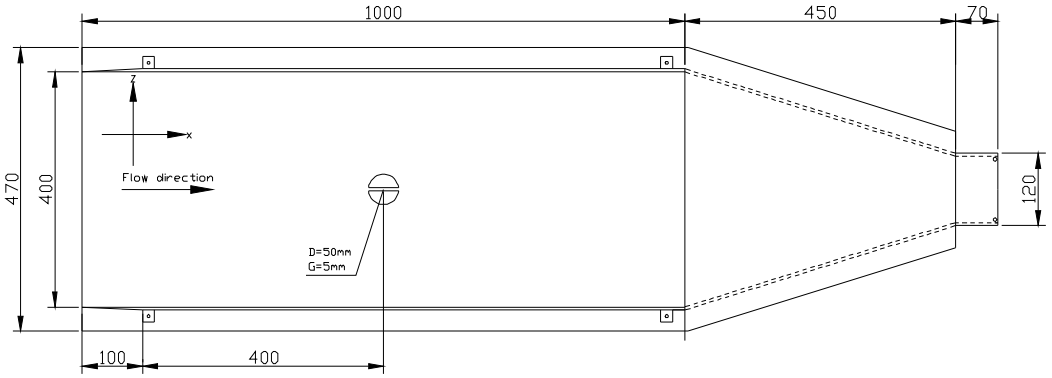

Figure 3.7. Test geometry of single slotted-cylinder in plan view plane (Dimensions in mm).

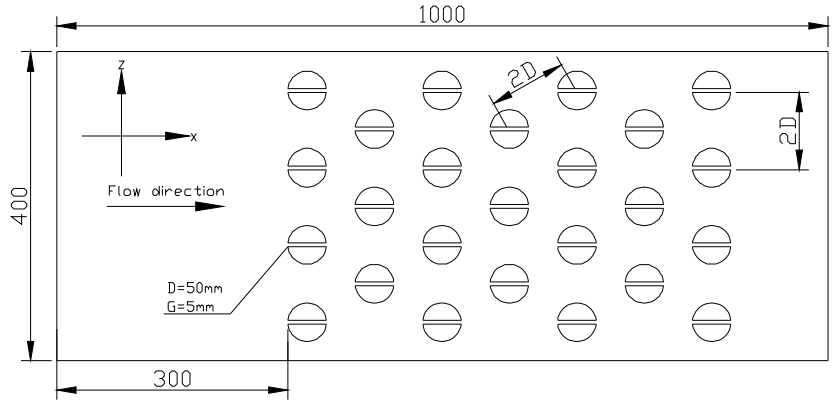

Figure 3.8. Test geometry of multiple staggered slotted-cylinders in plan view plane (Dimensions in mm).

4. RESULTS AND DISCUSSION

4.1. Experimental Study of Flow Details for a Single Cylinder and Slotted-Cylinder

4.1.1. Introduction

It is well known that, fin-tube heat exchangers which are similar to the rectangular duct geometry with narrow gap is mostly used in heat transfer devices.

A substantial energy demands in the world is due to the rate of population growth, the high rate of industrialization and social and economical development of countries. On the other hand, electricity generation used thermal power plants based on fossil fuels deteriorate the quality of environment in large scale. With this in mind, progress of technological development in heat exchanger systems must go on. Heat transfer problem in the heat exchangers is strongly related to the flow structure.

The flow characteristics past a cylinder exist in both practical life and engineering studies as they are frequently encountered in aircraft and automobile industries, heat exchangers, flow around bridge piers, building-ground junctions, etc. Therefore, in many engineering branches, such as in chemical, nuclear, coastal, marine, wind, hydraulics, and heat transfer engineering, this kind of flow configurations are investigated in order to produce information on the characteristics of juncture vortices occurred in the vicinity of circular cylinder in a confined flow. Furthermore, in this study, it is focused on investigating the flow characteristics around staggered slotted-cylinders which can be used in new design of fin-tube heat exchangers so as to get enhancement of heat transfer rate as a function of horseshoe vortex system

4.1.2. The Objective of the Present Work

In the case of flow passing bluff bodies, the flow is forced to separate and pass around the bluff body, the separation of the flow at the both sides of the body forms

wake vortices, and vortex shedding in the wake of the cylinder starts. Interactions between the cylinder wake, horseshoe vortex system, and the flat surface result a complex flow behavior. In order to understand that complex flow around the bluff body, the PIV technique is used and it is well known that PIV technique can give quantitative information on the instantaneous spatial structure of the velocity field. Therefore, in order to better understand the flow characteristics in the upstream and downstream regions of the single slotted-cylinder and multiple slotted-cylinders in the confined geometries flow, the PIV technique and dye visualization experiments are conducted to obtain instantaneous and time- averaged flow data in plan-view laser planes and the results are presented as shown in the following sections.

4.1.3. Test-Chamber Arrangement

The objective of the present work is to perform qualitative and quantitative flow studies in plan-view laser planes for a circular cylinder, a circular slotted-cylinder which are mounted on a bottom plate in the rectangular narrow gaped duct. for the purpose of revealing the structure of the flow details using instantaneous and time-averaged flow data. Plan-views of the test section, direction of the flow and the coordinate system are illustrated in Figures 4.1. and 4.2. The dimensions of the base plate are 1000mm x 400mm x 10mm. The diameter of the cylinder is d=50 mm, the width of the slot is 5 mm and the height (Gap) is h=20mm, respectively.

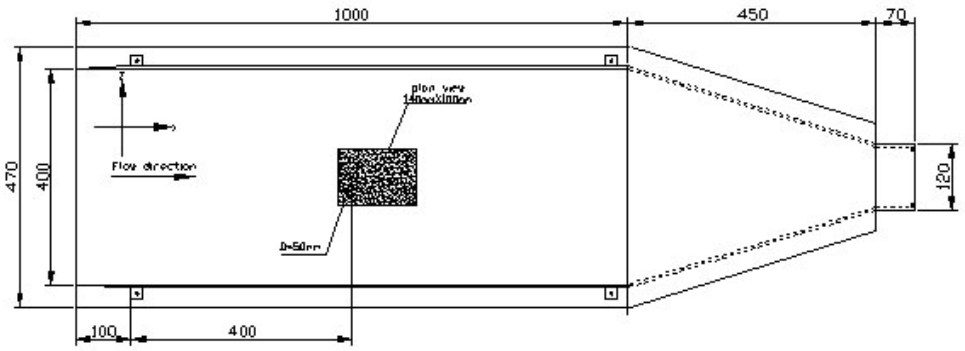

Figure 4.1. Test geometry, size of images, location of measuring planes in plan view plane (Dimansions in mm).

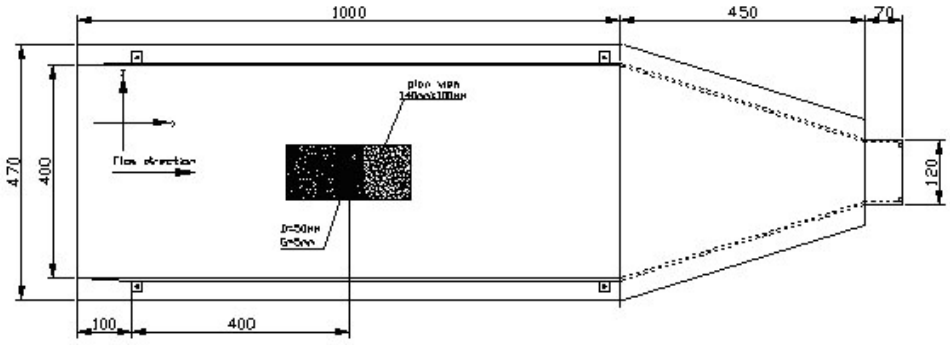

Figure 4.2. Test geometry, size of images, location of measuring planes in plan view plane (Dimensions in mm).

4.1.4 Dye Visualization of Flow Around A Single and Slotted-Cylinder

In figure 4.3 a well-seen saddle point occurs upstream of the cylinder surface. The region between the circumferential flow emanating from the saddle point and the surface of the cylinder involves upstream flow, which is associated with the horseshoe vortex in that region. Spiraling horseshoe vortex on both side of the

cylinder moves further downstream along the wake region. Almost a distance of one D starting from rear surface of the cylinder, between horseshoe vortices and shedding vortices interactions take place. These interactions increase the turbulence intensity of the flow to a higher level. The wake region downstream of the cylinder enlarges in the free-stream flow direction randomly. In other words, merging points of shedding vortices move forward and backward in the main flow direction. On the other hand horseshoe vortices on both sides of the cylinder wonder in the lateral direction giving rise the entrainment between wake flow and core flow regions. Along the shear layers Kelvin-Helmholtz vortices are developed predominantly. After merging of shear layers downstream of wake flow region Von Karman vortices occur.

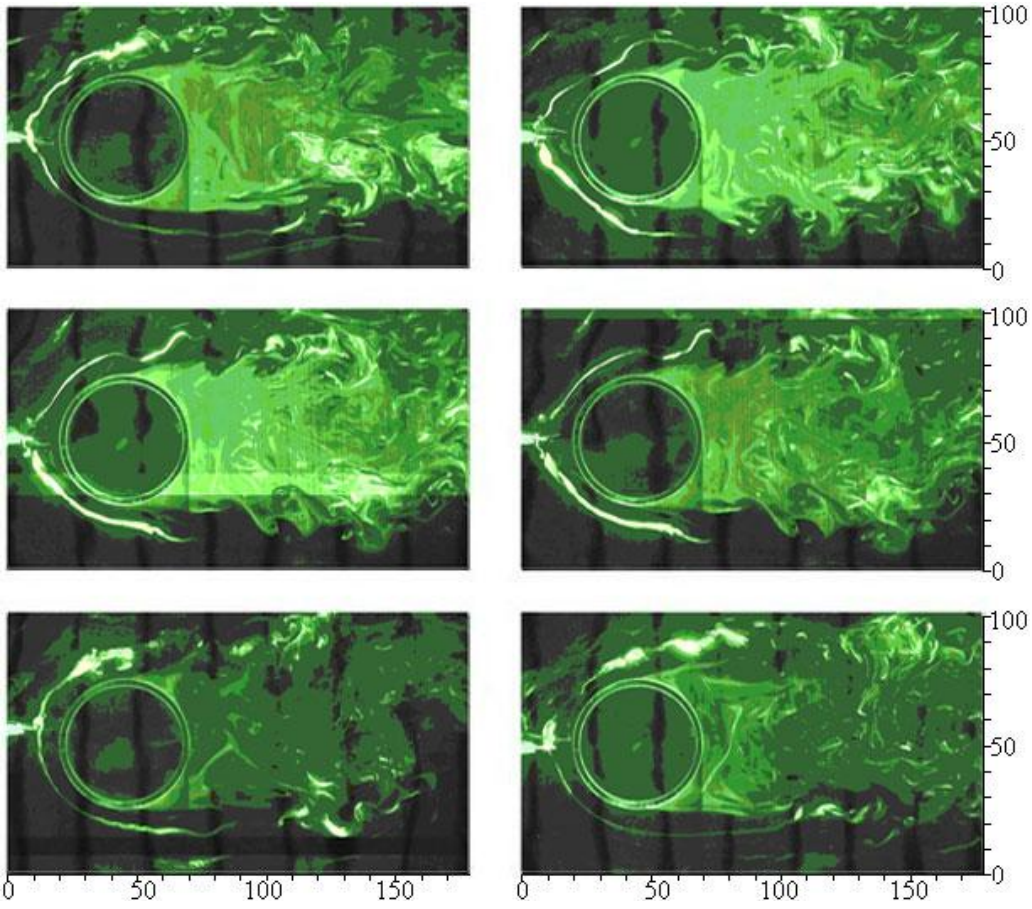

Figure 4.3. Instantaneous dye visualization of single cylinder for Re_d =1500, h_l/h_w=0.1

As can be seen in figure 4.4. a horseshoe vortex system which is developed in the forward face of the cylinder takes place closer to the forward face of the cylinder time to time having Reynolds number 4000 comparing the case of Reynolds number 1500. Because of increasing the Reynolds number from Re_d=1500 to Re_d=4000 this spiraling horseshoe vortices move in close region of the shedding vortices and hence interaction starts earlier between those two different types of vortices due to the high rate of momentum. It is clearly seen that the level of velocity fluctuations goes a higher level along the shear layers. This flow behavior stimulates mixing of main flow and wake flow. By increasing the rate of mixing fresh fluid and the fluid of wake flows enhance the rate of heat transfer to a certain level hydrodynamically. Outer regions of shedding vortices, Kelvin Helmholtz vortices are developed for all case at elevation of h_l/h_w=0.1 and both cases of Reynolds numbers. Starting from the merging point of shedding vortices which take place downstream of wake flow region a well defined Von Karman vortex street is developed. These flow behaviors happen for all cases of Reynolds numbers.

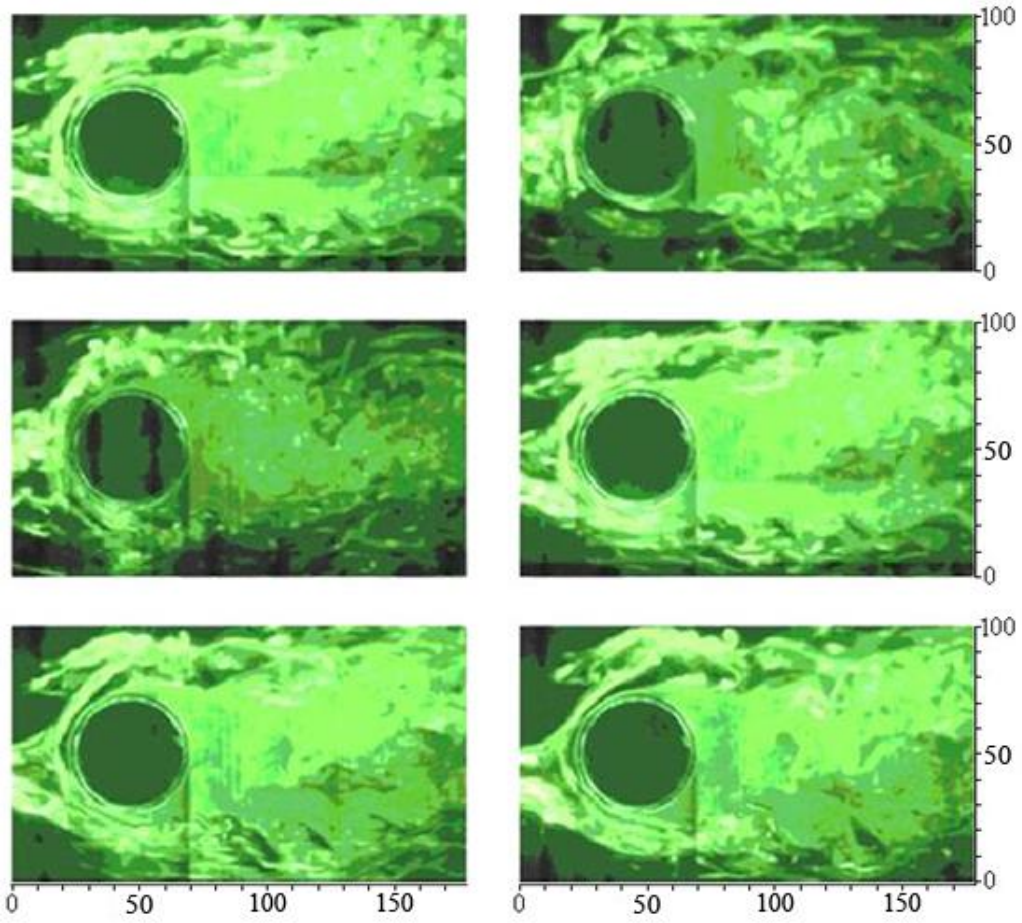

Figure 4.4. Instantaneous dye visualization of single cylinder for Re_d=4000, h_l/h_w=0.1

Patterns of time-averaged velocity, streamlines and vorticity at elevation of measuring planes of h_L/D=0.06 in deep water flow were established by Ozturk et al. (2009) for Reynolds number of Re_d=4000 based on the cylinder diameter and Re_h=87280 based on the hydraulic diameter of the open channel. They found that the approaching flow rolls up to generate horseshoe vortex system and wrap around the cylinder as seen in figure 4.5. Their instantaneous velocity vector map and streamline pattern indicate the presence of horseshoe vortex system as well as corresponding vorticity pattern, ω also indicates the occurrence of this horseshoe vortex system in the upper region of the cylinder.

With the primary vortex Nv_1, as illustrated in the last image of the third row of fig.4.5, three pairs of counter-clock-wise, Pv_1, Pv_2, Pv_3 and clock-wise Nv_1, Nv_2, Nv_3 rotating vortices grow rapidly. As time passes, the counter-clock-wise rotating vortices Pv_1, Pv_2 and Pv_3 grow in size, but decay in strength and later are washed away by the clock-wise rotating vortices Nv_1, Nv_2 and Nv_3 to allow for the formation of the primary vortex. A close examination of the time-averaged and the instantaneous vorticity contours reveal that along the upstream cylinder surface, counter-clock-wise rotating secondary type vortices occur. These vortices revolve vertically downwards along the cylinder surface toward the junction region.

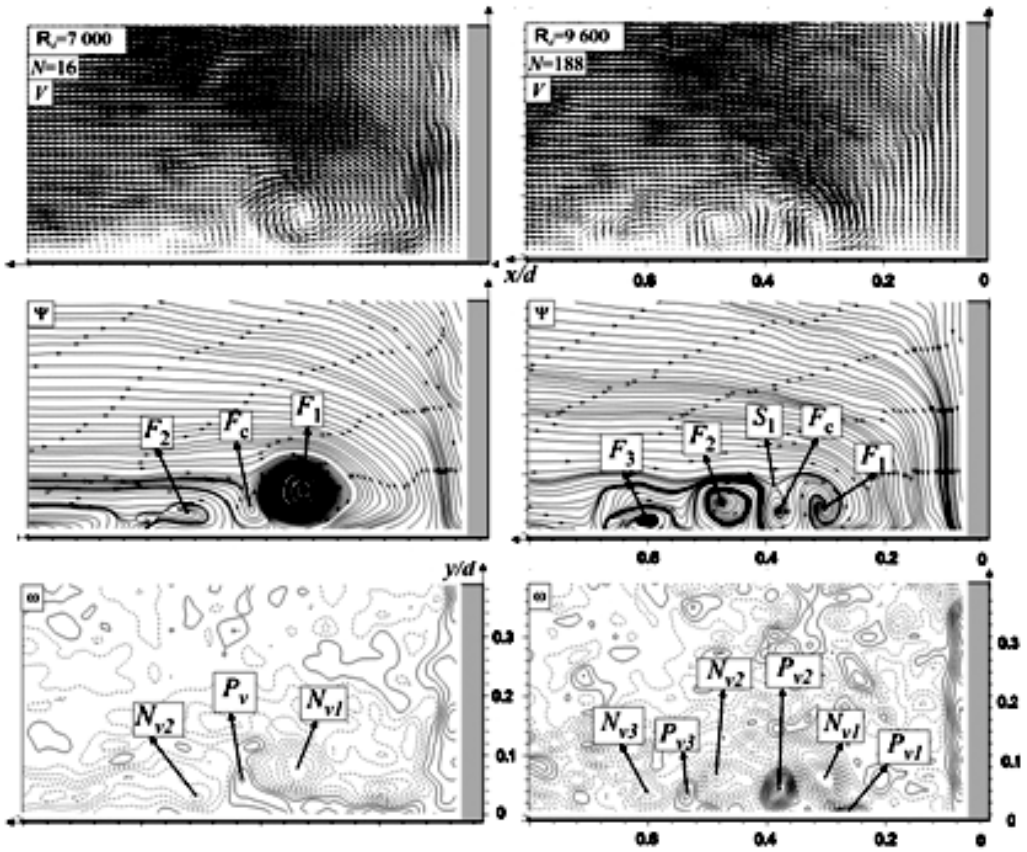

Figure 4.5 Instantaneous velocity vector map, V streamline patterns, ψ and vorticity contours, ω in the upstream base of the cylinder in side-view planes. Minimum and incremental values of vorticity are $\omega_{min}=\pm 3.5\ s^{-1}$ and $\Delta\omega=7s^{-1}$ (Ozturk et al, 2008)

Kirkil et al. (2005) stated that if the free stream flow is turbulent a wide range of turbulent scales are evident around the cylinder which controls the transport process. They reported that if the free stream flow is turbulent the location, size and intensity of vortices commonly known as horseshoe vortices are highly variable with time. Present dye visualization experiment also shows that these horseshoe vortices effect the turbulence structure in the upstream base of the cylinder when these vortices converted into 3D eddies. These horseshoe vortices are very sensitive to a flow parameters such as the height of the rectangular channel

In the work of Ozturk et al (2008) the patterns of streamlines reveals that there are three different saddle points, S and attachment of nodal points, N indicating the existence of three individual horseshoe vortices as seen in figure 4.6. They stated that through the observation of cinema of dye visualization in side view plane of their test geometry there were three different horseshoe vortices. These multiple horseshoe vortices in forward face of the cylinder merged to combine into one primary horseshoe vortex system in unsteady mode. In the present work, dye visualizations demonstrate that the side view images shown in figure 4.7 indicate that these vortices move backward and forward in the direction of the free stream flow. These vortices are often combines together to create a well defined horseshoe vortices. In last two images of figure 4.7 indicates two symmetrical primary vortices which are well defined. In the work of Ozturk et al. (2008), two identical developing large-scale swirling patterns of velocity vectors of approximately the same length, are observed close to the lower plate surface, and relatively wide and elongated primary swirls of velocity were detected close to the upper plate surface shown in figure 4.6. In order to demonstrate the capability of the horseshoe type vortices, the formation, development of these vortices in the side-view plane, upstream of the cylinder, are presented in this Fig. for Re_d = 4000. Studies of the instantaneous flow data shows that multiple vortices are formed in the vicinity of the upper and lower plates. Close to the lower plate, clock-wise rotating vortices occur and these are F, F_1, F_2 and F_3.

They reported that as soon as a half-node of attachment point, Na, appears focus F is formed which rolls up towards the plate-cylinder junction and gradually grows in size. It is worth mentioning that below each saddle point along the lower plate and

above each saddle point along the upper plate, counter-rotating secondary vortices, Vc interact with the developing and primary vortices. These secondary vortices, Vc prevent merging of developing vortices with the primary vortices temporarily as reported by Ozturk et al. (2008). Animation of their instantaneous flow data demonstrated that, as soon as these secondary or counter-rotating vortices, Vc disappear, the developing vortices combine with the primary vortices to form a large primary vortex which moves towards the plate-cylinder junction. The half-node of attachment point, Na on the lower plate surface is further away from the cylinder surface than the corresponding point, Na close to the upper plate. Both instantaneous velocity vector maps, V and corresponding streamline patterns, ψ clearly indicate that the size of the circulating flow region gradually increases as the flow moves towards the cylinder. In the present work the cinema of dye visualizations also reveal that the vortical flow structure is sometimes dominant along the lower plate, while sometimes dominant along the upper plate. In the present work as seen in figure 4.7 two identical developing large-scale vortices approximately the same size are observed close to the lower plate surface and close to the upper plate surface. These well-defined vortices rotate clockwise. Cinema of the dye visualization of the present work demonstrates same information as Ozturk et al (2008) obtained.

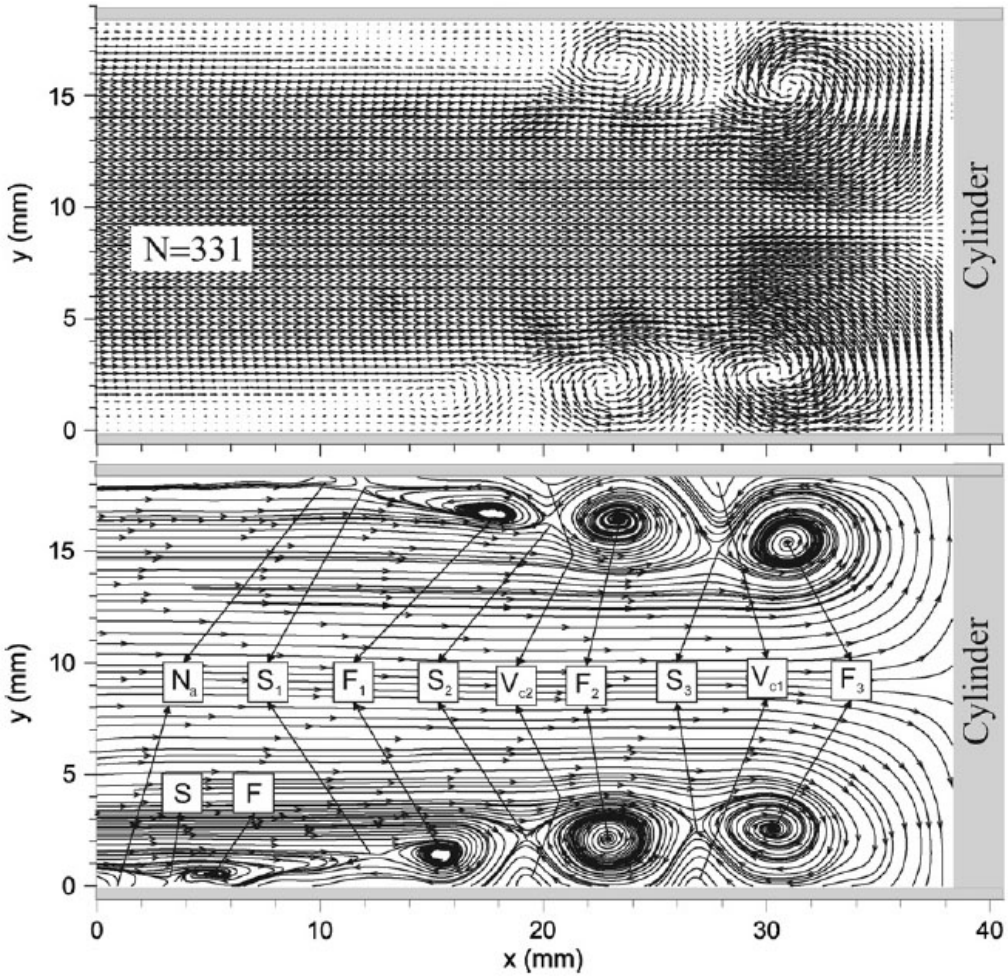

Figure 4.6. Instantaneous velocity vectors, V and streamlines patterns, ψ for Reynolds number Re_d=4000 (Ref. Ozturk et al. (2008)).

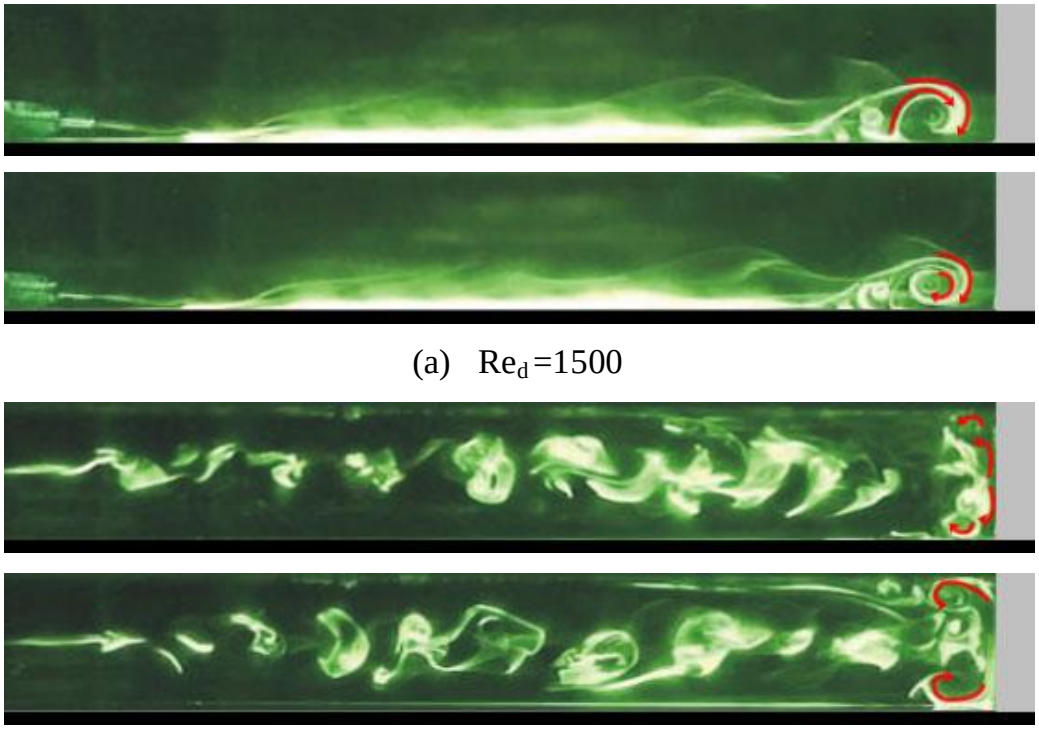

(a) Re_d =1500

(b) Re_d =4000

Figure 4.7. Instantaneous dye visualization in side-view in the upstream of the cylinder for Re_d = 1500 and 4000

The comparison of PIV results in figure 4.8 conducted by Ozturk et al (2008) a single cylinder mounted on the flat plate in deep water flow and dye visualization of the present work reveal that having slot at the center of the cylinder activates the wake flow region to the higher value. For example, as observed from cinema of the dye experiment a jet flow which is caused by slots goes through the center of the wake flow regions as seen in figure 4.9. This jet flow moves side to side in quasi periodic regime. This movement of jet flow increases the entrainment of the main flow across the shear layer. Again, this entrainment is expected to increase the rate of heat transfer in the cases of heat exchanger. Primary horseshoe vortex system moves further close to the slotted cylinder due to the suction of the flow by this slot and hence the level of interactions between horseshoe and shedding vortices increase. Because of this high level of interactions put the entrainment between main and wake flows to upper level.

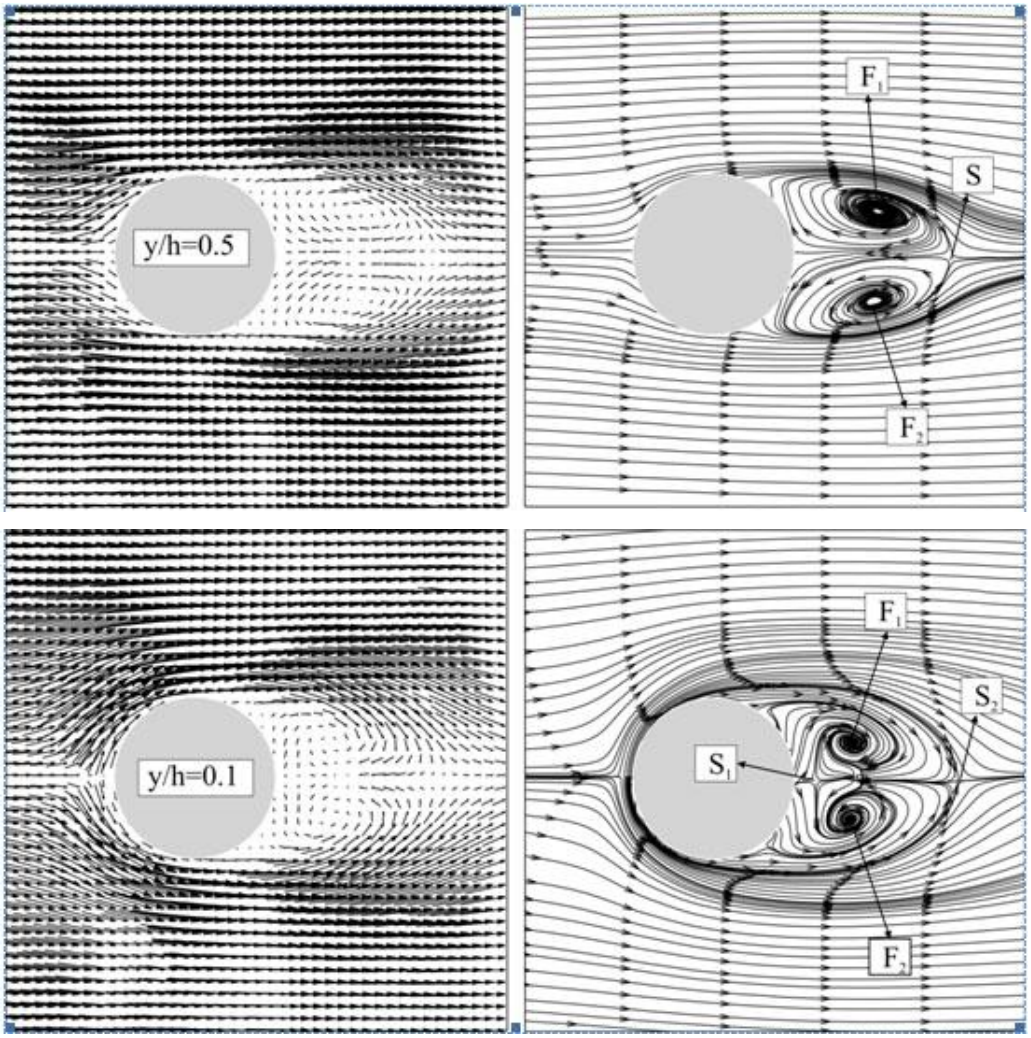

Figure 4.8. Patterns of time-averaged velocity, <V> and streamlines, <ψ> for Reynolds number Re_d=6150 (Ref. Ozturk et al. (2008)).

Examing figure 4.9 and 4.10 reveal that having 5 mm slot at central line of the circular cylinder vortical flow behavior around the slotted-cylinder is completely changed. For example, the saddle point in the upstream region of the slotted-cylinder move close to the forward face of the cylinder for both cases of Reynolds numbers. Furthermore, horseshoe vortices travels in the free stream flow direction close to the outer surface of the shedding vortices. Having flow jet through the slot a wake flow

region of the cylinder is further activated. As Fu (2004) stated that it is apparent that the base bleed through a slot can substantially retard the onset and development of large-scale vortical flow structures in the near-wake region, relative to those occurring from a complete cylinder. Confined flow past a cylinder gives rise to a horseshoe vortex about the upstream surface of the cylinder, and large-scale vortex formation occurs in the near-wake. Furthermore, existence of a negative base pressure on the downstream surface of the cylinder, in conjunction with time-averaged patterns of recirculation cells, are also well-known. The consequence of a streamwise slot through the cylinder is used to alter the patterns of the flow structure along the fore and base regions of the cylinder, as well as in its near-wake. Such alterations have important implications, not only for the steady and unsteady loading on the cylinder, but also the corresponding loading on the bed region about the cylinder. But, in the present study a slotted cylinder is placed in a narrow gaped rectangular channel. During the dye visualization it is seen that the horseshoe vortex that exists about the upstream surface of the complete cylinder or without a slot is altered significantly due to the flow extraction through a slot. Fu (2004) also stated that water flow jet available through the slot decreases the vertical gradient of circumferential vorticity along the plane of symmetry, in accordance with loss of the well-defined cluster of vorticity that represents the horseshoe vortex.

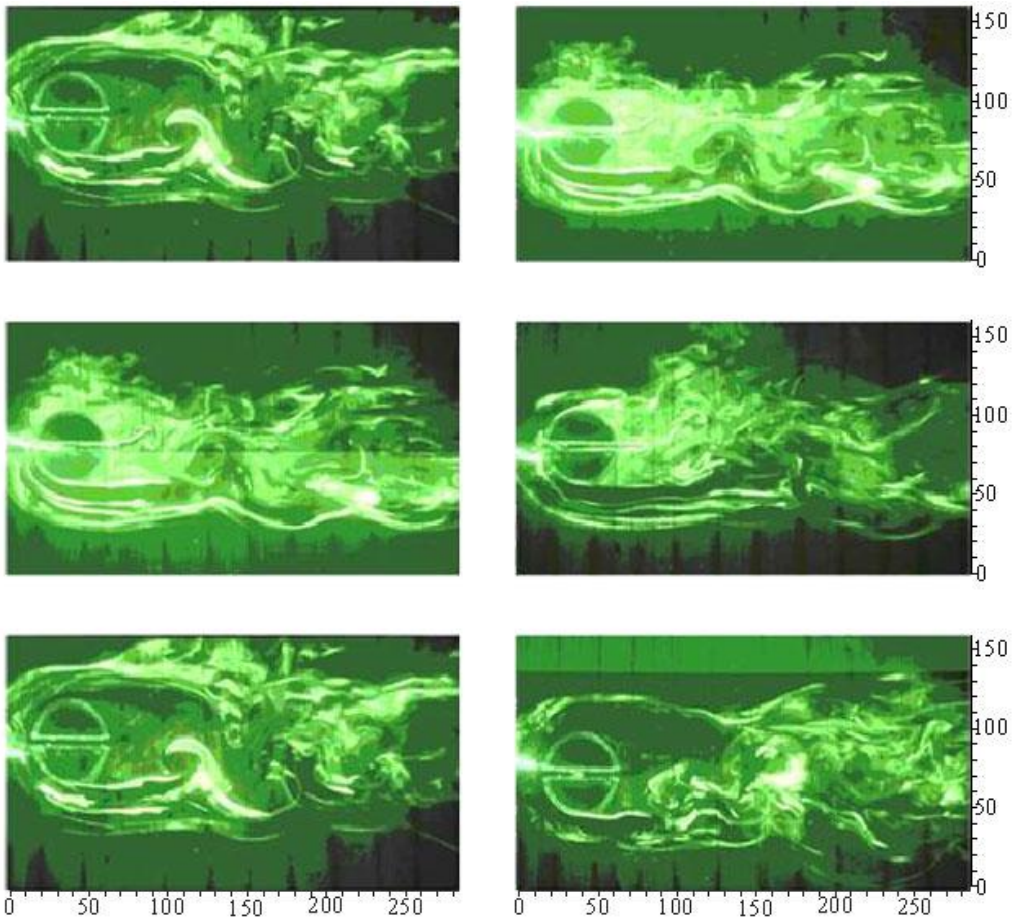

Figure 4.9. Instantaneous dye visualization of a single slotted-cylinder for Re_d =1500, h_l/h_w=0.1

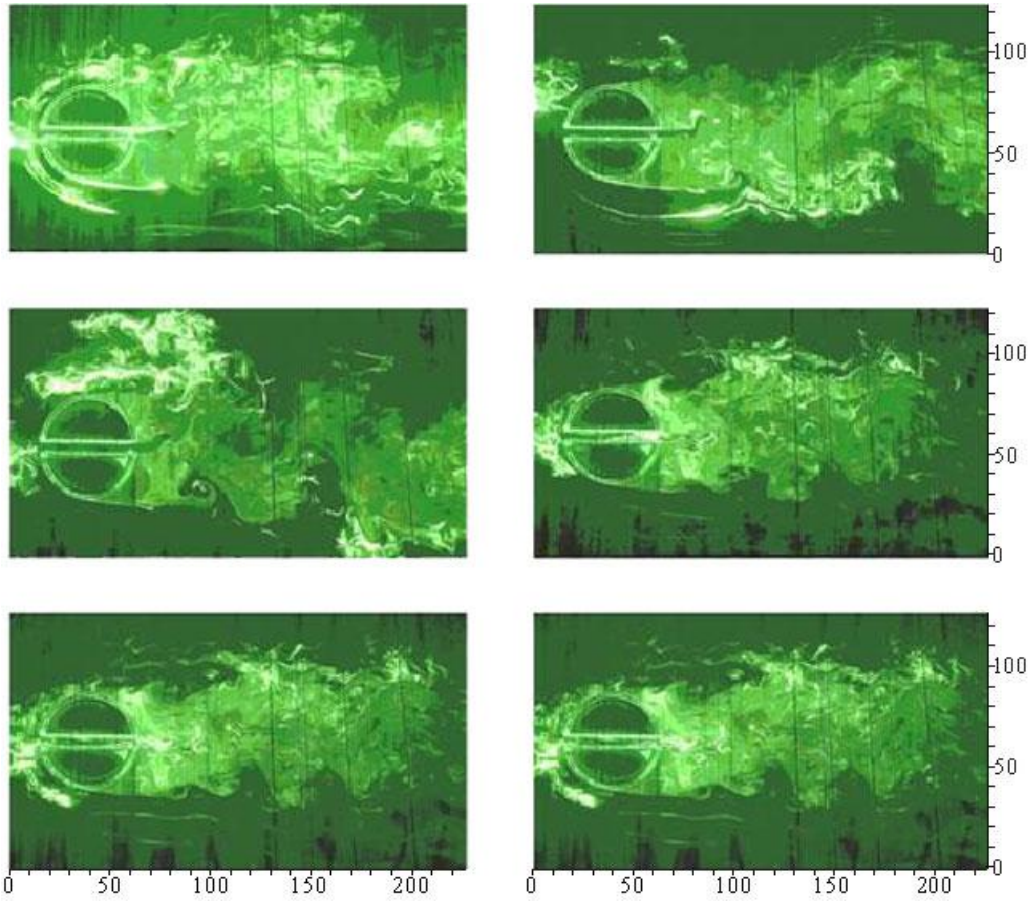

Figure 4.10. Dye visualization of a single slotted-cylinder for Re_d =4000, h_l/h_w=0.1

4.1.5. PIV Results of Single Cylinder and Single Slotted-Cylinder

Figure 4.11., shows the time-averaged velocity vector map at an elevation of h_l/h_w=0.1 above the base of the cylinder, for Re_d=1500 and Re_d=4000. The flow separation region is symmetric in both cases of Reynolds numbers. It is evident that, in the vicinity of the slot entrance, the magnitude of the velocity is small. On the other hand in the boundary layer around the cylinder, the magnitude of the velocity has a higher value.

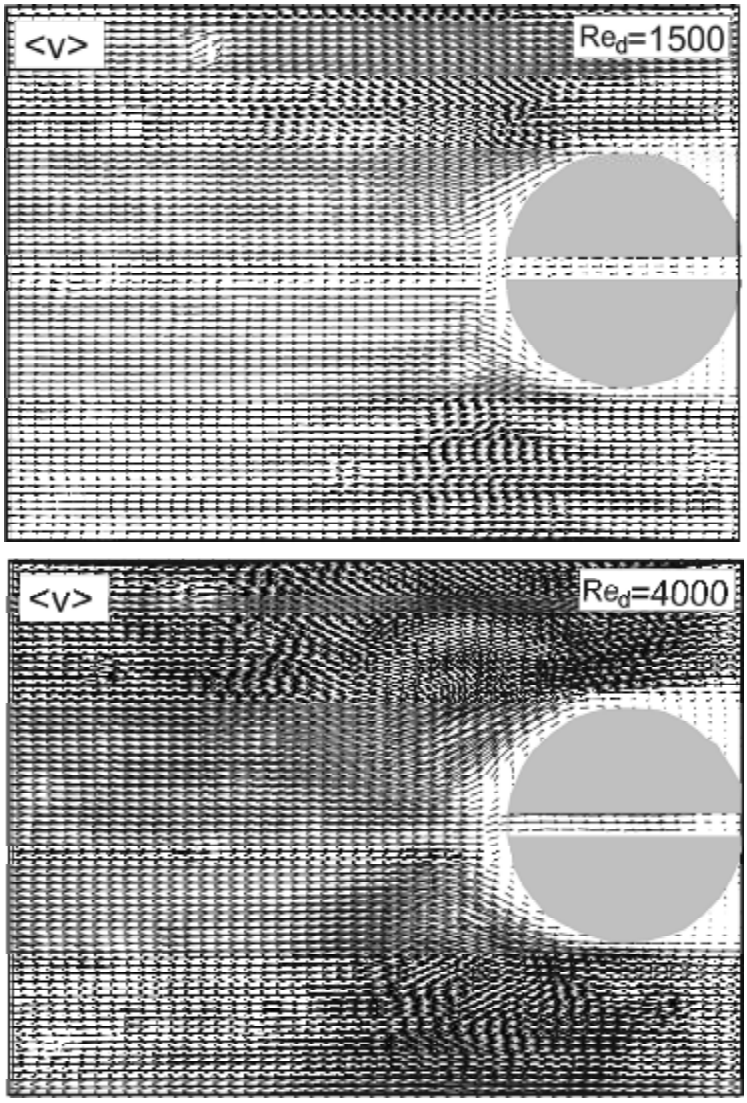

Figure 4.11. Time-averaged velocity vector map in the upstream region of single slotted- cylinder at elevation of h_l/h_w=0.1, for Re_d =1500 and 4000

The time-averaged vorticity contours <ω> in the upstream of single slotted-cylinder at an elevation of h_l/h_w=0.1 for Re_d =1500 and 4000 presented in figure 4.12. Time-averaged patterns of vorticity, <ω> illustrates that the horseshoe vortex which usually take place in the case of cylinder disappears in close region of the slot entrance, but the horseshoe vortices occur on both sides of the slotted-cylinder. A pair of negative and positive horseshoe vortices is developed next to the shedding

vortices for both cases of Reynolds numbers. It is also observed that the vorticity layers are symmetric with each other according to the plane of symmetry of the cylinder. It can be seen that the existence of horseshoe vortex system convecting downstream along the shear layers. The positive vorticity layers and the negative vorticity layers are drawn as solid and dashed lines, respectively. The minimum and the incremental values of the vorticity are $\omega=\pm 0.5 s^{-1}$ and $\Delta\omega=1 s^{-1}$, respectively.

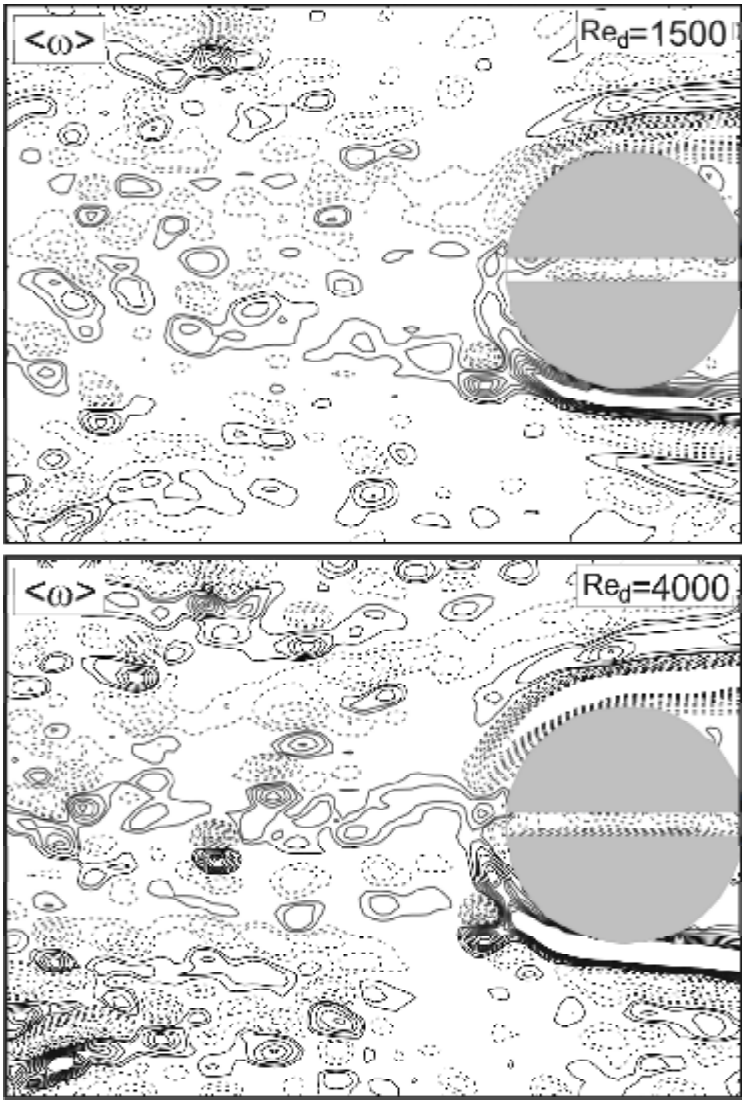

Figure 4.12. Time-averaged vorticity contours in the upstream region of single slotted-cylinder for $h_l/h_w=0.1$, Re_d =1500 and 4000. $\omega=\pm 0.5 s^{-1}$ and $\Delta\omega=1 s^{-1}$

Figure 4.13 presents <u/U> streamwise velocity distribution in the upstream region of the cylinder. The patterns of streamwise velocity indicates that the higher streamwise velocity occurs along outer region of the shear layers.

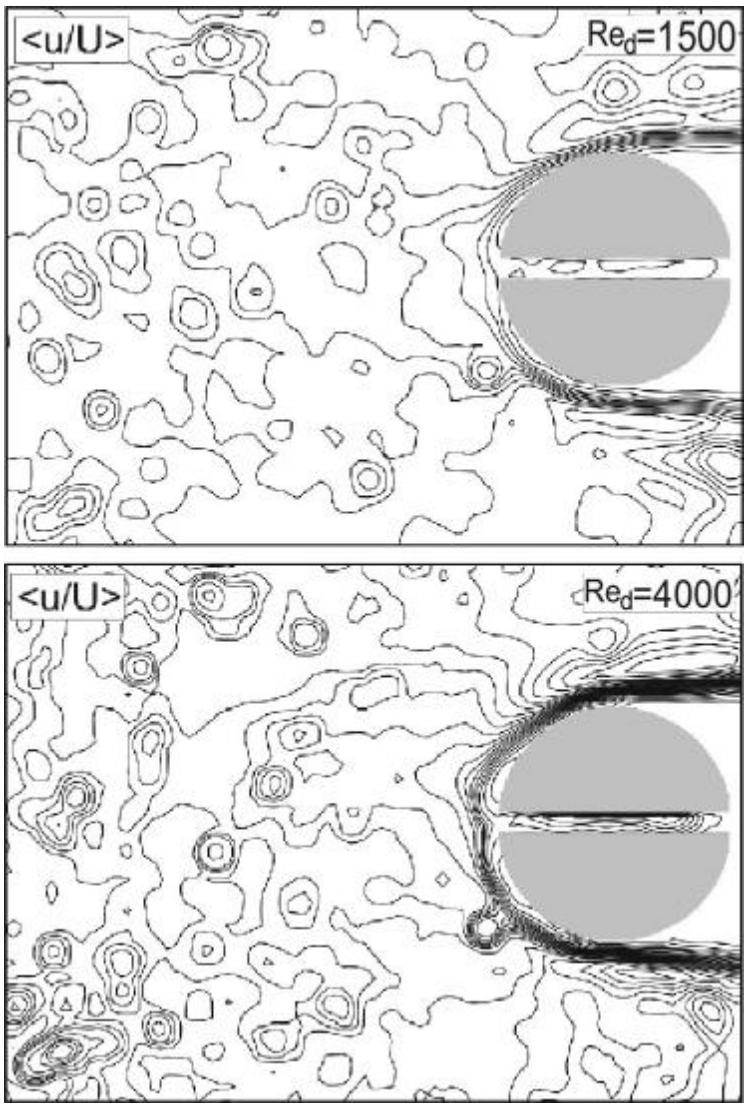

Figure 4.13. Streamwise velocity in the upstream region of single slotted-cylinder for h_l/h_w=0.1, Re_d =1500 and 4000

The root mean square of streamwise component, $<u_{rms}/U>$ normalized by a free stream velocity, U are presented in figure 4.14 for Reynolds numbers Re_d=1500 and Re_d=4000. For the purpose of comparison with the results of Sahin et al. (2009) who

performed similar work on the flow of a single cylinder in deep water flow the size of measuring images were intentionally taken the similar size with the work of Sahin et al. (2009). Relatively a low level of Reynolds stress $<u_{rms}/U>$ appear on the shoulder of the slotted-cylinder comparing to the results of Sahin at al. (2009). This situation may happen due to the suction of the flow through the slot. In other words, the horseshoe vortex may not as strong as in case of single cylinder without slot.

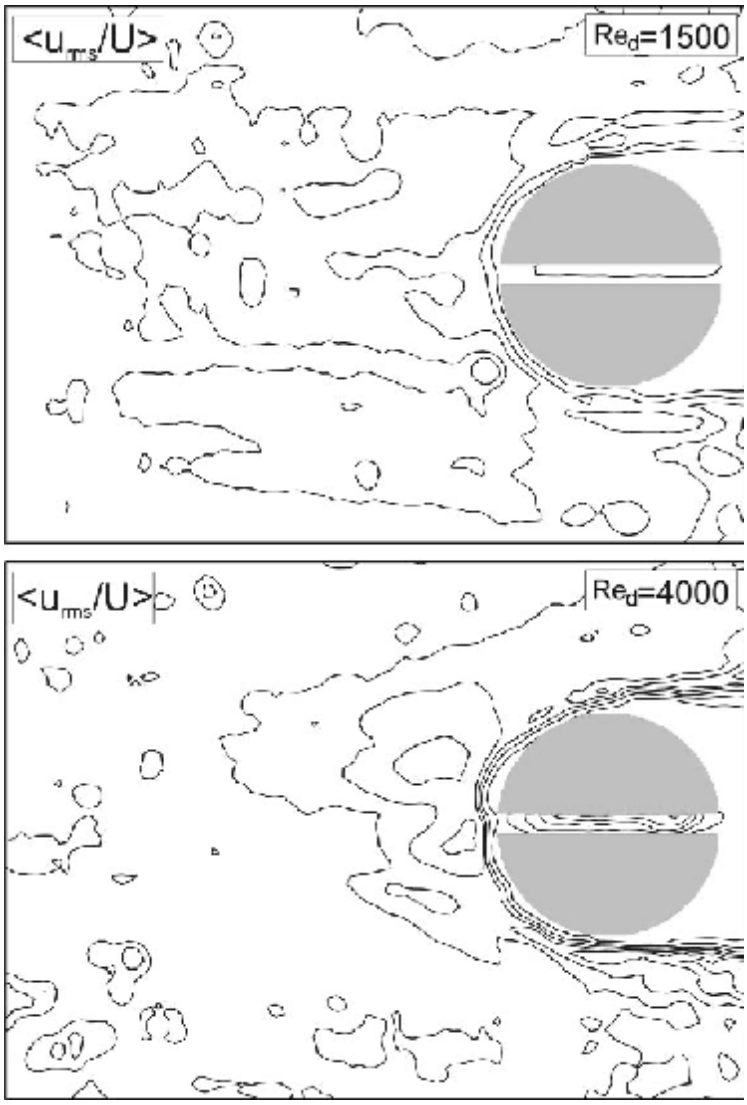

Figure 4.14. u_{rms} value in the upstream region of single slotted-cylinder for h_l/h_w=0.1, Re_d =1500 and 4000

Figure 4.15, shows the time-averaged velocity vector map of wake flow at elevation of h_l/h_w=0.1 above the base of the cylinder, for Re_d=1500 and Re_d=4000. Regarding the exit region of the slot, patterns of velocity vectors show the transformation from the slot flow to the free jet. The influence of the jet from the slot on the flow in the base region becomes apparent, as it induces two recirculation cells. The size of the wake region is obtained wider and two symmetric vortices rotating in opposite direction are clearly seen in both cases of Re_d =1500 and 4000. It seems that velocity vectors in the exit region of the slot is higher comparing to the case of a single cylinder without slot. This flow behavior can increase the heat transfer rate hydrodynamically.

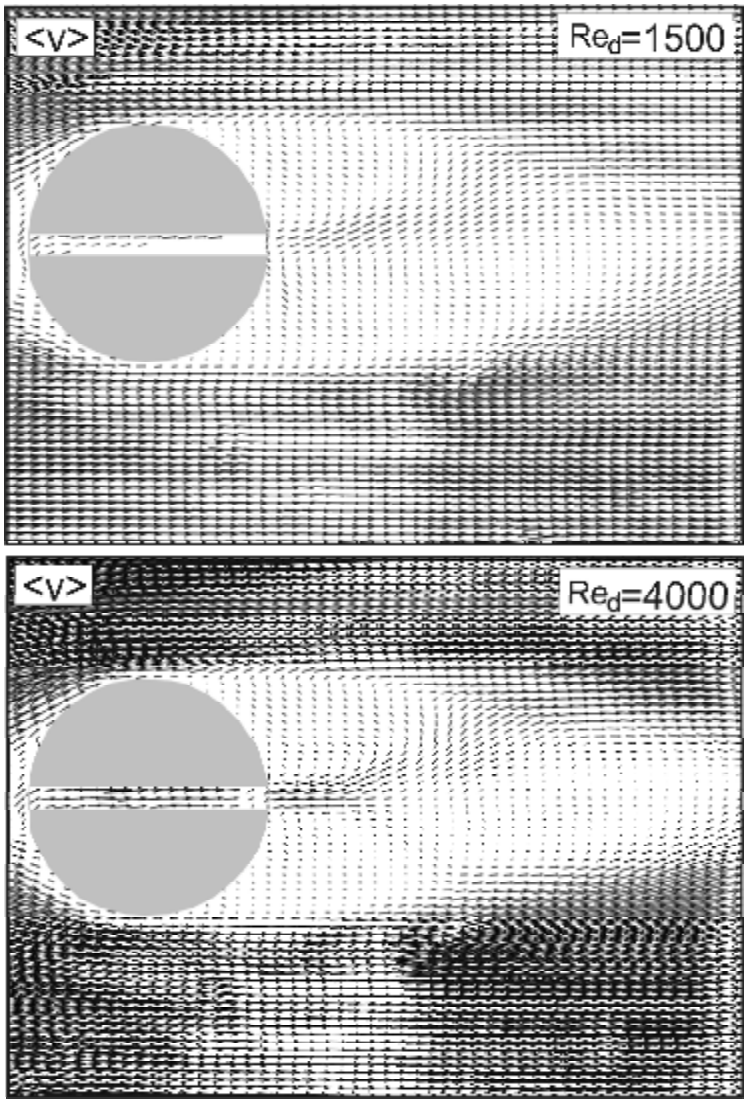

Figure 4.15. Time-averaged velocity vector map, <V> in wake flow of single slotted-cylinder for h_l/h_w=0.1, Re_d =1500 and 4000

Figure 4.16 demonstrates the time-averaged vorticity contours, <ω> at elevation of h_l/h_w=0.1 above the base of the cylinder, at Re_d =1500 and 4000. Regarding the exit region of the slot, patterns of time-averaged vorticity show the transformation from the slot flow to the free jet. It is clearly seen that the vorticity layers beginning from the slot entrance are convecting in the flow direction in the shear layer. It is observed that the vorticity layers are symmetric with each other

according to the plane of symmetry of the cylinder. Vorticity contours are seen nearly parallel with only mild deflections towards the wake centerline. A pair of vortices is developed at the wake region due to the jet flow emanating from the slot. Well defined shedding vortices along the shear layer moves further downstream in the free-stream flow direction a companying with horseshoe vortices.

The positive and negative vorticity layers diverge substantially and, in fact, tend to interact with the clusters of vorticity of the separating layers from the base of the cylinder. The positive vorticity layers and the negative vorticity layers are drawn as solid and dashed lines, respectively. The minimum and the incremental values of the vorticity are $\omega_{min}=\pm 0.5\ s^{-1}$ and $\Delta\omega=1\ s^{-1}$, respectively. Animation of instantaneous vorticity patterns demonstrates that horseshoe vortices along the shear layer moves in lateral direction in randomly. A well defined positive and negative cluster of vortices occur at exit of the slot. It prevails that the jet flow emanating from the slot activates the wake flow region.

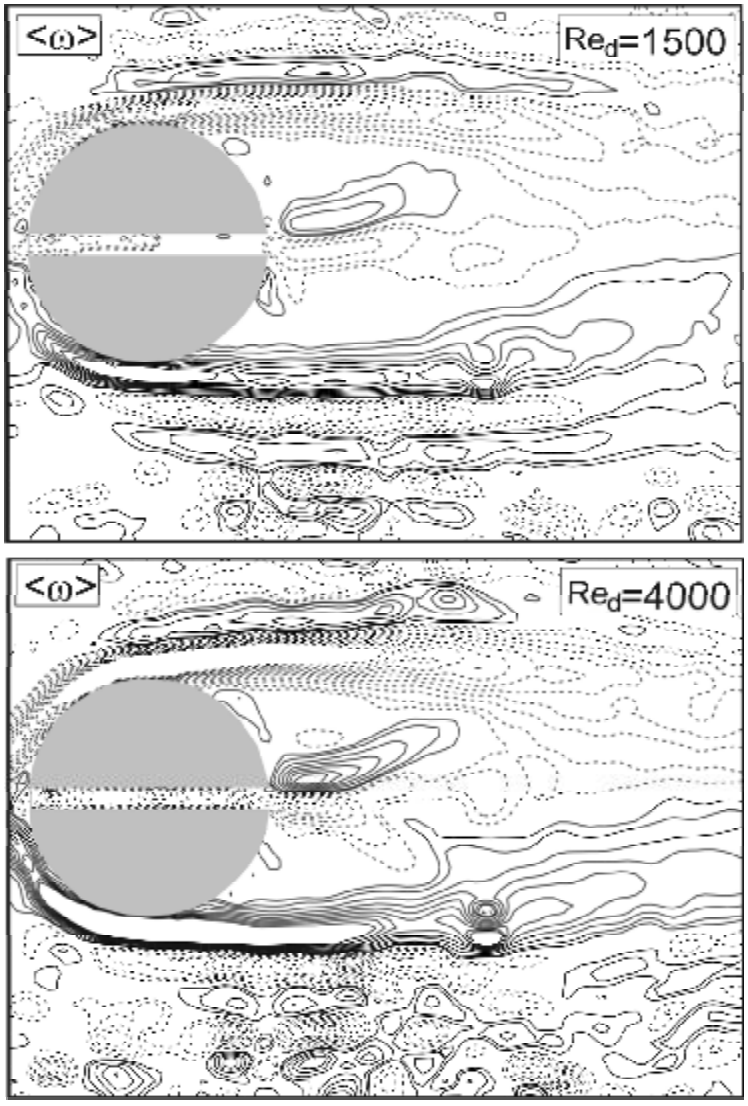

Figure 4.16. Time-averaged vorticity contours, <ω> in wake flow of single slotted-cylinder for h_l/h_w=0.1, Re_d =1500 and 4000, $\omega_{min}=\pm 0.5\ s^{-1}$ and $\Delta\omega=1\ s^{-1}$

4.1.6. Reynolds Stress Correlations for Both Cases of Single Cylinders

The images of Figure 4.17 show contours of constant Reynolds stress $<u'v'/U^2>$ in the near-wake region at an elevation of $h_l/h_w=0.1$ as seen that the peak values of Reynolds stress correlations, $<u'v'/U^2>$ are evident, regarding magnitudes of the Reynolds stresses at the bed. It is obvious that the unsteadiness associated with the developing jet emanating from the slot does not locally enhance the Reynolds stresses for $Re_d=1500$. On the other hand, it is evident that for $Re_d=4000$, momentum of the jet flow has a significantly large magnitude and therefore locally higher values of $<u'v'/U^2>$ are attainable in the region of jet formation. On the shoulder of the cylinder a small size cluster of the Reynolds stress correlations occur for the case of Reynolds numbers $Re_d=4000$ due to the existence of horseshoe vortices around the slotted-cylinder. However, the peak values of Reynolds stress correlation, $<u'v'/U^2>$ occur along the shear layer. In addition, jet flows emanating from the slot of the cylinder cause positive and negative clusters of Reynolds stress correlations $<u'v'/U^2>$ at a location a distance of a half diameter far from the rear surface of the cylinder in the downstream region. Similar experimental analysis was performed by Ozturk et al. (2009) without slot. Ozturk et al. (2009) have conducted experiment using the single cylinder placed on the ground in deep water flow in order to study the interaction of horseshoe vortices and shedding vortices having ground effect also. They concluded that minimum value of Reynolds stress correlations $<u'v'/U^2>$ for the case of elevation $h_L/D=0.06$ is developed comparing to higher elevation. He also stated that although a low level of Reynolds stress correlations $<u'v'/U^2>$ occur in the case of elevation, $h_L/D=0.06$, but it occupies a wider area comparing to the higher elevations in deep water flow cases.

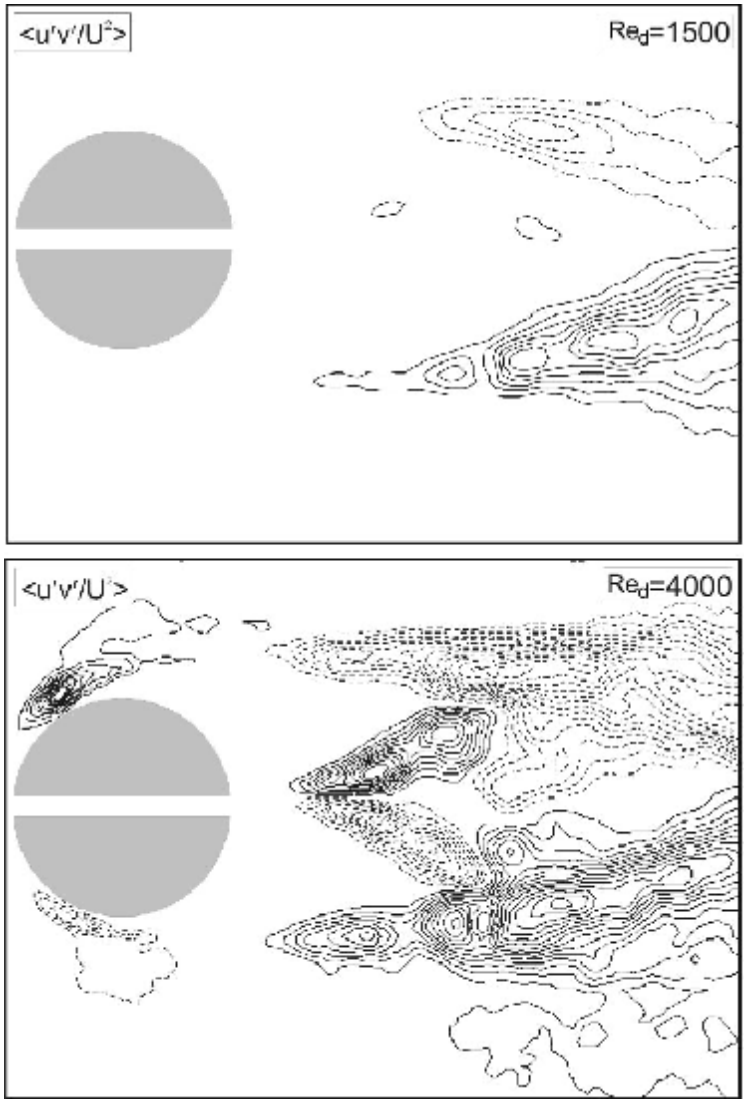

Figure 4.17. Time-averaged Contours of Reynolds stress correlations, $\langle u'v'/U^2 \rangle$ minimum and incremental values of Reynold stress correlation are $\langle u'v'/U^2 \rangle_{min} = \pm 0.005$ and $\Delta \langle u'v'/U^2 \rangle = 0.005$

Sahin and Ozturk (2009) conducted an experimental work on the behaviour of flow at the junction of the cylinder and base plate in deep water. They reported that the patterns of the time- averaged normalized streamwise velocity, $\langle u/U \rangle$ component for Re_d=1500 and 9600, the negative pockets of streamwise velocity component, u/U appears. But in the present case these negative pockets of streamwise velocity are

avoided by the water jet flow emanating from the slot which passes through the central axis of the cylinder as seen in figure 4.18

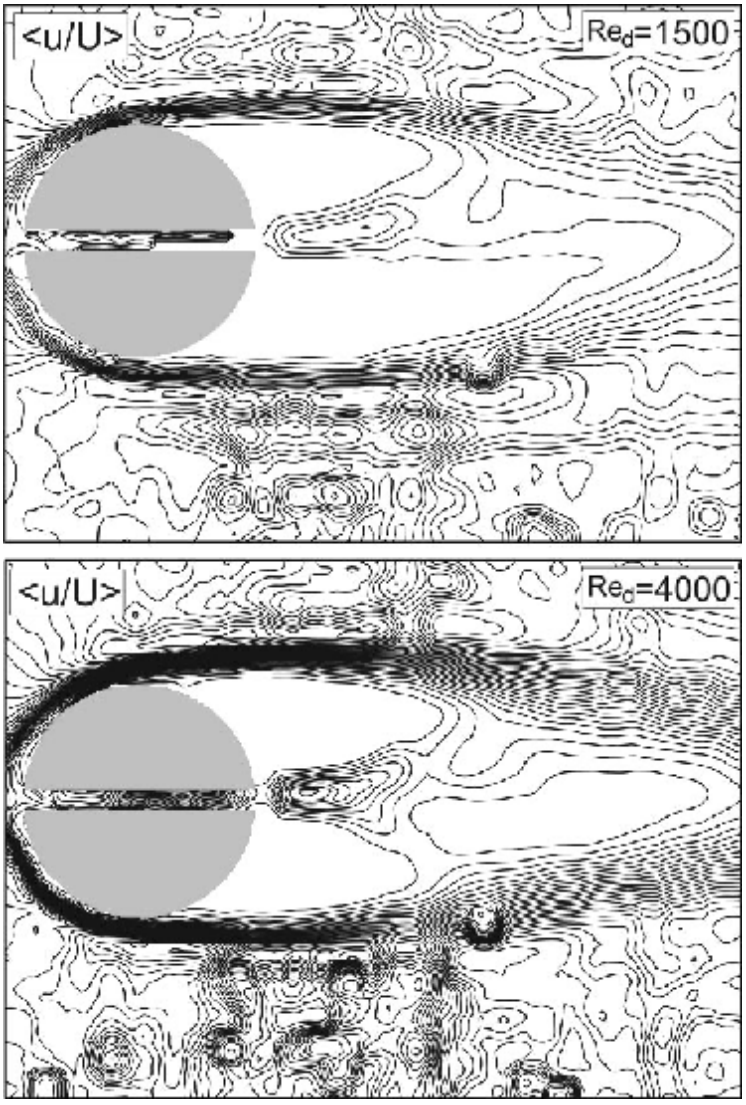

Figure 4.18. Time-averaged streamwise velocity around a single slotted-cylinder for h_l/h_w=0.1, Re_d =1500 and 4000, $\langle u/U \rangle_{min}$ =±1 and Δ $\langle u/U \rangle$ = 3

Figure 4.19 presents the distributions of the root mean square of streamwise velocity fluctuations, $\langle u_{rms}/U \rangle$ at an elevation of h_l/h_w=0.1 for Reynolds numbers of

Re_d =1500 and 4000. Higher values of fluctuations are developed along the shear layers and along the central axis of the slot due to the jet leaving the slot and moving in the direction of the free-stream velocity for both cases of Reynolds numbers. The flow with a high rate of velocity fluctuations occupies a larger region in the downstream direction comparing to the work of Sahin and Ozturk (2009). It is supposed that the water jet flow can cause velocity fluctuations further in downstream direction.

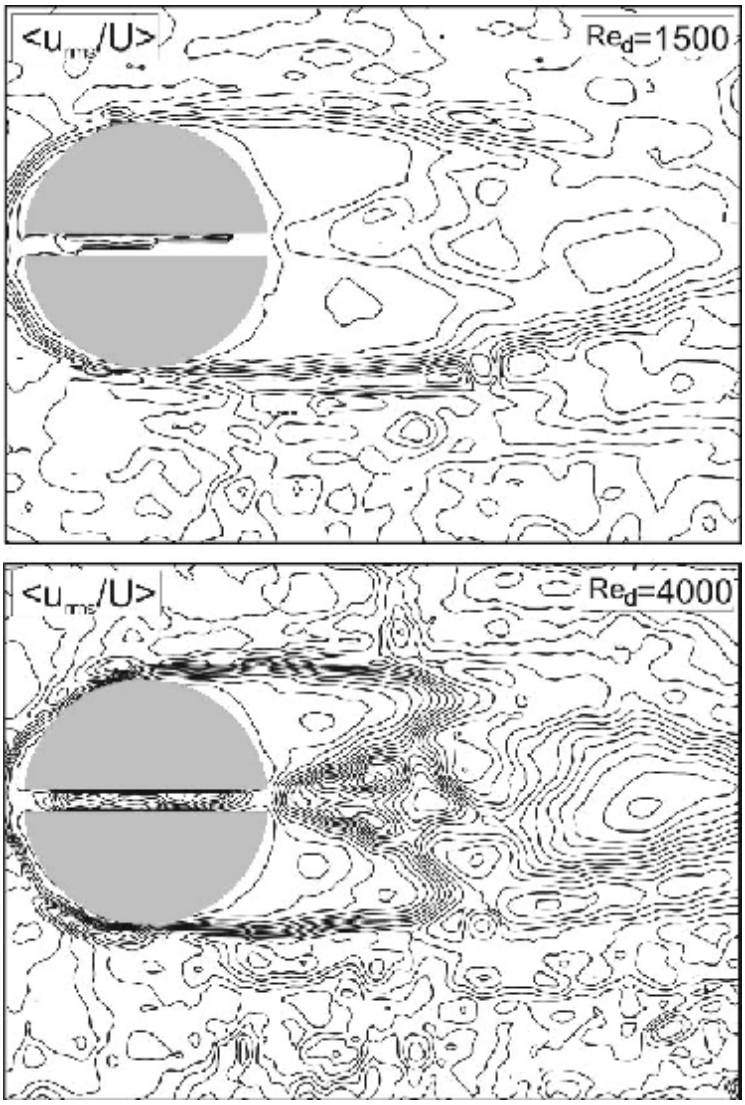

Figure 4.19. Time-averaged u_{rms} value in wake flow of single slotted-cylinder for h_l/h_w=0.1, Re_d =1500 and 4000, $<u_{rms}/U>_{min}$ =±0.01 and $\Delta <u_{rms}/U>$ = 0.01

Figure 4.20 presents the distributions of the time-averaged transverse velocity < v/U> at an elevation of h_l/h_w=0.1 for Reynolds numbers of Re_d=1500 and 4000. Contours of cross-stream velocity components v/U are involved in a switching of the orientation of the positive and negative values of < v/U> downstream of the cylinder as happened in the work Sahin and Ozturk (2009). In the case of Re_d=4000, on the upstream shoulder of the cylinder a maximum level or concentrations of positive and negative cross-stream velocity components, <v/U> are evident. While the flow moves further downstream the magnitude of cross-stream velocity, <v/U> fluctuations are gradually attenuated. It is expected that as the Reynolds number increases the level of fluctuation also increases due to the high rate of momentum of the flow.

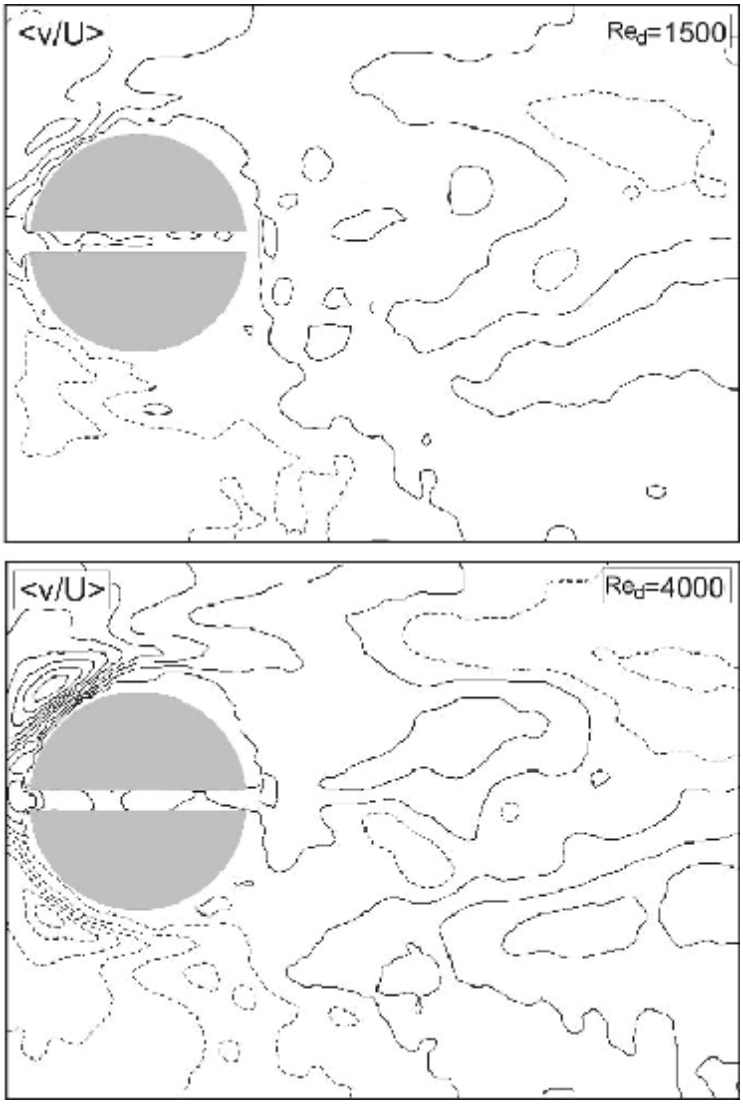

Figure 4.20. Time-averaged transverse velocity, < v/U> in wake flow of single slotted-cylinder for h_l/h_w=0.1, Re_d =1500 and 4000, $<v/U>_{min}$ =±1 and Δ <v/U> = 3

Figure 4.21 presents the distributions of the root mean square of transverse velocity fluctuations, $<v_{rms}/U>$ at an elevation of h_l/h_w =0.1 for Reynolds numbers of Re_d=1500 and 4000. Amplitude of the root mean square of cross-stream velocity fluctuations $<v_{rms}/U>$ for Re_d=1500 is low comparing to Re_d=4000 due to the lower rate of momentum of the fluid. Velocity fluctuations occupy the area where the

shear layers and horseshoe vortices pass through the area which includes the merging point of the shear layers emanating on both sides of the cylinder. In the case of Reynolds number Re_d=4000, the magnitude of velocity fluctuations in the wake region is also as high as other regions because of exiting the water flow jet through the slot.

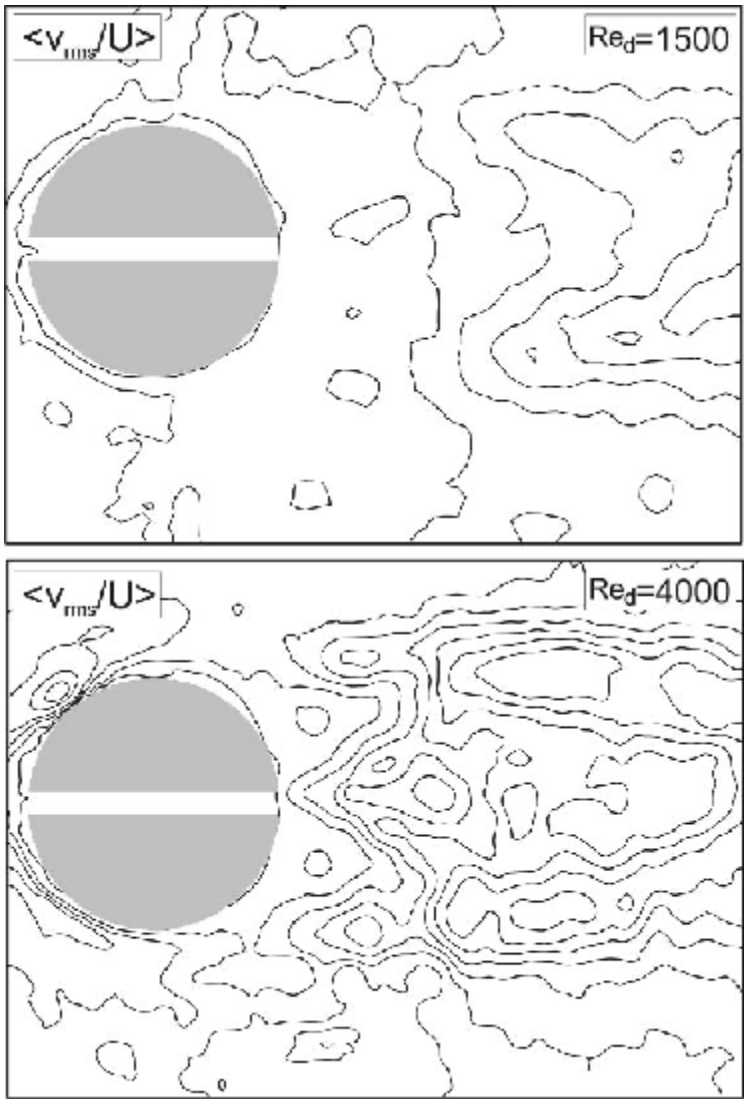

Figure 4.21. Time-averaged $\langle v_{rms}/U \rangle$ value in wake flow of single slotted-cylinder for h_l/h_w=0.1, Re_d =1500 and 4000, $\langle \mathbf{v}_{rms}/U \rangle_{min}$ =±0.01 and $\Delta < v_{rms}/U> = 0.01$

4.2. Dye Visualization of Multiple Slotted-Cylinders

4.2.1 Introduction

It is known that heat exchangers are one of the devices that can be developed further in the energy saving aspects and they are used in a wide variety of industrial applications. Therefore in recent years, there have been significant improvements in heat exchanger technology in order to save the loss of energy. Even though, the investigation of the flow characteristics through fin-tube heat exchanger will certainly be a challenge to those scientists who involve in sciences of thermal fluid mechanics in the future.

4.2.2. Scope of the Present Work

The aim of this study is to study the mechanisms of hydrodynamics of the heat exchangers experimentally which are mostly responsible for the performance. Main objectives of the present work are as follows.

I) Visualizing the structures of the vertical flow qualitatively and quantitatively through the confined staggered slotted-cylinders.

II) Analyzing the flow structure using data which consist of time series of streamwise and cross-stream velocity components measured in some selected cross-sections, at an elevation of $h_l/h_w=0.1$, in plan view planes. Reynolds stress correlations and root mean square of u and v velocity components, u_{rms} and v_{rms} were calculated.

III) Observation are focused in close region of cylinders-plate junctions and the central cross sections in order to see the effect of jets emanating from the slot on the wake flow, the generation and behavior of the horseshoe vortex system through the staggered slotted-cylinders and hence their effect on wake flow structures

IV) Finally it is aimed to observe vortices how they stimulate the entrainment between main flow and wake flow which enhances the heat transfer rate through flow passages hydrodynamically.

4.2.3. Arrangement of Test Chamber

As it has been known the flow in the passage of the fin tube heat exchanger is extremely complicated. It is rather difficult and time consuming to perform experiment in the case of having multiple tubes in staggered combination in between rectangular duct with narrow gap. Seven rows and seven columns of slotted-cylinders were mounted on the lower plate and later upper plate was pressed on the top of these slotted-cylinders. The width of this slot is 5 mm. Cylinders are located at the corners of equilateral triangles. The distance between cylinders was taken as 1D at all directions. The height of the flow passage was taken as h_w=20mm. The width of the rectangular duct was 400mm as seen in Figure 4.22. The upstream length of the flow passage starting from the central points of first column of cylinders was 325 mm. The length of downstream flow passage starting from the central points of last column of the cylinders was 150 mm. This narrow gaped rectangular duct was connect to the nozzle with included angle 90 degree. The locations of the measuring flow sections in the plan view indicated in Figure 4.22. The dimensions of plan view of measuring section are 160mmx120mm.This dimensions are chosen in order to see the interference of the multiple slotted-cylinders on the flow behaviors. The measuring plane was h_l/h_w=0.1 above the lower plate surface.

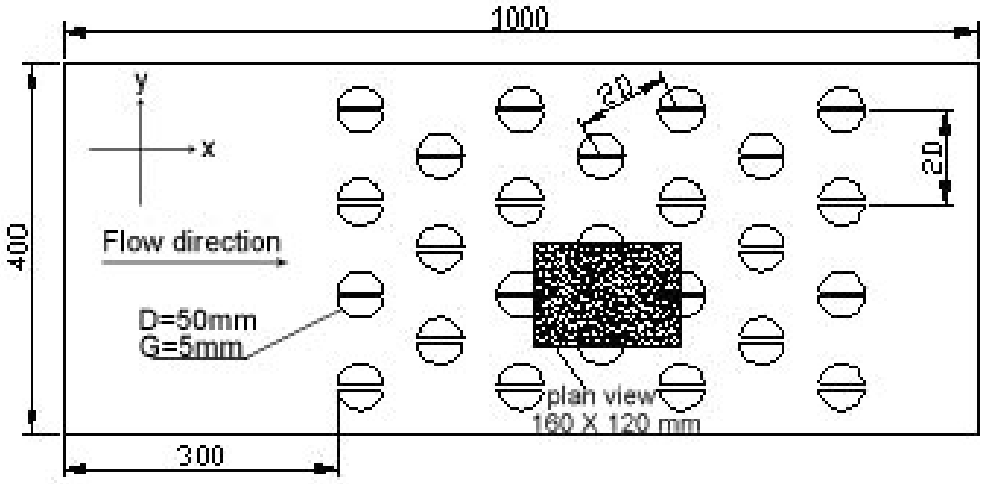

Figure 4.22. Overview of multiple slotted-cylinder combination, size of images and location measuring plane (Dimensions in mm)

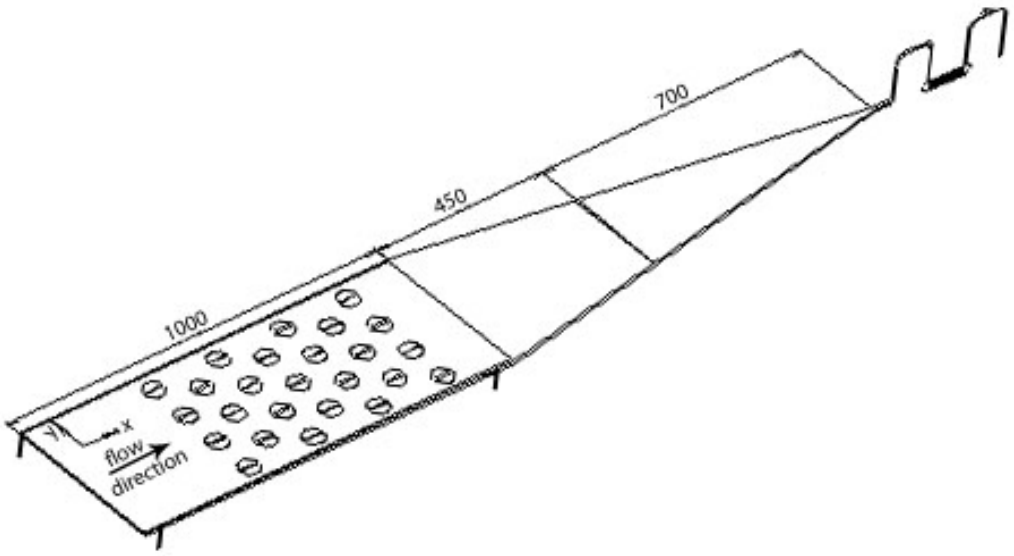

Figure 4.23. Isometric view of test geometry (Dimensions in mm)

4.2.4. Dye Visualization of Flows for Multiple Slotted-Cylinders

In general, the present combinations of staggered cylinders produce a complex flow characteristics. In the present work, the combination of staggered slotted-cylinders was the same as the work of Ozturk (2006) without slot and dye visualization experiment has also performed for multiple slotted-cylinders.

Comparison of flow structures in the forward face of the cylinder at an elevation of h_l/h_w=0.1 for a staggered slotted-cylinders array is presented in figure 4.22. The location of primary horseshoe vortex, in the forward face of the multiple slotted-cylinders shown in figure 4.24, is further closed to the surface of the cylinder comparing to the single cylinder shown in figure 4.3. This situation happens due to the configurations of the multiple staggered cylinders. It can be also concluded that horseshoes vortices moves further close to the surface of the cylinders due to the suction caused by water jet flow occurring through slots. Further more, on both side of the slotted-cylinder those spiraling horseshoe vortices travel in the direction of the main flow in the vicinity of shedding vortices having high rate of interactions. Shedding vortices arise from the shoulder of the cylinder which interact with horseshoes vortices provokes the shearing phenomenon. It is known that the flow characteristics downstream of cylinders are vitally important in terms of heat transfer rate comparing to the forward faces of cylinders since the occurrence of wake flow region deteriorates the rate of heat transfer hydrodynamically. Dye images shown in figure 4.24 illustrate that wake flow region is shortened in size compared with the results of single cylinder. There are two reasons to have flow characteristic in the present form. These are;

i) The compactness of the cylinder combinations and

ii) Jet flow occurring through slots.

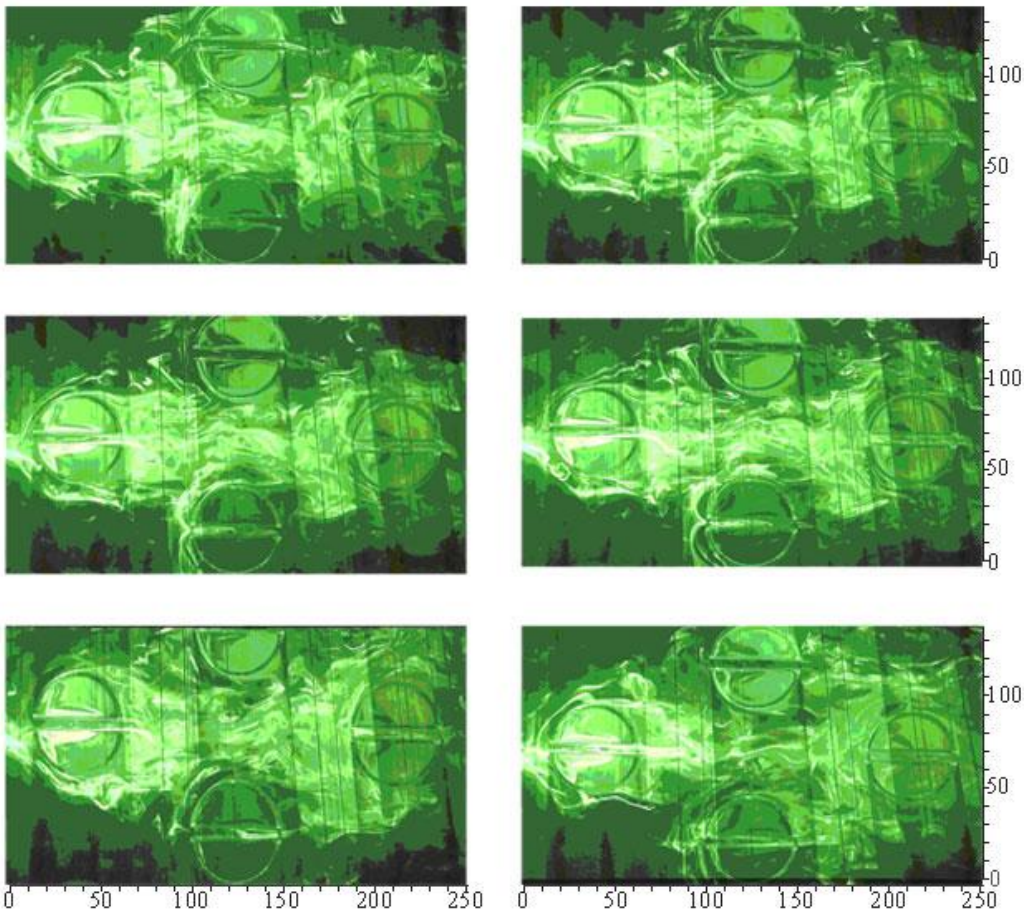

Figure 4.24. Instantaneous dye visualization of multiple slotted-cylinders for Re_d =1500, h_l/h_w=0.1

As seen view of dye images in figure 4.25 water jet flow is more effective on the suction of the horseshoe vortex in the forward face of the cylinder as well as in the wake flow regions. Horseshoe vortices move in the flow direction further close to the shear layers due to the existence of downstram cylinders and hence interactions of shedding vortices and horseshoe vortices increase significantly. The water jet flow exiting the slot moves in the lateral direction stirring the wake flow region to increase the entrainment to a higher level.

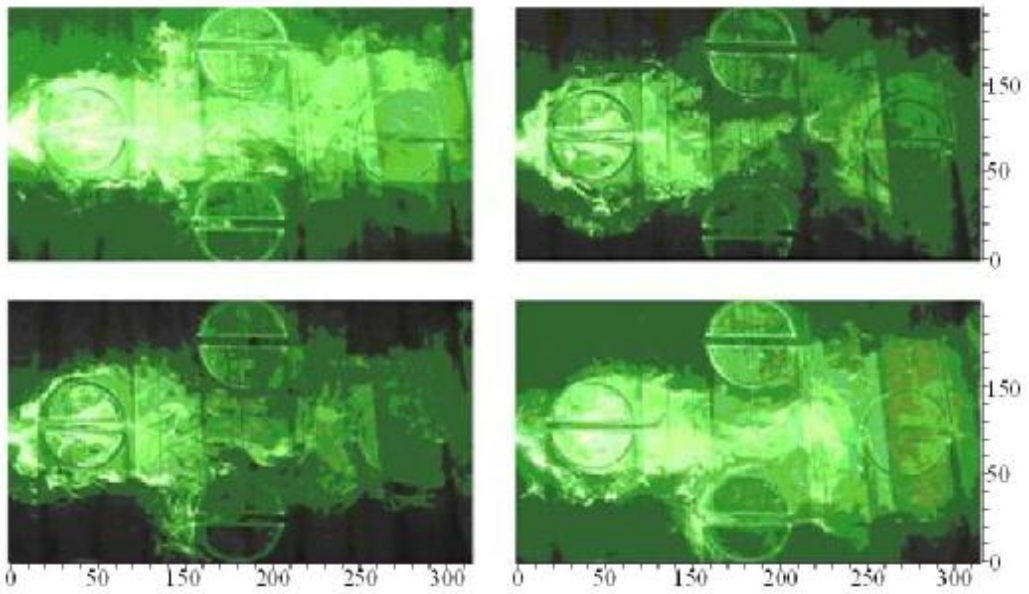

Figure 4.25. Instantaneous dye visualization of multiple slotted-cylinders for Re_d =4000, h_l/h_w=0.1

4.2.5. PIV Results of Multiple Cylinders and Multiple Slotted-Cylinders

In the work of Marakkos and Turner (2006) it has been indicated that the past experimental studies are limited due to the difficulties in measuring the unsteady flow data. Because of this reason, most of the past work on horseshoe vortex systems was qualitative using flow visualization, point-wise measurement of time-averaged velocity information and velocity spectra. In recent years and present time, particle image velocimetry gives an opportunity to the researcher to measure the instantaneous velocity distribution across a defined flow field quantitatively. In order to demonstrate the capability of the horseshoe type vortices, the formation, development of these vortices the PIV technique has been used in the present work along with dye visualizations.

In figure 4.26, time-averaged velocity vector distributions <V> is shown and images were taken at an elevation of h_l/h_w =0.1 for Re_d=1500 and 4000. Averaged velocity vector distributions, <V> images indicate that a high rate of velocity occurs on the shoulders of each cylinders and travel further downstream along the shear

layers with S shape. The curvature of the flow is repeated due to the configurations of cylinders. The wake flow region is rather small compared with the single cylinder case. This wake region is also smaller than the results of Ozturk (2006) who performed experimental test on the multiple cylinders without slot having the same configurations of the present work.

It is also seen in this figure that along the slot water jet flow is conveyed into the wake flow regions. Wake flow regions of staggered slotted-cylinders shrink in size comparing to the case of single cylinder. Shear layers emanating from the upstream of cylinders interfere with the shear layers of downstream cylinders resulting in a high rate of fluctuations.

Overall conclusions can be derived through the examinations of images as; the size of wake flow regions get smaller as soon as flow enters into the second columns of cylinders. Shear layers of upstream cylinders reattaches the shear layers of downstream cylinders causing high rate of turbulence.

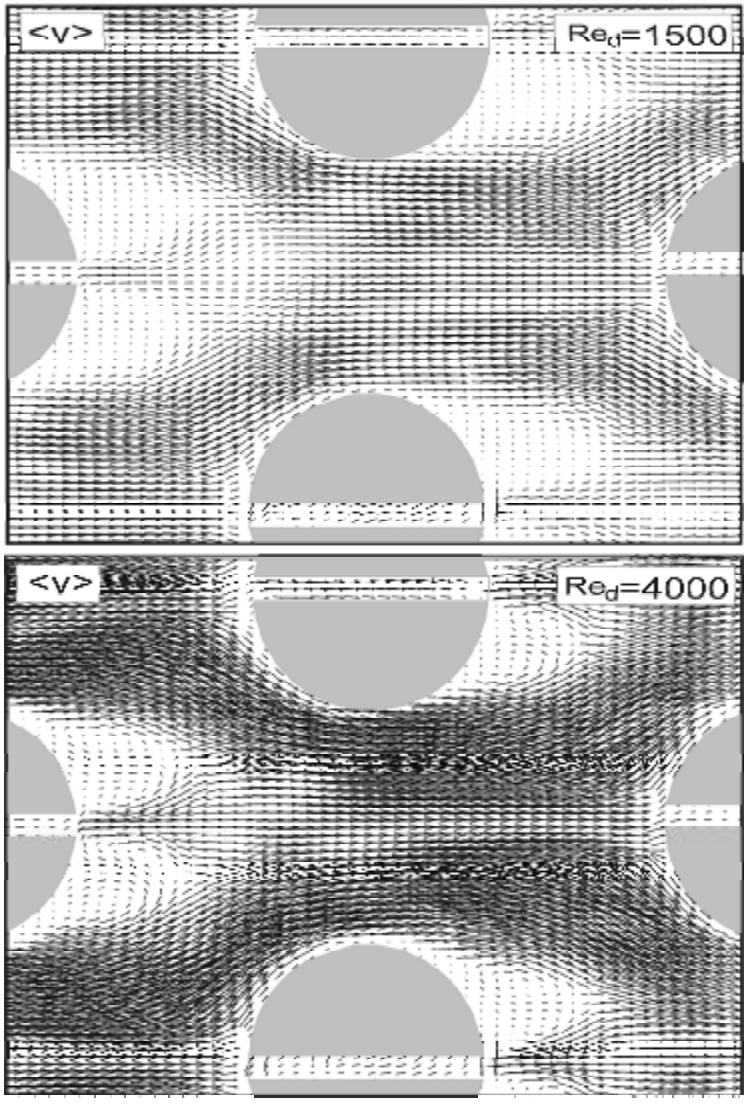

Figure 4.26. Time-averaged velocity vector map, <V> in wake flow of multiple slotted- cylinders for h_l/h_w =0.1, Re_d =1500 and 4000

Ozturk (2006) conducted experimental work on the flow structure at the base of staggered cylinders without slot having the same combination cylinders same as the present work. His results such as the time-averaged velocity vectors, <V>, the patterns of streamlines, <ψ> and contours of vorticity, <ω> at an elevation of h_l/h_w =0.05, are presented in figure 4.27 for both case of Reynolds numbers Re_d=1500 and 4000. Distributions of velocity vectors for both cases Reynolds numbers reveal that

the size of wake flow region downstream of the cylinder shrinks in size comparing to the case of a single cylinder. But the slotted cylinders reduce the wake flow size further.

In second column of figure 4.27 patterns of vorticity are presented. As seen in his figure the line of separation, L_s which crosses this saddle point, S surrounds both the cylinder and wake flow region. Corresponding vorticity contours $<\omega>$ also present that along the outer region of shear layer horseshoe vortex systems take place. Second and third row of images present the flow structures of multiple cylinders. Examining of these figure show that horseshoe vortices occurring in forward face of cylinders reveal that the saddle points, S are closer to the surface of the cylinders comparing to the single cylinder case. The size of wake flow regions is smaller. Foci, F_1 and F_2 that occur in the wake flow regions are closer to the surface of the cylinder. Patterns of streamlines indicate that fresh flow due to the hydrodynamics of horseshoes vortex system is transported in to the wake flow regions. Corresponding vorticity $<\omega>$ presents that, initially, horseshoe vortices has an elongated shape. While the main flow travels further downstream through the staggered cylinders this elongated shaped horseshoe vortices disappear.

Overall conclusions of Ozturk (2006) are; the size of wake flow regions get smaller as soon as flow enters into the second columns of cylinders. But these wake regions get slightly thicker in the lateral direction comparing to the case of single cylinder. Shear layers of upstream cylinders reattaches the shear layers of downstream cylinders causing high rate of turbulence. Separations lines, L_s crosses the upstream saddle points surrounds the cylinder on both sides and reattaches downstream of wake flow regions and extends to the saddle points of upstream of next cylinder as seen in the images of second row. Last row of images present the flow data of forth column of cylinders. In these images, patterns of streamlines indicate that separation lines, L_s surrounds its cylinder and wake flow regions and reattached at the saddle point of downstream.

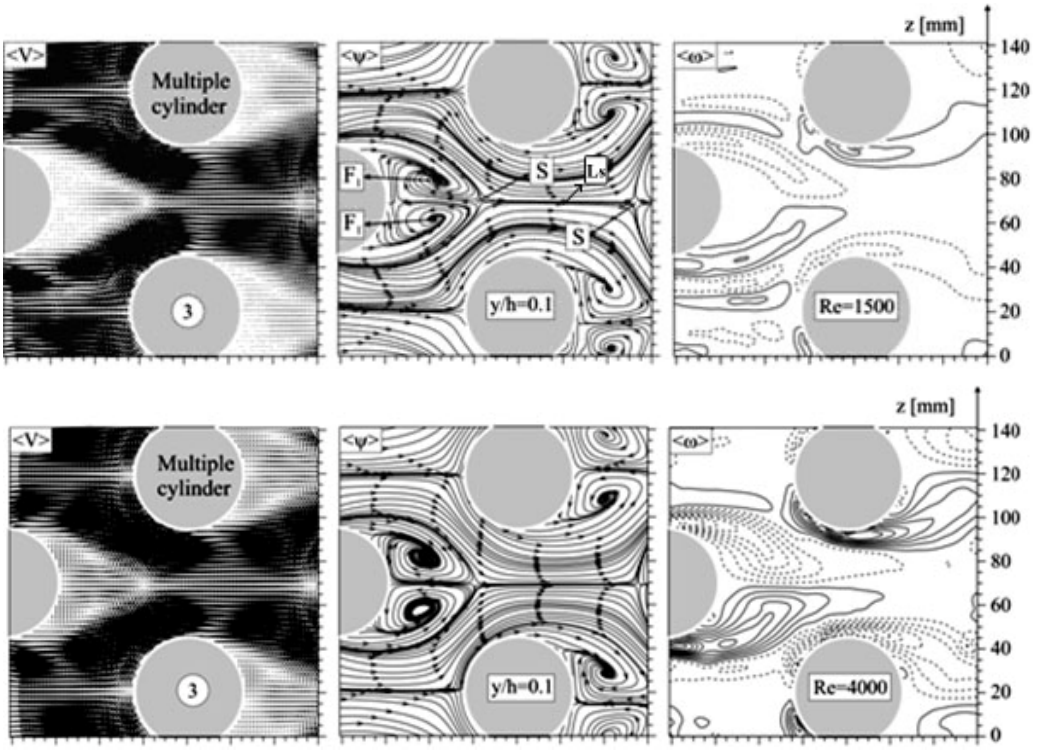

Figure 4.27. Comparisons of time-averaged flow data for Re numbers Red=1500 and Re_d=4000 at elevation of h_l/h_w=0.1 (Ozturk, 2006)

In Fig.4.28, vorticity contours <ω> also present that along the outer boundary of shear layers, horseshoe vortex systems take place. It seems that the water jet flow sucks the horseshoe vortex in a way that the primary horseshoe vortex comes very close to the inlet region of slots. In the image of vorticy patterns positive and negative shedding vortices are developed in close region of the inlet of slots.

The shear layers emerging from both sides of cylinders move downstream in between neighboring cylinders and interacts with the shear layers of other cylinders for y/h=0.1. It can be concluded that combinations of these cylinders stimulate the rate of turbulence and non steadiness. It may be thought that the entrainment enhances to further level because of interferences water jet flow caused by staggered slotted-cylinders. In addition, combinations of cylinders lead the main flow to accelerate and decelerate continuously in between staggered cylinders while the main flow moves in the forward direction. Patterns vorticity, <ω> also illustrate that wake

flow region is shortened in size compared with the results of Ozturk (2006). In addition, cluster of positive and negative vortices developed by the water jet flow at the centre of positive and negative elongated shedding vortices along by horseshoe vortices take place which merges into the shedding vortices. Finally, it can be concluded that having slots along cylinders improves the results of Ozturk (2006) further.

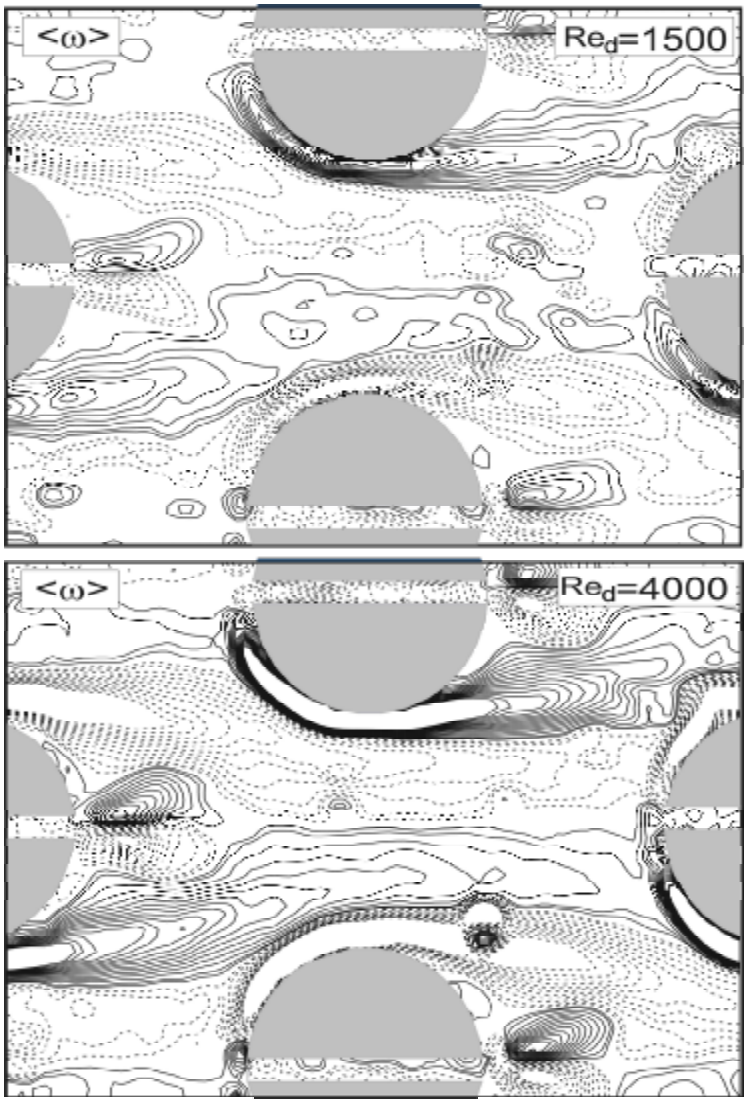

Figure 4.28. Time-averaged vorticity contours in wake flow of multiple slotted-cylinder for h_l/h_w=0.1, Re_d =1500 and 4000. $\omega_{min}=\pm 0.5 s^{-1}$ and $\Delta\omega=1 s^{-1}$

In the case of multiple slotted-cylinders arrangements, Clusters of negative and positive Reynolds stress correlations are occupied whole flow field as presented in figure 4.29. Maximum values of Reynolds stress correlations, $<u'v'>/U^2$ occur along the shear layer in close region of cylinder surface extended to the center of wake flow region. The distributions of velocity component are also indicates that the wake flow region is also energetic. This image present the time-averaged data of multiple cylinders at an elevation of $h_l/h_w=0.1$ for Reynolds number $Re_d=1500$ and 4000. Clusters of Reynolds stress correlations, $<u'v'>/U^2$ appear over the whole flow fields. Once again, the maximum value of Reynolds stress is located in close region of cylinder surface. It can be summarized that the distributions of Reynolds stress and velocity components declare that wake flow region is very energetic in the case of multiple slotted-cylinder arrangement comparing to the single cylinder case and multiple cylinders without slots as which are presented by Ozturk 2006.

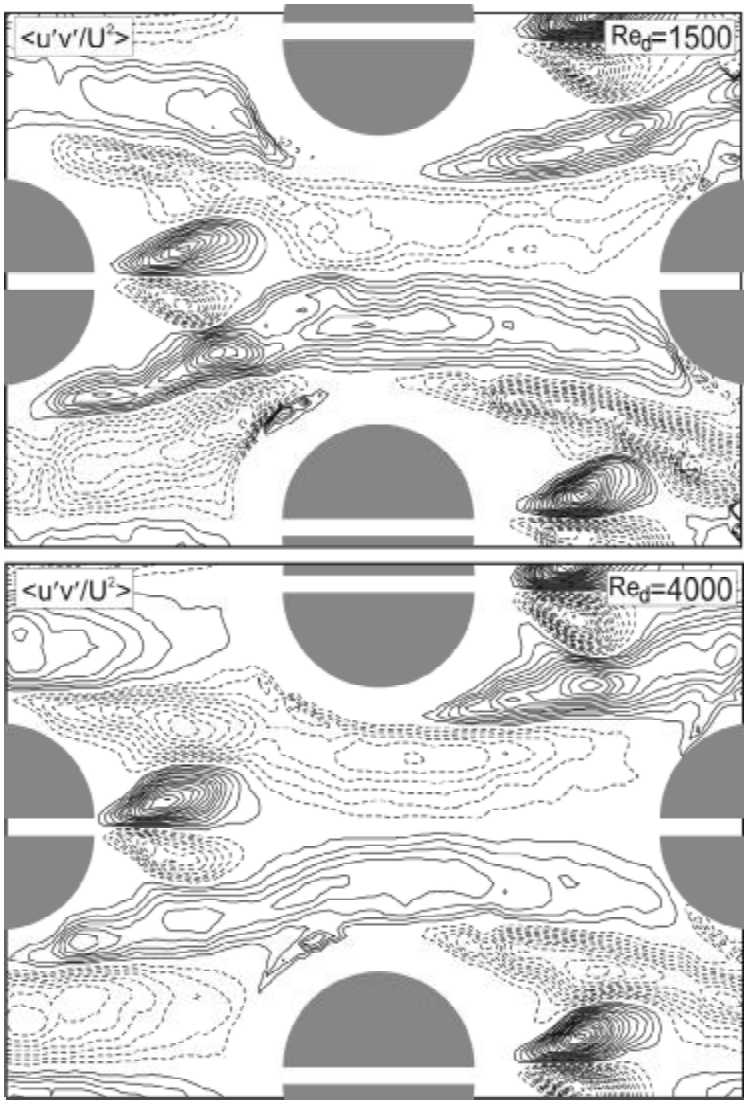

Figure 4.29. Reynolds stress correlation in wake flow of multiple slot-cylinders for h_l/h_w=0.1 , Re_d =1500 and 4000

In figure 4.30 the time-averaged streamline patterns, $<\psi>$ illustrates that separated flow regions are more compact since the water jet flow goes through slots directly into the wake flow region. Because of this water jet flow the size of foci are very small comparing to the results of Ozturk (2006). Patterns of streamlines indicate that fresh flow due to the hydrodynamics of horseshoes vortex system and from the slot is transported in to the wake flow regions to further extent. These foci F1, and F2 are almost symmetrical for both case of Reynolds numbers. There is a saddle point, S for each focus, F. In addition, focus is developed close to the surface of the cylinder comparing to the case of single cylinder and results of Ozturk (2006) due to enforcements of the curvature of the core flow region. Row of cylinders located downstream of the observed cylinder affect the upstream flow to merge into the wake flow region and water jet flow of slots. These are the reasons that wake flow area shrinks in size in the longitudinal direction and lateral direction. But the wake flow area in the work of Ozturk (2006) enlarges slightly in the lateral direction.

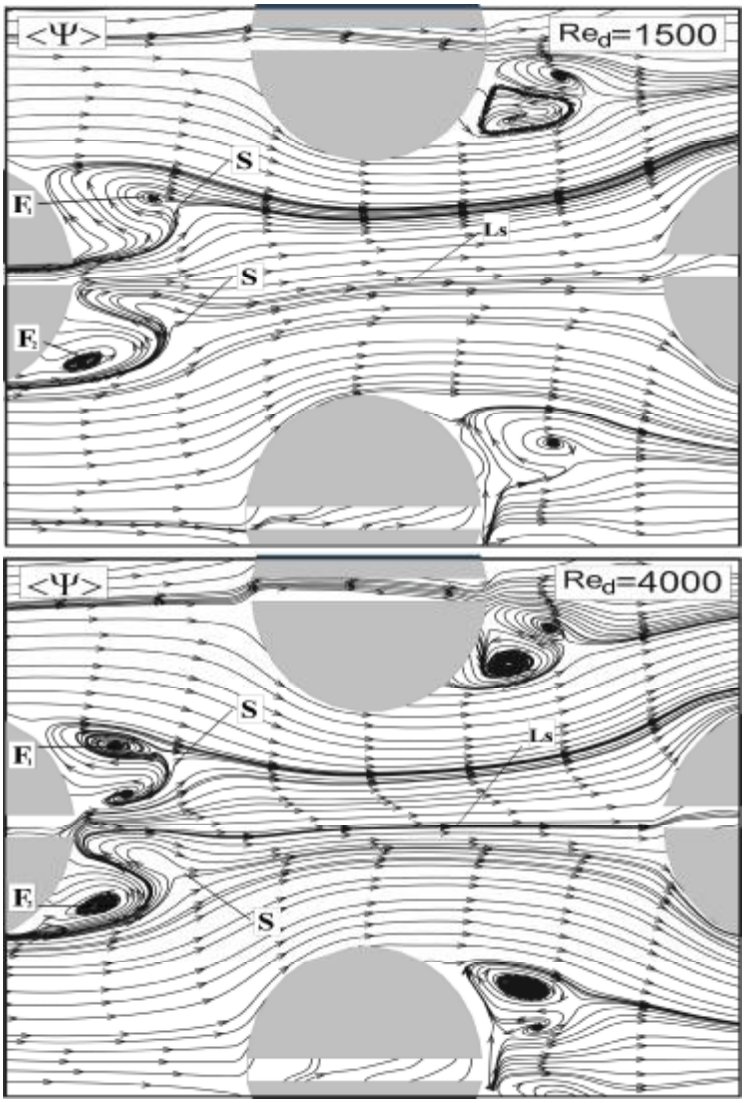

Figure 4.30. Time-averaged streamline pattern, <ψ> in wake flow of multiple slotted-cylinders for h_l/h_w=0.1, Re_d =1500 and 4000

Streamwise flow velocity distributions, <u/U> presented in figure 4.31 clearly indicates that the wake flow area is very small. This result reveals that wake flow region has a velocity distribution with high magnitude.

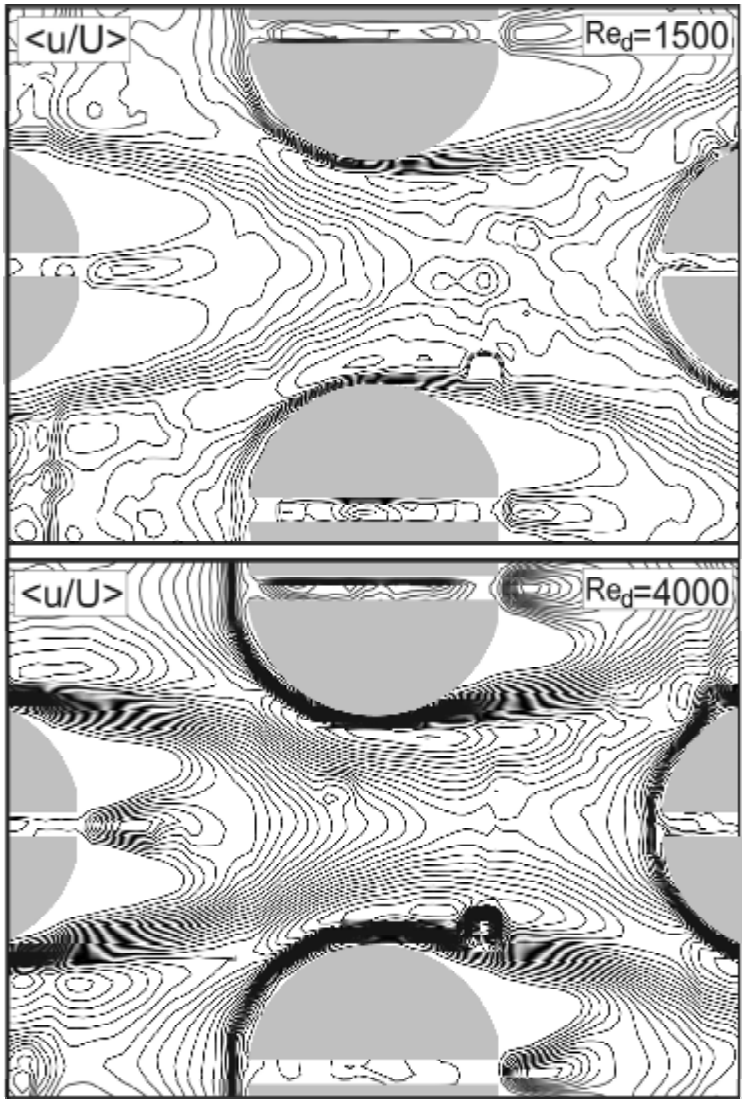

Figure 4.31. Streamwise velocity, <u/U> in wake flow of multiple slotte-cylinders for h_l/h_w=0.1, Re_d =1500 and 4000

Figure 4.32. presents the distribution of Urms showing that the high rate of fluctuations cover whole flow regions. The rates of fluctuations are higher than the results of multiple cylinders with the same combinations but without slots. The maximum value of u_{rms} occur along the shear layers and the merging points of these shear layers and water jet flow.

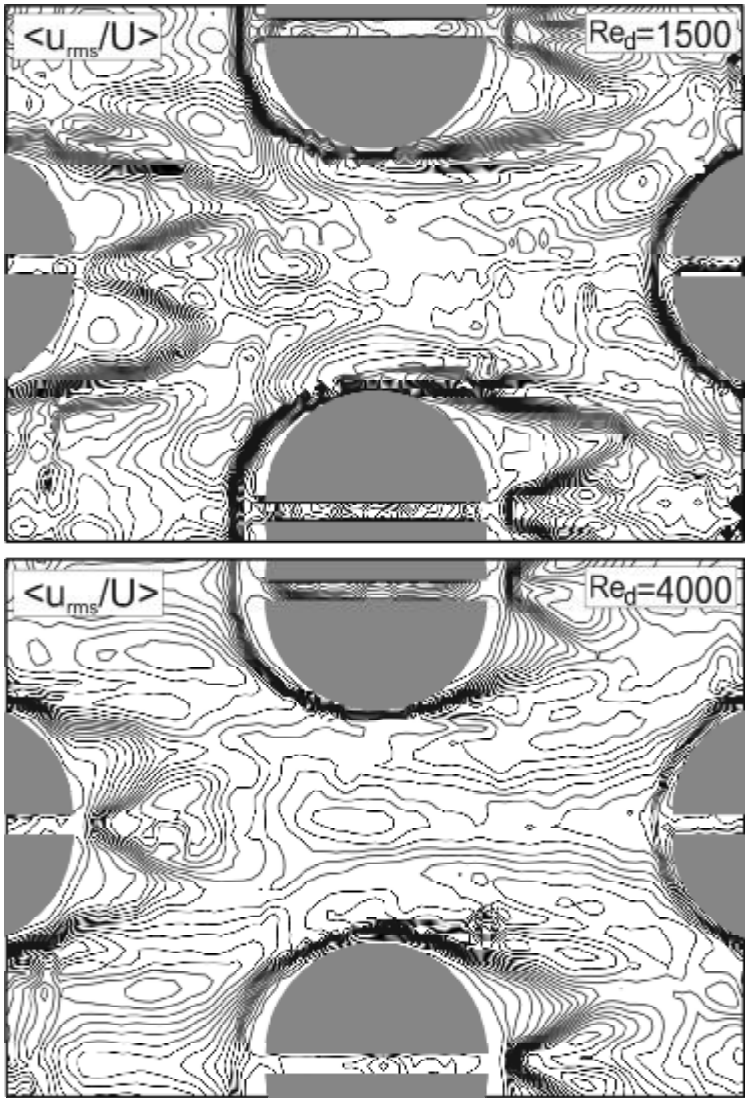

Figure 4.32. u_{rms} value in wake flow of multiple slotted-cylinders for h_l/h_w=0.1, Re_d =1500 and 4000

Figure 4.33 present the distributions of transverse velocity, <v/U>. It is interesting that a cluster of transverse velocity distributions are evident on shoulder of cylinders in the forward faces. Outlet of slot exit a low level of transverse velocity takes place. This indicates that in the case multiple slotted-cylinders, horseshoe

vortices combines with shedding vortices time to time causing high rate interactions between these two types of vortices.

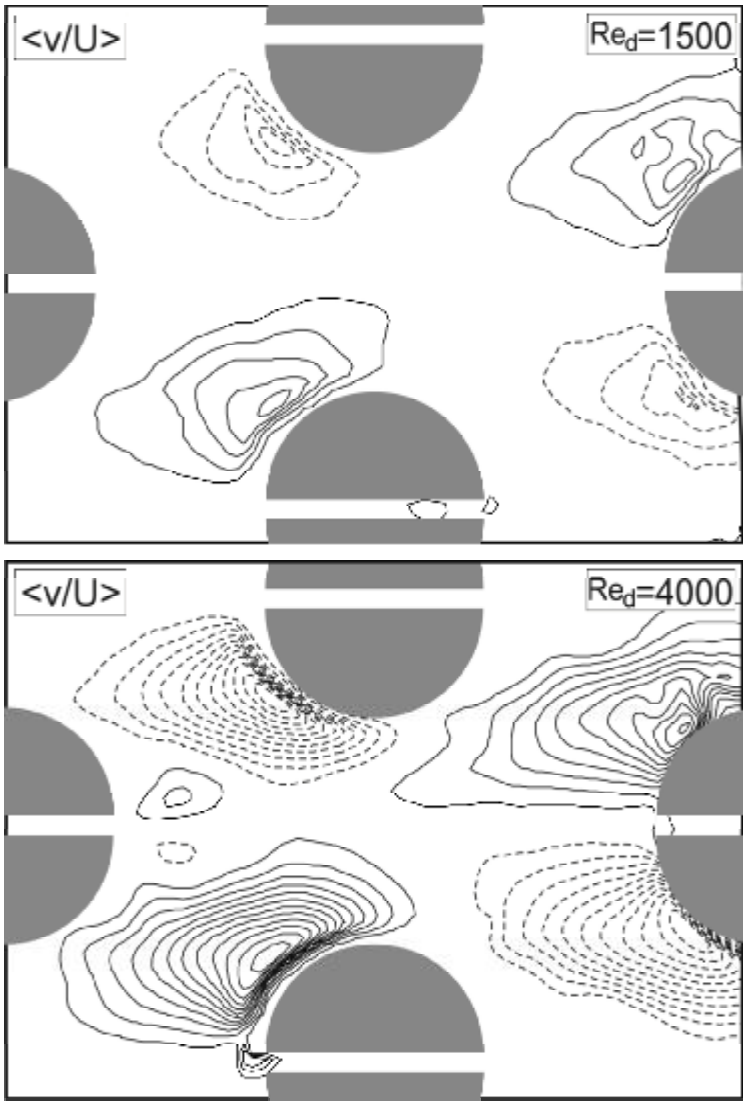

Figure 4.33. Time-averaged transverse velocity in wake flow of multiple slotted-cylinders for h_l/h_w=0.1, Re_d =1500 and 4000

Figure 4.34 present the distributions of the v_{rms} of transverse velocity component. The maximum value of v_{rms} occurs in the area where shear layers

emanating from both sides of slotted-cylinders and water jet flow combines together. The other part of the measuring suction also has a high rate of v_{rms}. This situation indicates that fluctuating of flow is high over whole measuring section. It can be concluded that the rate of heat transfer is improved to further extent hydrodynamically comparing to the same combinations of cylinder without slots.

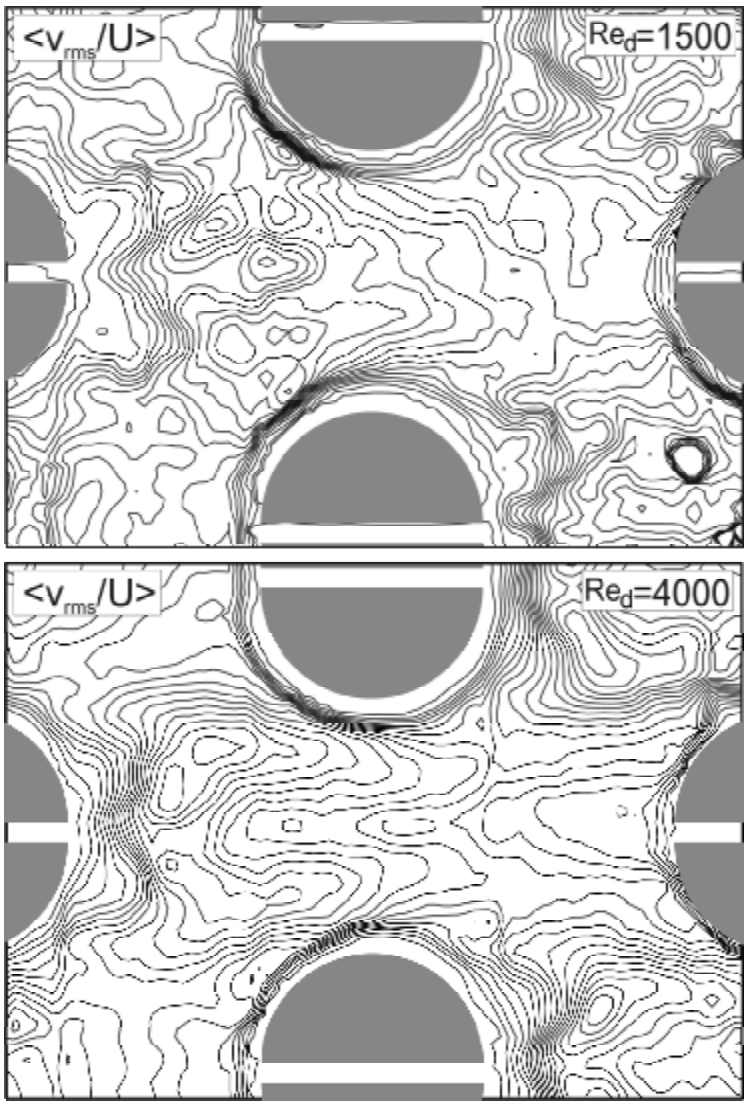

Figure 4.34. v_{rms} value in wake flow of multiple slotted-cylinders for h_l/h_w=0.1, Re_d =1500 and 4000

Overall conclusions can be derived through the examinations of all images as; the size of wake flow regions get smaller as soon as flow enters into the second columns of cylinders. Although in the work Ozturk (2006) these wake regions get slightly thicker in the lateral direction comparing to the case of single cylinder, in the present work even in the lateral direction the size of wake flow are is smaller. Shear layers of upstream cylinders reattach the shear layers of downstream cylinders causing high rate of turbulence. These conclusions are indicated in figures given above.

4.2.6. Instantaneous Vector Velocity Distributions for Multiple Slotted-Cylinders

Representative instantaneous flow data are presented in Figures 4.35 for multiple slotted-cylinder as a function of slot width B/D is equal to 0.1, for Re_d =1500 and 4000. Throughout the PIV experiment 350 images were taken for each test sets and all patterns are phase-referenced according to the same phase of the cycle of vortex formation. The patterns of V indicate that vortex formation occurs immediately adjacent to the base of the cylinder and as these horseshoe vortices immigrate in the direction of the free stream flow they also flap in the lateral direction in unsteady fashion. It is obviously seen that near wake vortex formation changes periodically due to jet flow from slot into wake flow region. Image 5 shows that jet flow from slot goes along the slot axis and there is no any undulation in the near wake flow. Image 10 shows the jet flow from the slot changes direction to the right hand side. Large-scale of swirling patterns of velocity vectors are evident in the downstream base of the cylinder, corresponding patterns of vorticity shows that the shear layer is pushed to the base region causing a well defined concentration of vorticity as seen in image 10. Image 15 shows the direction of jet flow to the left hand side in wake flow region and it is clear that lateral undulation is occured.

The patterns of velocity images show a higher frequency level, transverse undulation comparing for Re_d=1500. These characteristics of the flow clearly indicate the existence of the horseshoe vortex system.

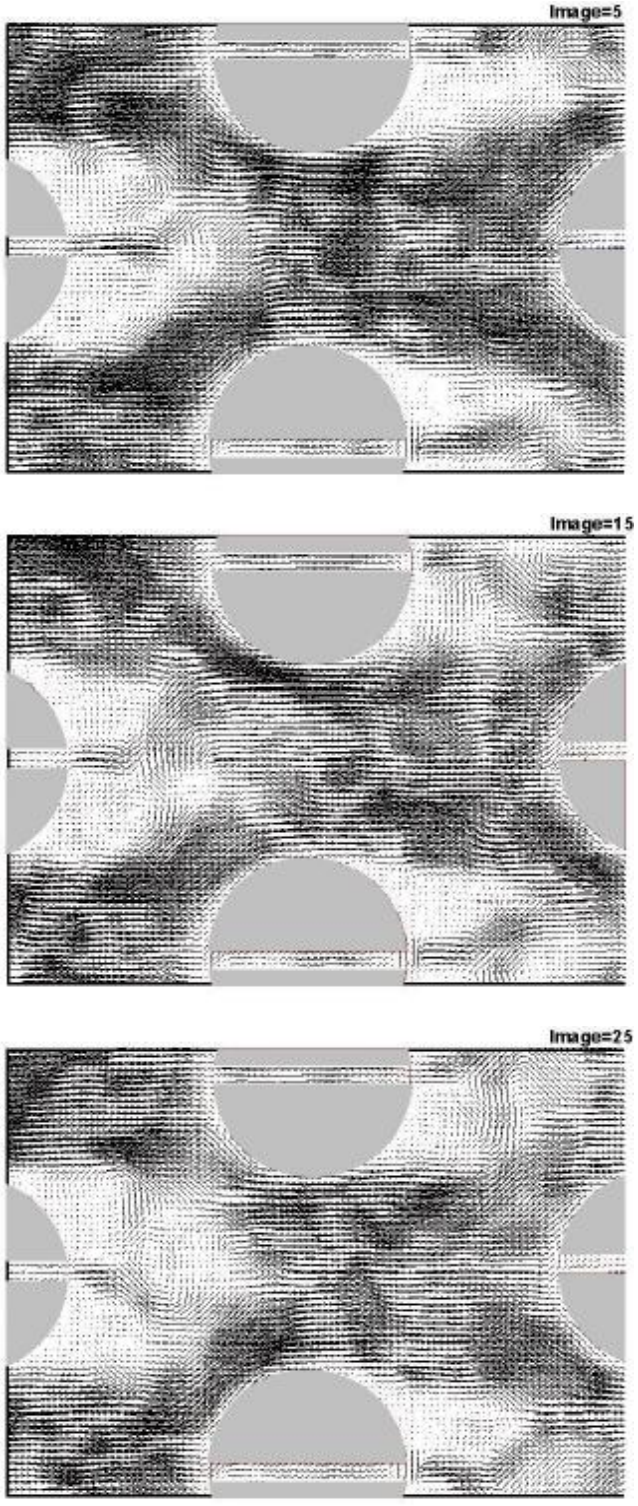

Figure 4.35. Instantaneous velocity vector map,V for Re_d=1500, h_l/h_w=0.1

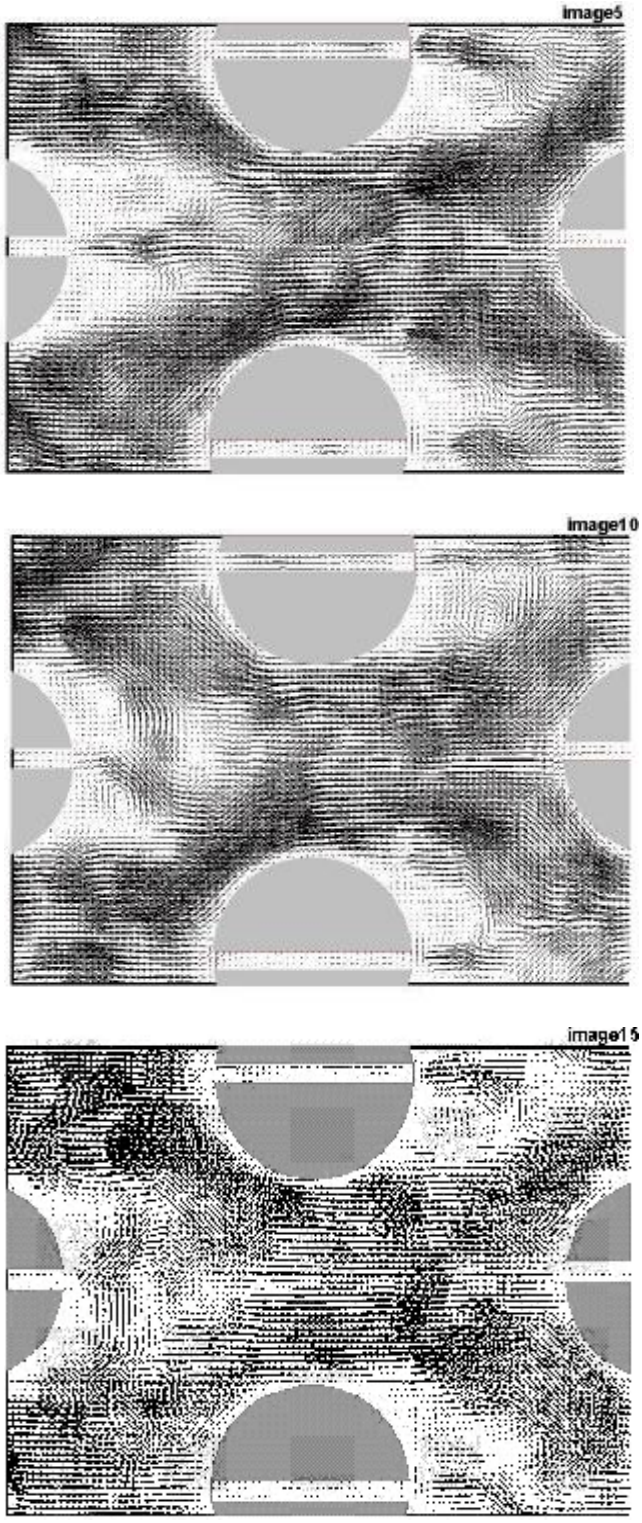

Figure 4.36. Instantaneous velocity vector map,V for Re_d=4000, h_l/h_w=0.1

4.3. Concluding Remarks

The flow structure in a plate fin and tube heat exchanger thermal unit composed of staggered slotted-cylinders arrangement is continuously accelerated and decelerated due to the arrangement of cylinders. Cylinders are located at the corners of equilateral triangles. Due to the compactness of this type of heat exchanger the distance between cylinders surfaces is 1.0 D. On the other hand, the distance between lower and upper plates is 0.4 D. Horseshoe vortices are developed on both surface of the plate in close regions of the cylinders. Flow structures are restless due to the continuous developing flow process. Flow jet layers appear along the outer of the shear layers. Entrainment processes due to the high rate of circulatory flow motion on vortical flow structure is extremely high engender energetic wake flow structure. In summary, staggered slotted-cylinder arrangements enhance the heat transfer rate hydrodynamically even in wake flow regions but they cause pressure losses. Comparing with complete staggered cylinders, pressure losses are less for staggered slotted-cylinders and flow structure supplies more efficiency for heat transfer rate.

5. CONCLUSIONS AND RECOMMENDATIONS

5.1. Flow Structure Around Single and Multiple Staggered Slotted-Cylinders

Heat exchangers, which are used in wide variety of industrial applications, are one of the devices that can be developed further in regard to energy-saving, from the hydrodynamics point of view. Therefore the main aim of the present study is to investigate details of flow structure in the upstream and downstream of a circular single slotted-cylinder and multiple staggered slotted-cylinders mounted on a flat surface in a narrow gaped rectangular duct in the case of confined flow which is used in plate-fin-and-tube type of heat exchangers.

It is known that multiple cylinders in staggered arrangement are more efficient than in-line tube arrangement in the case of heat transfer. With this in mind, this study examines the effect of a combination of multiple slotted-cylinders on flow characteristics. Therefore the effect of staggered arrangement of slotted-cylinders on the flow characteristic in confined flow was investigated both using dye visualization and the PIV technique. PIV experiments were carried out for single-slotted cylinder and multiple staggered slotted-cylinders.

The width of the slot is 5 mm, the diameters of the cylinders are 50 mm and the ratio of B/D is 0.1, the gap ratio G/D is 2 where the slot width is B, diameter of the cylinder is D and distance between the centers of the cylinders in the lateral direction is G. The laser sheet was located parallel to the bottom surface of the water channel at the elevation of $h_l/h_w=0.1$.

The slotted-cylinders significantly change the flow characteristics in downstream directions. The most important change occurs on the Reynolds stress concentrations and it substantially decreases the peak concentration of Reynolds stress.

Water jet-flow passing through the slot was remarkably effective for the gap ratio B/D=0.1 in case of staggered cylinder arrangements. The jet-like flow changed direction and switched from one side to the other randomly. Jet-flow between cylinders was effective and almost symmetrical wake region in downstream direction

for Re_d=1500 and Re_d=4000. At the bottom surface plane (h_l/h_w=0.1), the analysis of the instantaneous flow data and time-averaged velocity vectors map, <V> patterns of streamlines, <ψ> and corresponding vorticity contours, <ω>, Reynolds stress correlations $<u'v'>/U^2$ and fluctuations of the velocity components show that the horseshoe vortices take place in the base of the cylinder in three dimensional forms causing a scour mechanisms. These vortices also magnify the entrainment process and circulatory motions between core and wake flow regions downstream of the cylinder mounted on the flat plate in confined flow

Control of jet-like-flow both on the shoulders of slotted-cylinders and in the slot along the cylinder provides the absence of biased flow. In terms of the size of the wake region, wake region elongates in streamwise direction due to the momentum transfer from the slot of the cylinder in case of single slotted-cylinder. The vortex shedding., Kelvin-Helmholtz instabilities in the shear layer become effective on the flow characteristics downstream of the cylinder.

.

5.2. Flow Control Around Slotted-Cylinders

In this section, flow characteristics of circular slotted-cylinders arrangement Has been investigated experimentally. Experiments were only carried out for the gap ratio of G/D=2 and B/D=0.1. During the experiments, Reynolds numbers were changed between 1500 and 4000. The cylinders having same slot widths were used during the experiments. All experiments were carried out at elevation of h_l/h_w=0.1. The slot width has an effect on the flow characteristics. The peak value of Reynolds shear stress concentration decreases due to slot width.

Following conclusions can be derived from the overall experimental studies.

- A test model geometry comprised of multiple slotted-cylinders row surrounded by a fin plate configuration should be considered in the context of optimization and design of plate fin and tube heat exchangers. Fluid flow and corresponding heat transfer characteristics of multiple row heat exchanger geometry can be extended to investigate for different ratio of B/D for fin and tube heat exchangers.

- Tube row number, tube arrangement with slot, fin configuration and Reynolds number are important governing design parameters for the plate fin and tube heat exchangers.
- The heat transfer rate increases with an increase of the Reynolds number.
- Staggered slotted-cylinders arrangements enhance the heat transfer rate hydrodynamically, even in wake-flow region compared to the arrangement of multiple in-line cylinders since staggered cylinder arrangements activate the flow behaviours further because of the repetition of boundary-layer development.
- The magnitude of the pressure drop along the tube surface in the staggered slotted arrangement is found to be lower comparing staggered arrangement without slot.
- A continous flow development, involving shearing phenomena and interactions of shedding and horseshoe vortices, causes a high rate of fluctuations and heat transfer over the whole flow field. For the staggered arrangement with slot has higher heat transfer rate than for the inlined arrangement.
- The distributions of the time-averaged flow data for multiple slotted-cylinders demonstrate that the wake-flow region is shortened in size in the longitudinal direction but slightly enlarged in size in the lateral direction, comparing with the same configuration of cylinders without slots.
- The size of the wake region differs slightly depending on the Reynolds number for single slotted-cylinder but not multiple slotted-cylinders. As the Reynolds number is increased, the size of the wake region becomes smaller.
- The positive and the negative vorticity layers are approximately equal and symmetric with each other.

5.3. Recommendations for Future Work

The present work focused on the flow control for single and staggered slotted arrangement of cylinders in confined flow which is similar to heat exchanger flow passage. The flow behavior in the heat exchanger flow passage is really a complex, three-dimensional and unsteady with flow separation, reattachment, recirculation zones, and vortices in the wake of the cylinders.

The present study can be further extended heat transfer aspect of plate fin and tube heat exchangers. Different control techniques can be also used to control vortex formation around staggered arrangements of slotted-cylinders.

In addition to that, the study may be further extended to investigate effects of tube diameter, slot width, effects of different tube shapes having oval or elliptical configurations, and effects of transverse and longitudinal distance between the tubes on the flow and heat transfer characteristics of plate fin and tube heat exchangers.

Besides three dimensional experimental investigations with 3-D PIV system can be undertaken to measure the third velocity component over a complete flow field of the confined flow of multiple slotted-cylinders.

REFERENCES

ADRIAN, R. J., 2005. Twenty Years of Particle Image Velocimetry. Experimental Fluids, Vol. 39, pp. 159–169.

ADRIAN, R.J., YAMAGUCHI, E., VANKA, P., PLATTNER, T., LAI, W., 1997. Validation of micro PIV measurements in PDMS micro-channel flow geometries. Department of Theoretical and Applied Mechanics, University of Illinois, Urbana, İllinois.

AKAR, A,. 2008. Vortex control behind side by side circular cylinders in shallow waters. Ph.D. thesis, Cukurova University.

ANAGNOSTOPOULOS, P., 1997. Computer aided flow visualization and vorticity Balance in the laminar wake of a circular cylinder. Journal of Fluids and Structures, 11: 33-72.

AKILLI, H., AKAR, A., and KARAKAUS, C., 2004, Flow Characteristics of Circular Cylinders Arranged Side-By-Side in Shallow Water, Flow Meas. Instrum., 15, pp. 187–197.

AKILLI, H., and ROCKWELL, D., 2002. Vortex formation from a cylinder in shallow water. Physics of Fluids, 14 (9): 2957-2967.

AKILLI, H., KARAKUS, C., AKAR, A., SAHIN, B. and TUMEN, N. F., "Control of Vortex Shedding of Circular Cylinder in Shallow Water Flow Using an Attached Splitter Plate", J. Fluids Eng. 130, 041401, 2008.

AKILLI, H., SAHIN, B. and ROCKWELL, D., 2001. Control of Vortex Break-down by a Transversely-Oriented Wire. Physics of Fluids, Vol. 13, No.2, pp. 452-463.

AKILLI,H., SAHIN,B., and TUMEN, N.F., 2005, Suppression of Vortex Shedding of Circular Cylinder in Shallow Water by a Splitter Plate, Flow Measure. Instrum., 16, pp. 211–219.

AKKOCA, A., 2004. Computational modeling of turbulent heat transfer in plate fin and tube heat exchangers. PhD thesis, Cukurova University, Institute of Natural and Applied Sciences, Department of Mechanical Engineering, 230p.

AKKOCA, A,.2004. Computational modeling of turbulent heat transfer in plate fin-and-tube heat exchangers, PhD thesis, Department of Mechanical Engineering, Institute of Natural and Applied Sciences, Cukurova University, Adana, Turkey

BAKER, C. J., 1979. The laminar horseshoe vortex. Journal of Fluid Mechanics, 95, 347-367.

BECKER, S., LIENHART, H., DURST, F., 2002. Flow around three-dimensional obstacles in boundary layers. Journal of Wind Engineering and Industrial Aerodynamics, 90, 265-279.

BOURIS, D., PAPADAKIS, G., BERGELES, G. 2001. Numerical Evaluation of Alternate Tube Configurations for Particle Deposition Rate Reduction in Heat Exchanger Tube Bundles. International Journal of Heat and Fluid Flow, 22, 525-536.

CHANG, K.A., HSU, T.J., LIU, P.L.F., 2005. Vortex generation and evolution in water waves propogating over a submerged rectangular obstacle, Part II: Cnoidal waves. Coastal Engineering, 52, 257-283.

CONSTANTINESCU, G., KOKEN, M., 2005. Time dependent and time averaged turbulence of flow past a surface mounted cylinder. 4st International Conference on Computational Heat and Mass Transfer, Paris-Cachan, France.

COTTET, G.H., PONCET, P., 2004. Simulation and control of three-dimensional wakes. Computers and Fluids, 33, 697-713.

FARACI, C., FOTI, E. and BAGLIO, S., 2000. Measurements of sandy bed scour processes in an oscillating flow by using structured light. Measurement 28, 159-174.

FU, H., ROCKWELL, D., 2005. Shallow flow past a cylinder,transition phenomena at low Reynolds number. Journal of Fluid Mechanics, 540, 75-97.

FU, H., 2004. Shallow flow vortex formation and control, PhD Thesis, Lehigh University, Bethlehem, Pa.

GOSSLER, A.A., MARSHALL, J.S., 2001. Simulation of normal vortex-cylinder interaction in a viscous fluid. Journal of Fluid Mechanics, 431, 371-405.

GROSCHE, F.-R., MEIER G. E. A., 2001. Research at DLR Göttingen on bluff body aerodynamics, drag reduction by wake ventilation and active flow control. Journal of Wind Engineering & Industrial Aerodynamics, 89, 1201-1218.

GURSUL, I. and YANG, H.,1995. On Fluctuations of Vortex Breakdown Location, Physics of Fluids, Vol. 7, No. 1, pp. 229-231.

HASSAN, Y.A., BARSAMIAN, H.R., 2004. Tube bundle flows with the large eddy simulation technique in curvilinear coordinates. Int.J. of Heat and Mass Transfer, 47: 3057-3071

IGARASHI,T., TERACHI, N.,2002. Drag reduction of flat plate normal to airstream airstream by flow control using a rod. Journal of Wind Engineering and Industrial Aerodynamics, Volume 90:359-376

IGARASHI, T., 1984. Characteristics of the flow around two circular cylinders arranged in tandem (2nd Report), Bull. JSME 27 (233) 2380–2387.

IGARASHI, T., TSUTSUI T., 1989. Flow control around a circular cylinder by a new method, Trans. JSME 55 (511) 701–713.

IGARASHI, I., ITOH, S., 1993. Drag reduction of a square prism. 1st report, flow control around a square prism using a small vortex shedder, J. Fluids Eng. 59: 3701–3707.

INOUE, O., YAMAZAKI, T., 1999. Secondary vortex streets in two-dimensional cylinder wakes. Fluid Dynamics Research, 25, 1-18.

IWAKI, C., CHEONG, K.H., MONJI, H., MATSUI, G., 2004. PIV measurement of the vertical cross-flow structure over tube bundles. Experiments in Fluids, 37: 350-363.

JANG, J.Y., WU, M.C., CHANG, W.J., 1996. Numerical and Experimental Studies of Three- Dimensional Plate Fin and Tube Heat Exchangers. International Journal of Heat and Mass Transfer, 39(14): 3057-3066.

JANG, J.Y., CHEN, L.K., 1997. Numerical Analysis of Heat Transfer and Fluid Flow in a Three- Dimensional Wavy Fin and Tube Heat Exchanger. International Journal of Heat and Mass Transfer, 40(16): 3981-3990.

KAHRAMAN, A., SAHIN, B., and ROCKWELL, D., 2002. Control of vortex formation a vertical cylinder in shallow water: Effect of localized roughness elements. Experiments in Fluids, 33: 54-65.

KELSO, R. M. and SMITH, A. J., 1995. Horseshoe vortex system resulting from the interaction between a laminar boundary layer and a transverse jet. Physics of Fluids, 7, 19, 153-158.

KIM, N.H., YUN, J.H., WEBB, R.L., 1997. Heat Transfer and Friction Correlations for Wavy Plate Fin- and- Tube Heat Exchangers. Journal of Heat Transfer, Transactions of the ASME, 119: 560-567.

KIM, J.Y., SONG, T.H.,2002. Microscopic Phenomena and Macroscopic Evaluation of Heat Transfer From Plate Fins/Circular tube Assembly Using Naphthalene Sublimation Technique. International Journal of Heat and Mass Transfer, 45: 3397-3404.

KIRKIL, G., CONSTANTINESCU, S.G. AND ETTEMA, R., 2005. The horseshoe vortex system around a circular bridge pier on equilibrium scour bed. World Water and Enviromental Resources Congress, Canada

KONSTANTINIDIS, E., BALABANI, S., YIANNESKIS, M, 2004. Phase-average mean flow and turbulence structure in a staggered cylinder array subjected to pulsating cross-flow. Journal of Fluids Engineering, 126: 323-336

KUNDU, D., SKEIKH, A.H., LOU, D.Y.S., 1992. Heat Transfer in Crossflow Over Cylinders Between Two Parallel Plates. Numerical Heat Transfer, Part A, 114: 558-564.

KUPPAN, T., 2000. Heat Exchanger Design Handbook, Marcell Dekker, Inc., New York, Basel, ISBN: 0-8247-9787-6, 1119 p.

KUROSAKA, M., KİKUCHİ, M., HİRANO, K., YUGE, T., and INOUE H., 2003 2003. Interchangeability of Vortex-Breakdown Types. Experiments in Fluids, Vol. 34, pp. 77–86.

KWON K., CHOI, H., 1996, Control of laminar vortex shedding behind a circular cylinder using splitter plates. Physics of Fluids 10:479– 485.

LAM, K.M., DAI, G.Q., 2002. Formation of vortex street and vortex pair from a Circular cylinder oscillating in water. Experimental Thermal and Fluid Science, 26, 901-915.

LEE, T. and BASU, S. 1997. Nonintrusive measurements of the boundary layer developing on a single and two circular cylinders. Exps. Fluids 23, 187–192.

LEI,C. K., KAVANAGH, L., Force and vortex shedding characteristics of a circular cylinder near a plane boundary, Proc. 7th Int. O¤shore and Polar Engineering Conf., USA, 25-30 May 1997,

LEU, J.S., WU Y.H., JANG, J.Y., 2004. Heat transfer and fluid flow analysis in plate fin-and-tube heat exchangers with a pair of block shape vortex generators. Int J. of Heat Mass Transfer 47:4327–4338

LIENHARD, J. 1996. Synopsis of Lift, Drag, and Vortex Frequency Data for Rigid Circular Cylinders.

LIM, H.C. AND LEE, S.J., 2002. Flow control of circular cylinder with longitudinal Grooved surfaces. AIAA Journal 40, 10, 2027-2036.

LIN, C. CHIU, P.H. AND SHIEH, S.J., 2002. Characteristics of horseshoe vortex system near a vertical plate-base plate juncture. Experimental thermal and Fluid Science, 27, 25-46.

LOZZA,G., MERLO, U., 2001. An Experimental Investigation of Heat Transfer and Friction Losses of Interrupted and Wavy Fins for Fin-and-Tube Heat Exchangers. Int. J. Refrigeration, 24: 409-416.

MADI, M.A., JOHNS, R.A., HEIKAL, M.R., 1998. Performance Characteristics Correlation Two- Row Tube and Plate Fin Heat Exchanger. J. Heat Transfer, Trans ASME, 106: 627-632.

MAVRIDIS,C., BAKROZIS, A., KOUTMOS, P., PAPAILIOU,D.,1998. Isothermal and non-premixed turbulent reacting wake flows past a two-dimensional square cylinder. Experimental Thermal and Fluid Science, 17, 90-99.

MARAKKOS, K., and TURNER, J. T., 2006. Vortex generation in the cross-flow around a cylinder attached to an end-wall. Optics & Laser Technology, 38, 277-285.

MARTINUZZI, R. J., HAVEL, B., 2004. Vortex shedding from two surface mounted cubes in tandem. International Journal of Heat and Fluid Flow, 25, 364-372.

MENDEZ, R. R., SEN, M., YANG, K.T., MCCLAIN, R., 2000. Effect of Fin Spacing on Convection in a Plate Fin and Tube Heat Exchanger. Int. J. Heat Mass Transfer, 43: 39-51.

MITTAL S., KUMAR, V. and RAGHUVANSHI A.,1997. Unsteady incompressible flow past two cylinders in tandem and staggered arrangements. International Journal for Numerical Methods in Fluids, 25:1315-1344

MITTAL, S. and KUMAR, V., 2001 Flow-induced oscillations of two cylinders in tandem and staggered arrangement,Journal of Fluids and Structures, 15: 717-736

MITTAL, S., KUMAR, V., 2004. Vortex induced vibrations of a pair of cylinders at Reynolds Number 1000, International Journal of Computational Fluid Dynamics, Volume 18: pages 601 – MITTAL, S., RAGHUVANSHI, A., 2000. Control of vortex shedding behind circular cylinder for flow at low Reynolds numbers. International Journal for Numerical Methods in Fluids.

MON, M. S.R., GROSS, U., 2004. Numerical study of fin-spacing effects in annular finned tube heat exchangers: International Journal of Heat and Mass Transfer, 47, 1953-1964

MUZAMMIL, M. and GANGAHARIAH, T., 2003. The mean characteristics of horseshoe vortex at a cylinder pier. Journal of Hydraulic Research, 4, 3, 285-297.

NAKAMURA, H., IGARASHI, T., TSUTSUI, T., 2001. Local heat transfer around a wall mounted cube in the turbulent boundary layer. International Journal of Heat and Mass Transfer. 44: 3385-3395.

_____, 2003. Local heat transfer around a wall mounted cube at 45 degrees to flow in a turbulent boundary layer. International Journal of Heat and Fluid Flow, 24, 807-815.

NAKAMURA, Y., 1996.Vortex shedding from bluff bodies and a universal Strouhal Number, Fluids and Structures Volume 10, Issue 2, Pages 159-171

NORBERG, C., 1994. An experimental investigation of the flow around a circular cylinder: influence of aspect ratio. Journal of Fluid Mechanics, 258: 287-316.

OZONO S., 1999, Flow control of vortex shedding by a short splitter plate asymmetrically arranged downstream of a cylinder. Physics of Fluids 11(10):2928 –2934.

OZTURK, N.A,. 2006. Investigation of Flow Characteristics In Heat Exchangers of Various Geometries. Ph.D. thesis, Cukurova University.

OZTURK, N.A., AKKOCA, A., SAHIN, B., 2008. PIV measurements of flow past a confined cylinder Received: Exp Fluids 44:1001–1014

OZTURK, N.A., AKKOCA,A., SAHIN, B., 2008. Flow details of a circular cylinder cylinder mounted on a flat plate. 46:344-355

OZTURK, N.A., AKCAYOGLU, A., SAHIN, B., 2009. Downstream PIV measurements of a circular cylinder-plate junction. J. Mechanical Engineering Science 223:1-13

PARK, C.W., LEE, S.J., 2004. Effects of free-end corner shape on flow structure around a finite cylinder, Journal of Fluids and Structures. 19, 141-158.

PARK D., LADD, D., HENDRICKS, E., 1994. Feedback control of von Karman vortex shedding behind circular cylinders at low Reynolds numbers. Physics of Fluids 6(7):2390 –2405

PATTENDEN, R.J., TURNOCK, S.R., ZHANG, X., 2005. Measurements of the flow over a low-aspect-ratio cylinder mounted on a ground plane. Experiments in Fluids. 39, 10-21

PERSILLON, H. and BRAZA, M., 1998. Physical analysis of the transition to Turbulence in the wake of a circular cylinder by three-dimensional Navier-Stokes simulation. Journal of Fluids Mechanics, 365, 23-88.

PRAISNER, T.J., SABATINO, D.R., and SMITH, C.R. 2001 Simultaneously Combined Liquid-Crystal Surface Heat Transfer and PIV Flow-Field Measurements, Experiments in Fluids, vol 30, no.1, pp. 1-10.

ROHSENOW, W. M., HARTNETT, J.P., CHO, Y.I., 1998. Handbook of Heat Transfer. Third Edition. McGraw Hill, ISBN 0-07-053555-8, New York, 1330 p.

ROULUND, A., SUMER, B. M., FREDSOE, J., MICHELSEN, J., 2005. Numerical and experimental investigation of flow and scour around a circular pile. Journal of Fluid Mechanics, 534, 351-401.

ROUSSOPOULOS, K. 1993. Feedback control of vortex shedding at low Reynolds numbers. Journal of Fluid Mechanics 24, 267-296.

LIN,J.C., ROCKWELL, D., 2001.Vortex Breakdown Edge Ineraction, Consequence of Edge Oscillations. AIAA Journal, Vol. 39, No.55, pp. 865-876.

SAHIN, B., AKKOCA, A., OZTURK, N.A., AKILLI, H., 2006. Investigations of flow characteristics in a plate fin and tube heat exchanger model composed of single cylinder, International Journal of Heat and Fluid Flow 27 3: 522–530.

_____ , 2007. Horseshoe vortex system in the vicinity of the vertical cylinder mounted on a flat plate, Flow Measurement and Instrumentation 18: 57–68

SAHIN, B., OZTURK, N.A., GURLEK, C., 2008. Horseshoe vortex studies in the passage of a model plate-fin-and-tube heat exchanger. International Journal of Heat and Fluid Flow 29:340–351

SAHIN,B., OZTURK, N.A., 2009. Behaviour of flow at the junction of cylinder and base plate in deep water, Measurement 42: 225–240

SAHIN, B., AKILLI, H., KARAKUS, C., AKAR, M. A., OZKUL, E., 2010. Qualitative and quantitative mmeasurements of horseshoe vortex formation in the junction of horizontal and vertical places. Measurement 43: 245–254

SAKAMOTO, H., ARIE, M., 1983. Vortex shedding from a rectangular prism and a circular cylinder placed vertically on a turbulent boundary layer. Journal of Fluids Mechanics, 126, 147-165.

SANTIAGO, J.G., MEINHART, C.D., WERELEY, S.T., BEEBE, D.J., ADRIAN, R.J., 1998. A particle image velocimetry system for micro fluidics. Experiments in Fluids, 25: 316-319.

SARPKAYA, T., 2004. A critical review of the intrinsic nature of vortex-induced vibrations. Journal of Fluids and Structures, 19, 389-447.

SAU, A., HWANG, R. R., SHEU, T. W. H., YANG, W. C., 2003. Interaction of trailing vortices in the wake of a wall-mounted rectangular cylinder. Physical Review, E 68, (1–15)

SCHIWIETZ, T., WESTERMANN, R., 2004, GPU- PIV Vision, Modeling and Visualization

SHEPPARD, D., Prof. Dr., 2004. Course Notes of the Lecture "EOC 6430 Coastal Structures", University of Florida, Civil and Coastal Engineering Department

SIMSON, J., 2001.Junction Flows. Annual Review of Fluid Mechanics, 33, 415-443

SOUZA, F. DE, DELVILLE, J., LEWALLE, J., BONNET, J.P., 1999. Large scale coherent structures in a turbulent boundary layer interacting with a cylinder wake. Experimental Thermal and Fluid Science, 19, 204-213.

SUMER, B.M., CHRISTIANSEN, N., FREDSOE, J., 1997. The horseshoe vortex and vortex shedding around a vertical wall mounted cylinder exposed to waves, Journal of Fluid Mechanics, 332, 41-70.

SUMNER, D., HESELTINE, J.L., DANSEREAU, O.J.P., 2004, Vortex shedding from a finite circular cylinder of small aspect ratio, Proceedings of the Canadian Society for Mechanical Engineering Forum 2004 - CSME Forum 2004, London, Canada, pp. 625-633.

SUMNER, D., PRICE, S. J., and PAIDOUSSIS, M. P., 2000. Flow-pattern identification for two staggered circular cylinders in cross-flow. Journal of Fluid Mechanics, 411: 263-303.

____ , 1997. Investigation of Impulsively-Started Flow Around Side-by-Side Circular Cylinders: Application of Particle Image Velocimetry. Journal of Fluids and Structures 11, 597-615.

TAO, J, S., HUANG X,Y., CHAN, W,K., 1996. A flow visualization study of feedback control of vortex shedding from a circular cylinder. Journal of Fluids and Structures 10:965 –970.

TSAI, S.F., SHEU, T.W.H., 1998. Some Physical Insights into a Two- Row Finned Tube Heat Transfer. Computers and Fluids, 27(1): 29-46.

TONY W. H. SHEU, T.W. H., TSAI, S. F., CHIANG, T. P., 1999. Numerical study of heat transfer in two-row heat exchangers having extended fin surfaces. Numerical Heat Transfer, Part A: Applications, 35, 797-814.

TORIKOSHI K., NAKASZAWA Y., and ASANO H., Flow and heat transfer performance of a plat-fin and tube heat exchanger, 1st report: Effect of fin pitch, Proceeding of the 10th International Heat Transfer conference, 411-416, 1994

TSENG, M-H. YEN, C-L., SONG, C. C. S, 2000. Computation of three-dimensional flow around square and circular piers. International Journal for Numerical Methods in Fluids, 34, 207-227.

TUTAR, M., AKKOCA,A., 2004. Numerical analysis of fluid flow and heat transfer characteristics in three-dimensional plate fin-and-tube heat exchangers. Numerical Heat Transfer; Part A: Applications, 46, 301-321.

TWARI, S., BISWAS, G., and PRASAD SUDIPTA BASU, P. L. N., 2003. Numerical Prediction of flow and heat transfer in a rectangular channel with a build-in circular tube. Transactions of the ASME, Journal of Heat Transfer, 125, 413-421.

UMEDA, S. and YANG, W.-J., 1999. Interaction of Von Karman vortices and intersecting main streams in staggered tube bundles. Experiments in Fluids, 26, 389-396.

WANG, H.F., ZHOU, Y., CHAN, C.K., WONG, W.O., LAM, K.S., 2004. Flow structure around a finite length square prism. 15th Australian Mechanics Conference, The University of Sydney, Sydney, Australia, 13-17

WANG, C. C., FU, W. L., CHANG, C. T., 1997. Heat Transfer and Friction Characteristics of Typical Wavy Fin-and-tube Heat Exchangers**.** Experimental Thermal and Fluid Science, 14: 174-186.

WANG, C.C., LIN, Y.T., LEE, C.J., CHANG, J.Y., 1999a. . Investigation of Wavy Fin- and- tube Heat Exchangers: A contribution to Databank. Experimental Heat Transfer, 12:73-89.

WANG, Z. J., ZHOU, Y., 2005. Vortex interactions in a two side-by-side cylinder near-wake, International Journal of Heata nd Fluid Flow Volume 26, Issue3, June 2005, Pages 362-377

WARUI, H.M. and FUJISAWA, N. 1996. Feedback control of vortex shedding from a circular cylinder by cross-flow cylinder oscillations. Experiments in Fluids 21, 49-56

WEI, T., and SMITH, C.R., 1986. Secondary vortices in the wake of circular. Journal of Fluid Mechanics, 169:513-533.

WILLIAMSON, C. H. K., 1996. Vortex dynamics on the cylinder wake. Annual Review Fluid Mechanics, 28, 477-539.

WUNG, T. S., CHEN, C. J., 1989. Finite analytic solution of convective heat transfer for tube arrays in crossflow: Part I. Flow field analysis. Journal of Heat Transfer, Transactions ASME, 111, 3, 633-640

XU G., ZHOU, Y., 2004. Strouhal numbers in the wake of two inline cylinders. Exp. Fluids 37 248–256.

YAN, W.M., SHEEN, P.J., 2000. Heat Transfer and Friction Characteristics of Fin and Tube Heat Exchangers. Int. J. Heat Mass Transfer, 43: 1651-1659.

ZDRAVKOVICH M.M., 1988. Review of interference-induced oscillations in flow past two parallel circular cylinders in various arrangements, J. Wind Ind. Aerodyn. 28 183–200.

ZHANG, H.J., and ZHOU, Y., 2001. Effect of unequal cylinder spacing on vortex streets behind three side-by-side cylinders. Physics of Fluids, 13 (12): 3675-3686.

ZIADA, S., 2006. Vorticity Shedding and Acoustic Resonance in Tube Bundles. J.of the Braz. Soc. of Mech. Sci & Eng. 28: 186-199

ZHOU, Y., YIU, M.W., 2006. Flow structure, momentum and heat transport in a two-tandem-cylinder wake, J. Fluid Mech. 548: 17–48.

ZHOU, Y., ZHANG, H. J. and YIU, M. W., (2002). The turbulent wake of two side-by- side circular cylinders, J. Fluid Mech. 458: 303.

CIRRICULUM VITAE

Suat ÖNAL was born in 1961 in Osmaniye. He was graduated from Mechanical Engineering Department of Cukurova University in 1982. After he had completed his military service in 1984, he worked as an engineer for goverment for 4 years. He was attended as Instructor to Osmaniye Vocational Higher School of Cukurova University in 1989 and had professional education in the United Kingdom for 9 months in 1990 under Industrial Training Project agreement between the World Bank and Turkish Higher Education Council.

He had a master degree in 1993 at Erciyes University. He also graduated from Economy faculty of Anadolu University in 1999. He has been to Sweden, England, Germany and Spain for project studies of EU Leonardo da Vinci Mobility and Grundtvig programmes

He has still been teaching at Korkut Ata University of Osmaniye. He is married and has got 2 children.